IN-18
64085
p. 74

NASA Technical Memorandum 106895

Static Stability of the Space Station Solar Array FASTMast Structure

John F. Shaker and Thomas H. Acquaviva
Lewis Research Center
Cleveland, Ohio

August 1995

National Aeronautics and Space Administration

STATIC STABILITY OF THE SPACE STATION
SOLAR ARRAY FASTMast STRUCTURE

by:

John F. Shaker
Solar Array Branch
Power Technology Division
Aerospace Technology Directorate

Thomas H. Acquaviva
Experiment Definition Branch
Space Experiments Division
Space Flight Systems Directorate

TABLE OF CONTENTS

LIST OF TABLES

LIST OF FIGURES

LIST OF FIGURES (continued)

ACKNOWLEDGMENTS

EXECUTIVE SUMMARY

The FASTMast is a deployable truss structure designed and able to carry a given set of axial, shear, bending, and torsion loads. Stability of this structure is being investigated to determine if the mast can carry loads beyond those to which it was originally designed. An investigation of the stability failure modes for the FASTMast system under a combined load state was successfully completed. The work presented herein attempts to explain the FASTMast behavior at points of instability. This was accomplished through a combination of static testing and nonlinear large displacement analyses. The goal of this task was to identify stability failure modes and develop nonlinear analytical models capable of predicting failure levels. Identification of primary FASTMast instability failure modes and the development of two test-verified nonlinear finite element models were the fundamental results of this effort.

Instability is precipitated by longeron misalignments due to events associated with a transition of the mast system to a secondary stiffness state. As the FASTMast structure evolves into this nonlinear state, system stiffness is reduced by approximately an order of magnitude. The nonlinear response state, which is most readily associated with slackening of the diagonal elements, gives rise to alternate load paths for which load resistance is greatly reduced. The effects of altered load paths, in conjunction with combined loading and changes in mast geometry, lead to a state of static instability. Principal FASTMast failure modes are kinematic in nature and involve undesirably large displacements of the elbow joints combined with large longeron compressive loads. However, the FASTMast linear response state, for which diagonals remain taut, exhibited no instabilities for all combinations of applied loads. Therefore, the onset of instability can be expected to occur at a point when system stiffness is reduced dramatically and alternate load paths attempt to accommodate transverse, torsion, and bending loads applied to the mast.

In order to develop the interaction curves required to define failure surfaces associated with the failure modes given above, it is necessary to develop analytical models of the flight FASTMast design. Due to the probabilistic nature of an instability failure event, a large sample of data would be required to develop a 3-sigma failure load level. The ability to apply Finite Element (FE) techniques to this problem was verified by the successful model correlation effort. With the knowledge gained from this activity, it would be possible to proceed successfully with a detailed nonlinear characterization effort. However, the practical value of continuing FASTMast characterization into the nonlinear response regime should be weighed very carefully in terms of International Space Station (ISS) Program objectives.

A final point relative to the failure mode discussion must address the post-buckled capability of the FASTMast. A post-buckled state in this case refers to a situation in which the FASTMast system enters a nonlinear response state. The fact that the critical failure modes have been kinematic in nature, leads to the question of post-buckling strength of the mast. There are two very important points that quickly provide focus to this significant question. First, it is very clear from the ultimate moment tests that once a longeron column has been involved in a buckling instability event the axial/bending capability is reduced by 30%. Secondly, continuous application of an applied load beyond the critical threshold will result in a catastrophic collapse. The reduction in strength is most likely due to permanent longeron misalignment that resulted from local yielding of several mast components. Strength reduction observed from test data was only possible because the applied loads were removed at the onset of unstable behavior. It is reasonable to assume that in the actual service environment an applied load causing instability will not be detected and therefore continue unabated. Therefore, a conservative engineering conclusion based on available test and analysis data is that the post-buckled strength of the FASTMast is zero.

INTRODUCTION

The combined loads test of the 3-Bay FASTMast marks the end of the Lewis Research Center (LeRC) effort to characterize the behavior of the principal Space Station solar array support structure. The primary objective of this test and analysis effort was to develop a method to predict structural stability failure modes under flight-like applied loads.

Included at the beginning of this report is a brief historical perspective of the hardware design development and FASTMast structural stability problem evolution. Once an understanding of the solution process has been established, test and analysis details are presented and related to the postulated failure theories.

The combined load test series subjected the structure to a combination of transverse, moment, and torsion loads similar to that expected in the service environment. Nonlinear Finite Element (FE) models were developed and large displacement analyses were performed to support the test effort and failure mode predictions. Details of the test configuration as well as test and analysis results are presented. The results were then critiqued to establish valid and successful support of the failure mode assessments. Finally, study conclusions are drawn and recommendations for safe operation of FASTMast structure are presented for consideration.

DESIGN DEVELOPMENT AND LOADING ENVIRONMENT BACKGROUND

An integral part of the Space Station Freedom (SSF) Electrical Power System (EPS) design is the 110 ft. long by 37 ft. wide Solar Array Wing. Each Solar Array Wing has two blankets consisting of 82 rigid-framed solar panels that have 200 solar cells. The Solar Array Blankets fold into a flat package for launch and are deployed and retracted once on-orbit. These blankets are deployed, supported and retracted by the Solar Array Mast structure.

The design and development of the Space Station Freedom (SSF) was divided into several work packages and a different NASA Center managed each work package. NASA's LeRC in Cleveland, Ohio was assigned the Work Package Four (WP-04). LeRC was responsible for the Electrical Power System of SSF. The prime contractor for LeRC was the Rocketdyne Division (RD) of the Rockwell International Corporation. The Solar Array Wing was designed and built by the Lockheed Missile and Space Co. (LMSC). The Solar Array Mast was designed and built for LMSC by AEC-Able Engineering Corporation.

One important concern of the LeRC loads and structural engineers was the ability of the Solar Array Wing to withstand the loads it may encounter during its service lifetime. When the impact of the Shuttle Reaction Control System (RCS) Jet Plume loads on the Solar Array became known, the load carrying capability of the Solar Array Mast became a continuous topic of debate. LeRC engineers have spent considerable time and energy in an attempt to characterize the structural capability of the Solar Array Mast.

Presented below is a brief history on the evolution of the Solar Array Mast design as well as a description of the latest design features. A characterization of the load path in response to an applied mechanical load and a detailed description of the FASTMast deployment and retraction operations is also included.

This report illustrates how the scope of 3-Bay FASTMast test objectives matured. An explanation will be included of how these strength evaluation efforts lead to the most recent mast combined-loads testing and structural stability assessment. With the description of earlier work serving as a foundation, a detailed characterization of the mast response to several combinations of applied loads is presented and conclusions are drawn related to the structural behavior of the Solar Array Mast.

Solar Array Mast Design Development History

In December 1987 the Solar Array Mast design was a Nut-Deployed Coilable Boom or Mast. This mast had a triangular cross-section with three continuous vertical members called longerons. The longerons were pultruded (i.e., continuous pulling through a form) fiberglass fibers in an epoxy matrix. This composite material enabled the longerons to be flexible enough to "coil-up" in the mast storage canister. A rotating screw-type nut, within the walls of the mast's housing and located at the tip of the storage canister, would deploy and retract the structure. This system has full structural capability when "partially deployed" or, simply, the mast is at full strength throughout the deploy/retract cycle.

This design was based on technology developed for the Solar Array Flight Experiment/Dynamic Augmentation Experiment (SAFE/DEA) flown on Shuttle flight STS-41D in September 1984, see figure 1. The SAFE/DEA investigation qualified advanced solar array and large space structure technologies. The SAFE/DEA Wing had several features that were marked improvements over rigid solar panel arrays designed to date. The most significant was the ability to store and protect the "flexible-blanket" wing in a relatively small Shuttle cargo package during the launch and then be able to deploy the large structure once on-orbit.
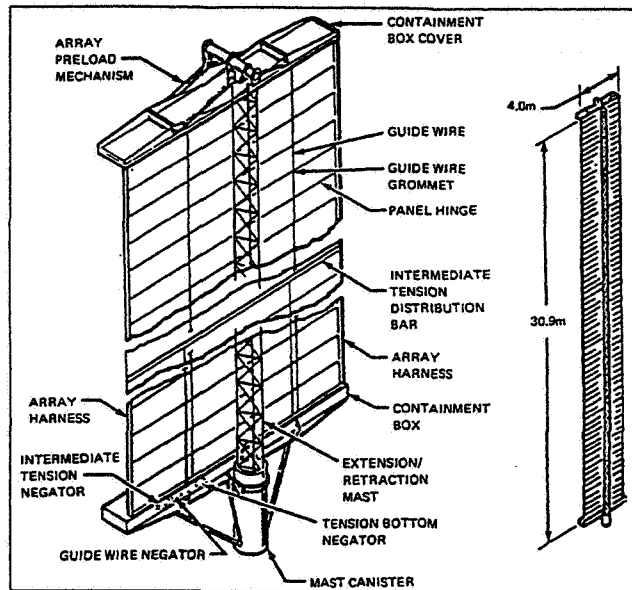
Figure 1. SAFE/DEA Wing

Several events took place in December 1989 that had a profound effect on the Solar Array Mast design. The most significant was the dramatic increase of the power requirements for Space Station Freedom. To comply with the new requirements, the area of the each Solar Array Blanket was expanded by increasing the number of panels per blanket from 68 to 82 panels. This increase in array area had an adverse effect on the Solar Array Mast service loads. It was apparent the service loads, although ill defined, were going up. The coilable longeron mast was considered not adaptable enough to prevent delays in hardware delivery if the loads were to change again.

The strength capability of the coilable longeron mast is dependent on two things, (1) the diameter and length of the mast storage canister and (2) the mast longeron diameter. It would be necessary to adjust both to increase the capability of the mast. Increasing the size of the mast canister would make packaging in the Shuttle Cargo Bay difficult. An increase of the longeron diameter would dangerously increase the stored energy of the stowed mast. In addition, the long lead time needed to manufacture the monolithic deploying nut in the mast canister and the continuous fiberglass longerons in the mast, would delay Solar Array hardware delivery if a change was necessary due to an adjustment in the applied loads.

The Folding Articulated Square Truss Mast (FASTMast) design allowed the SSF program to overcome these problems. The mast contractor, AEC-Able Eng. Co., used a FASTMast design on the Tethered Satellite System (TSS) launched on STS-46. TSS employed a FASTMast design that used a deploying nut similar to that of the coilable longeron mast. The SSF program was interested in the newer lanyard-deployed FASTMast that did not utilize a deploying nut, this eliminated possible delays in the manufacture of this item. Another aspect of the FASTMast design is the use of noncontinuous aluminum longerons, eliminating the need for the continuous fiberglass longerons which are difficult to fabricate. In February 1990, the SSF Program decided to abandon the coilable longeron mast design in favor of the lanyard-deployed FASTMast. Design flexibility and TSS flight program history were the primary reasons.

At the Solar Array Mast Preliminary Design Review (PDR) in June 1990, several Review Item Discrepancies (RIDs) were submitted concerning the lanyard-deployed FASTMast design. The most notable problem concerned the four lanyards that deployed and retracted the mast if one lanyard failed, the mast could not be retracted. Another problem arose from the sticking between the array blanket panels during deployment of the Solar Array. This sticking would have caused bending loads beyond the capability of a partially deployed mast. These unresolved problems compelled the contractor to reconsider the nut-deployed FASTMast design.

2

The mast contractor developed a "modified" deployment nut design. TSS used a deploying nut height equal to one FASTMast bay height. In the SSF FASTMast, the bay height was increased slightly and a "half-bay" deployment nut design was incorporated. This provided the strength needed during the solar array deployment operations. This change did not affect the mast canister height and weight enough to cause packaging problems in the Shuttle Cargo Bay.

LeRC engineers were concerned about possible delays due to the manufacture of the deploying nut, a problem first recognized in the coilable longeron mast. The mast contractor stated that limited adjustment to the FASTMast bending strength capability could still be done without affecting the nut diameter. In August 1990 the nut deployed FASTMast design was established as the baseline design for the Solar Array Mast.

In October 1991, the Solar Array contractors were given direction to base their hardware design and analysis activities on the internal structural loads furnished in reference 1. The Solar Array hardware internal structural loads, detailed in this book, increased on all the SSF Stage Configurations (SC). This was caused by the Shuttle RCS Jet Plume Impingement events on the SSF Pre-Integrated Truss Design, the Man-Tended Configuration (SC-17) is shown in figure 2. All the contractors working on the EPS were requested to design the WP-04 hardware to accommodate the structural loads encountered on the SSF Man-Tended Configuration. For earlier SSF Stage Configurations, an "operational work around" was expected to reduce any applied loads that caused negative margins of safety in the WP-04 hardware.
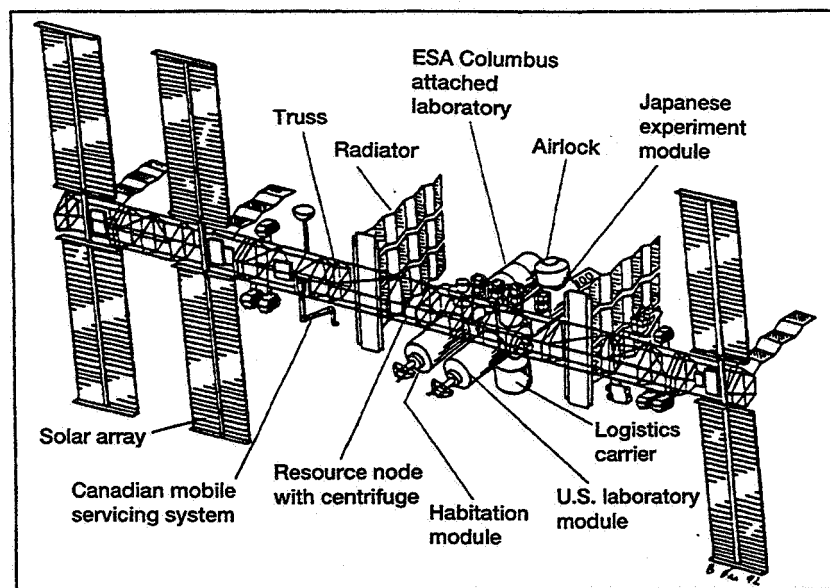
Figure 2. SSF Man-Tended Configuration (SC-17)

This new design requirement resulted in the next significant Solar Array Mast design change in December 1991. The design changes now involved the longerons and rigid battens of the FASTMast. The mast longerons were thickened in the middle (hence the term "tapered" longeron) to increase their buckling capability. The mast contractor implemented this change to increase the FASTMast system bending capability. The Rigid Battens were redesigned to allow the tapered longerons to stack close together, reducing the impact to the stored mast stack height.

Since the most recent design changes were carried out, there has been much concern whether this structure can withstand the latest on-orbit service loads. Even so, to date the FASTMast design and deployment method have not changed and flight hardware is presently being built and delivered for the International Space Station (ISS).

Space Station Solar Array Loading Environment

In order to begin the structural assessment of the FASTMast, it is necessary to understand the source of the external loading expected in service. The principal source of mast loading is imparted to the structure during Shuttle/ Space Station docking, Module/Space Station berthing and Shuttle approach maneuvers. These loads are caused by docking/berthing impacts, and Shuttle Reaction Control System (RCS) and/or Attitude Control System (ACS) jet

exhaust plume impingement on the solar array blankets. Docking/berthing loads are impulsive excitations transmitted down the truss of the Space Station to the base of the solar array assembly. The loads due to exhaust plumes can be considered either a dynamic or quasi-static surface pressure acting on the solar array panels. Typical surface pressures are on the order of 0.01 lb/in^2. Applied loads from docking, berthing and plume events result in transverse, torsion, axial, and moment loads on the mast structure. In order to better understand the manner in which the solar array mast is externally loaded, it is important to clearly understand these events.

One of the most dramatic loading events associated with Shuttle operations is the action of RCS and ACS jet plume impinging on the solar array. Shown in figure 3 is the Shuttle position during the last stages of approach to the Space Station Freedom. In order to engage the docking port the astronauts must guide the vehicle through an approach cone whose apex is the docking port. Control of vehicle position is maintained manually by firing RCS jets as shown in figure 4. There are 44 ACS and RCS jets located throughout the Shuttle and they are displayed pictorially in figure 5. The ACS jets fire at a 25 lb$_f$ rate and the RCS jets emit a thrust of 55 lb$_f$. Although their use is restricted to circumstances of great need, the Primary Reaction Control System (PRCS) jets can be used during maneuvers and are rated at 870 lb$_f$ of thrust. Real-time simulations of Shuttle/Space Station docking maneuvers indicate several large solar array loading conditions result from thruster plume impingement.
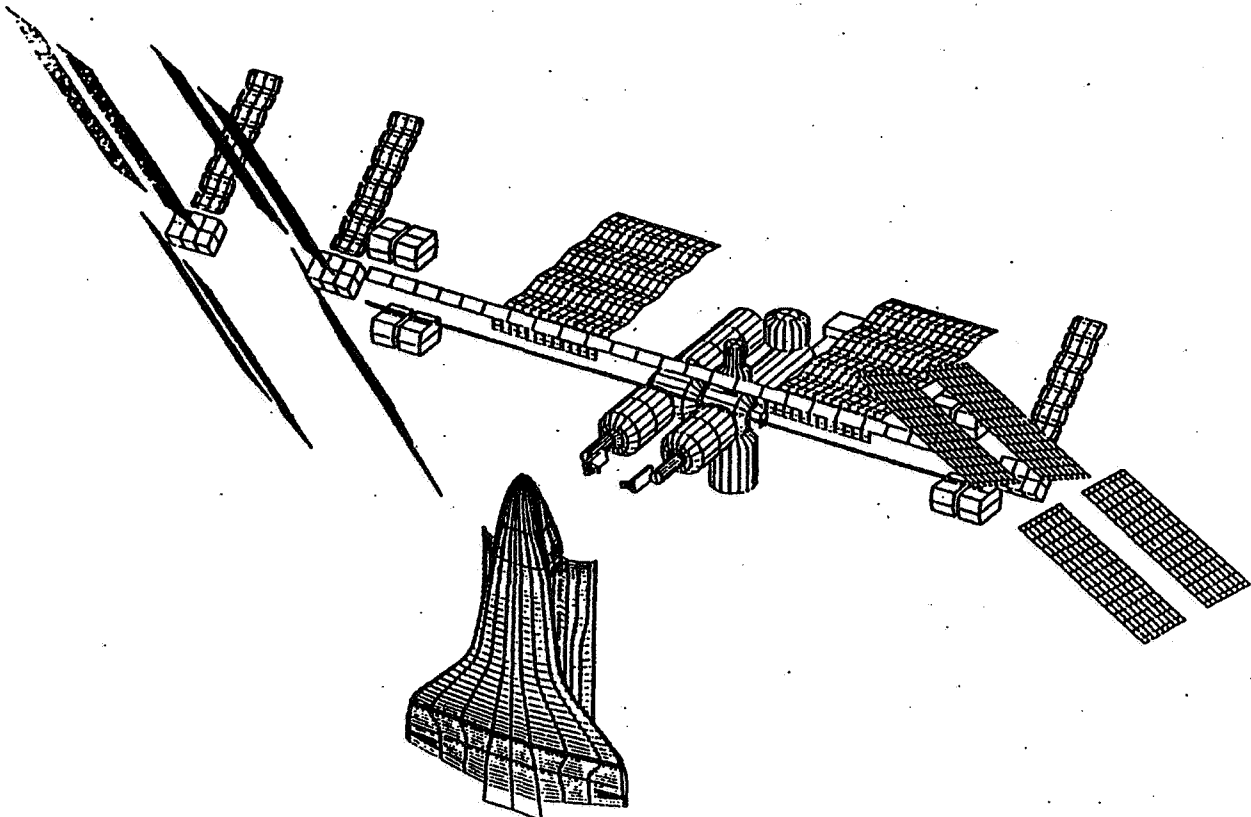
Figure 3. Shuttle Approach to Space Station (Typical).
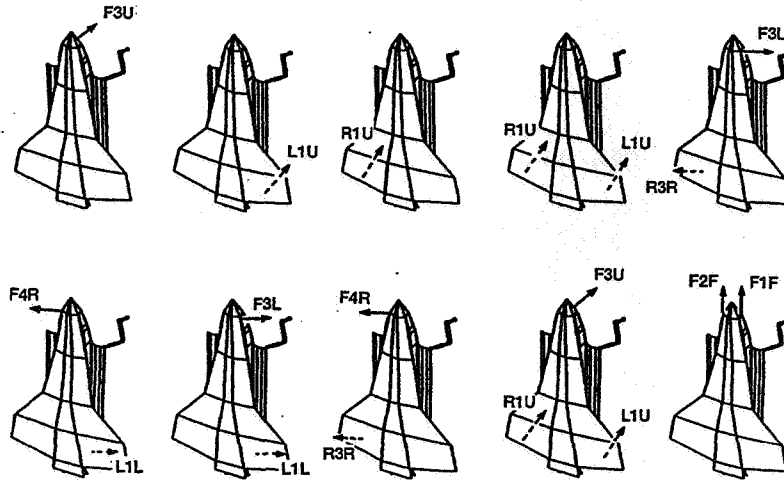
Figure 4. Shuttle Thrusters Used for Space Station Approach
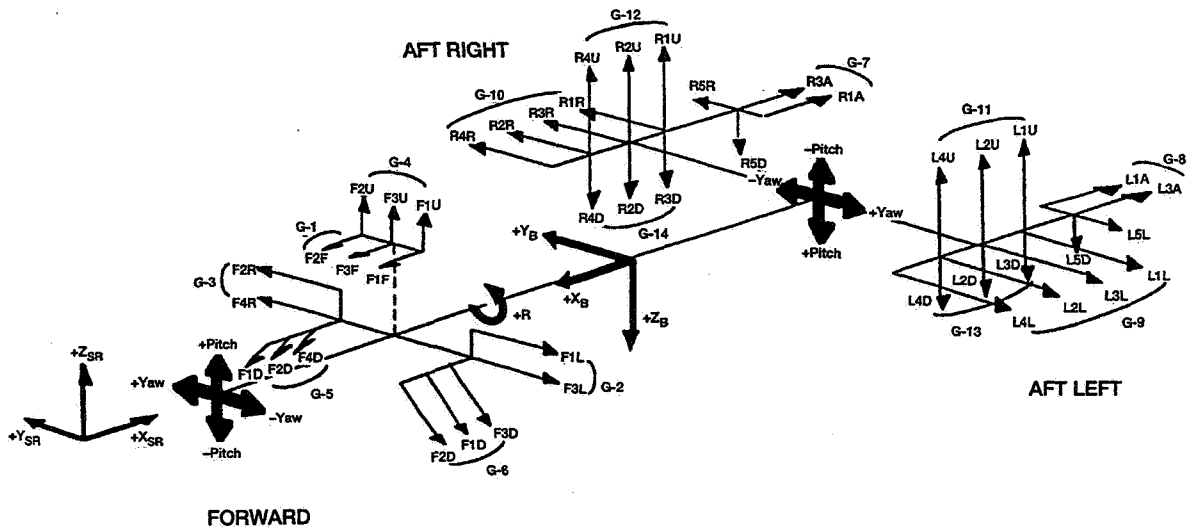
Figure 5. Shuttle Thruster Location Layout

The plume loading event can be either quasi-static or dynamic in nature. Shuttle approach to the space station is generally slow and deliberate. The pilot will continually fire the control jets in order to guide the craft into the docking mechanism capture device as is shown in figure 6. Therefore, the actual thrust pulses emitted from the rockets will occur in small bursts whose duration will generally be on the order of milliseconds. Depending on the amplitude and frequency of the force, pulse loading of this type could cause dynamic amplification of solar array response. This is in contrast to a maneuver that requires the Shuttle to execute a long duration thruster firing which would result in a quasi-static pressure load. An example of quasi-static loading could include a "breakout" maneuver requiring the Shuttle to quickly move away from the Space Station to avoid an undesirable alignment or collision. This maneuver would require a long duration firing which would result in a quasi-static loading. The net result of this action is very similar to that of a sailboat mast under conditions of wind loading. In order to reduce applied loads caused by plume impingement, Shuttle/Space Station operational fixes, such as array feathering and alternate approach routes, have been incorporated into flight plans. Although a detailed description of Shuttle maneuvers and thruster firing profiles have been omitted here, it should be clear that both static and dynamic thruster plume events must be included in the definition of the loads.

5
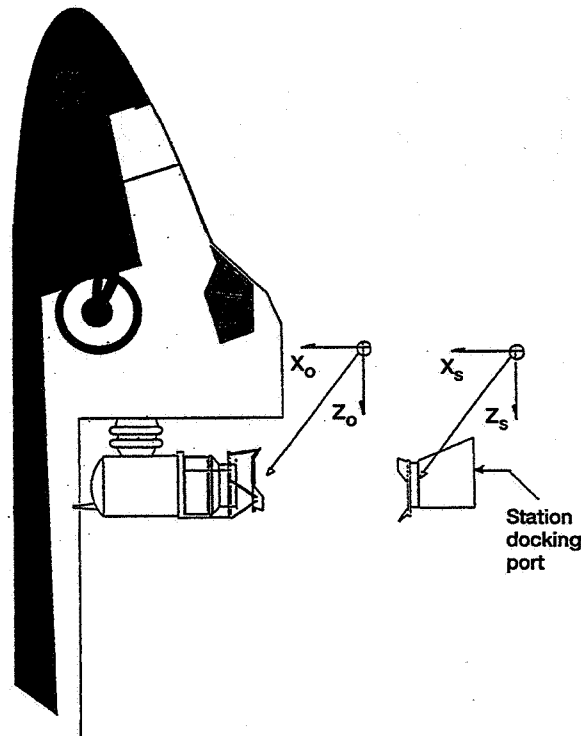
Figure 6. Shuttle Docking Interface with Space Station

The second type of dynamic loading event considered involves impact forces due to docking and berthing. Docking loads result from an impact between the Shuttle and Space Station docking mechanisms. Berthing loads are developed as the modules are attached to the existing Space Station structure during construction. In either case, impulsive loads transmitted to the truss structure result in a lateral base excitation of the solar array assembly. Solar array load levels induced during these events have also pushed the hardware to its design limit. Again, the magnitude of the applied load transmitted to the structure will depend to a large degree on the manner in which astronauts execute docking and berthing maneuvers. In general, large array responses are associated with high impact velocities. Other factors affecting force transmission during impact events include stiffness of mating mechanisms and Shuttle/Space Station mass ratios. Once docking/berthing scenarios and mating stiffnesses have been defined, the profile of the forcing function can be developed.

HARDWARE DESCRIPTION

The primary on-orbit function of the Folding Articulated Square Truss Mast (FASTMast) is to support the large and flexible Solar Array Blankets. It is also necessary to store the Solar Array Mast for launch in a compact package in the Shuttle Cargo Bay. To accomplish both functions, the mast design must be lightweight and strong. This section presents a brief hardware description emphasizing key aspects of the FASTMast's physical design. Also, load path description and details of the deployment and retraction operations of the mast are included.

Design Features of Principal Mast Parts

The FASTMast is a mechanism that deploys into a truss structure that is approximately 1296 in. tall and has a 30.4 in. square cross-section. The structure consists of 32 interconnected bays that are 40.5 in. tall. Figure 7 shows one face of one bay and pictorially locates the principal components of the mast bay. Each bay has an upper and lower section and the principal components are: a Flexible Batten Frame, four vertical members called longerons (four upper and four lower per bay), a Rigid Batten Frame, and the wire rope diagonals.

Corner roller

Longeron

Diagonal

Elbow roller

Elbow fitting

Flex batten

Longeron roller

Corner fitting

Rigid batten
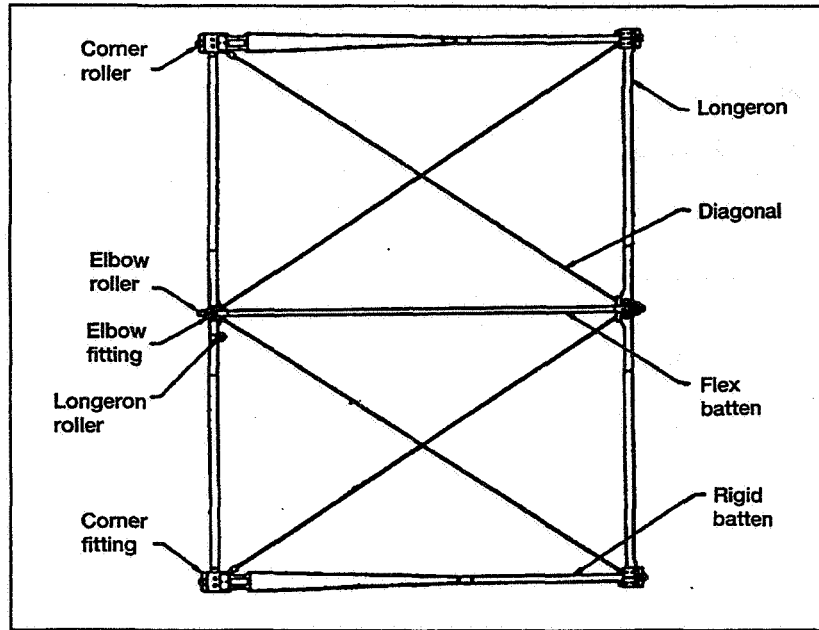
Figure 7. One Bay of the SSF FASTMast

The major elements of the Flexible Batten Frame are four post-buckled fiberglass flexible (flex) battens and four elbow fittings. The flex-battens are 0.375 by 0.275 in. fiberglass/epoxy pultruded rods. Each flex-batten is buckled to a strain of 0.5 percent when the mast is fully deployed and 1.5 percent when the mast is stowed in the storage canister. The elbow fittings react the 50 lb nominal pre-load of the strained flex-battens into the stainless steel wire rope diagonals. Each elbow fitting also provides a pair of pivot hinges that allow the longerons to stow and deploy during the mast extension/retraction operations.

The vertical members consist of an upper and lower bay aluminum longeron separated by an elbow fitting. There are two types of longerons in the FASTMast: "tapered"; found in the bottom 20 bays, and "straight"; found in the top 12 bays. The "tapered" longeron has a 0.590 by 0.590 in. cross-section that begins approximately 4.5 in. from each end, it then tapers to a 0.545 by 0.545 in. cross-section at the ends. The "straight" Longerons are effectively 0.500 by 0.500 in. in cross-section from end to end. The top bay of the Mast uses tapered Longerons to react the launch loads. Longerons are the primary axial and bending moment load carrying elements of the FASTMast structure.

The Rigid Batten Frames, at the top and bottom of each bay, provide transverse and torsional load resistance transmitted to them through the pre-strained diagonals. Each frame has four aluminum corner fittings interconnected by 0.5 in. outside diameter aluminum tubes that has a 0.035 in. wall thickness. The corner fitting has a C-channel cross-section. The height tapers from 1.4 in. at the corner to 0.5 in. at the aluminum tube. The thin profile of the C-channel allows the upper and lower "tapered" longerons to fit close to each other when the mast is stowed. The corner fittings also provide the other pivot point for the longerons to stow and deploy.

The elbow fittings in the FASTMast serve many purposes, several of which were mentioned above. Another important feature is the ability to prevent a failure mode called "elbow fitting rollover". There are interference backstops in the elbow fitting design that prevents the back rotation (i.e., opposite the fold-up direction) of the upper and lower longerons.

A longeron pair can fold next to each other to allow deployment and retraction of the FASTMast. Figure 8 shows how the upper and lower longerons can be thought of as the legs of a card table that fold in perpendicular directions to each other. Longeron pin axis-of-rotation or clocking orientation is also pictured at the elbow fitting locations. This clocking orientation forces the longerons to rotate in one direction. Figure 9 shows Flex-Batten movement during the extension and retraction operations of the mast.
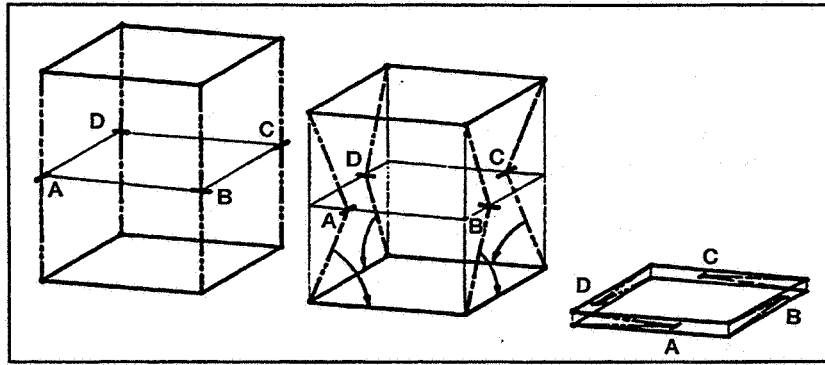
Figure 8. Longeron Movement
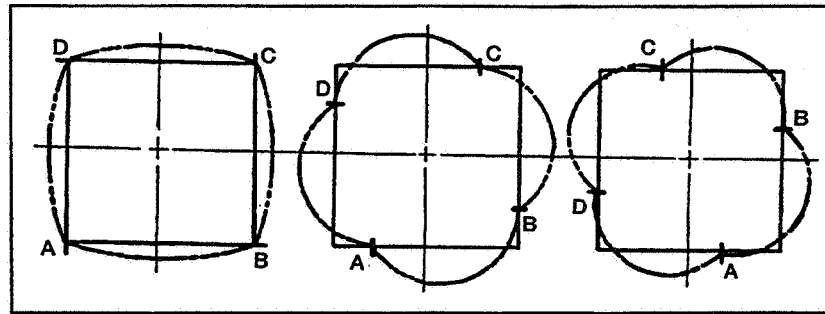
Figure 9. Flex-Batten Movement

FASTMast Deployment/Retraction Operations

The FASTMast can be deployed from a height of approximately 90 in., when completely stowed, to a height of 1296 in., when fully deployed. The figures 10 to 14 will show the mast deployment cycle from the fully stowed to fully deployed condition. It should be noted that this sequence can be reversed at any point during deployment. The mast stowage canister will not be shown.
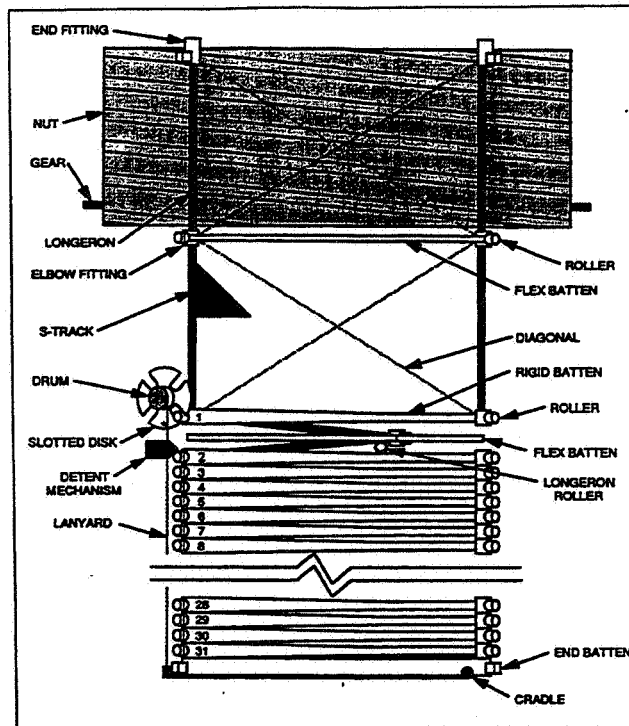
- The first rigid batten corner roller is engaging the slotted disk of the stack advance mechanism.
- The second rigid batten is below the detent mechanism.

Figure 10. Step One: Fully Stowed Mast
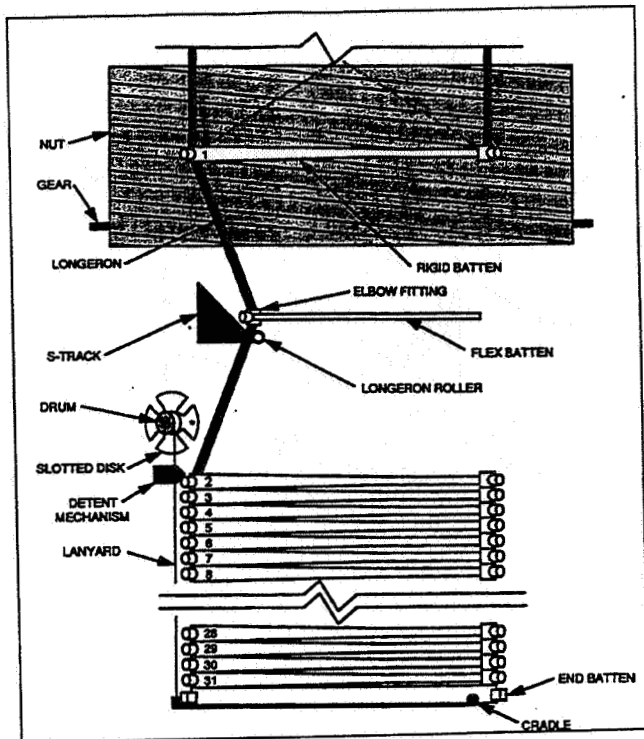
- The longeron roller engages the S-track.
- The stack advance mechanism has rotated one-quarter turn.
- The second rigid batten has not moved yet, it is still below the detent mechanism.

Figure 11. Step Two: First Stowed Bay - Deploying
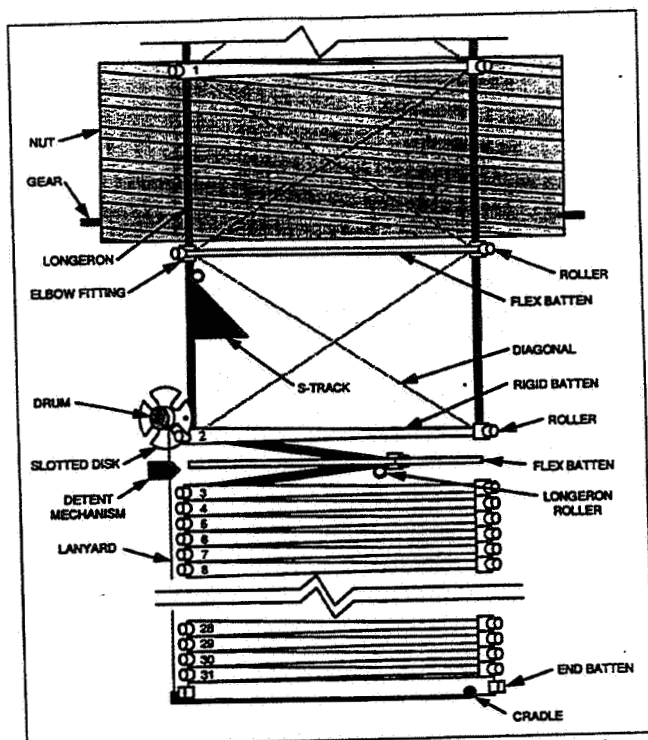
- The second rigid batten corner roller pulls through the detent and engages the stack advance.
- The third rigid batten has not advanced to the detent mechanism.

Figure 12. Step Three: First Bay - Erect

9
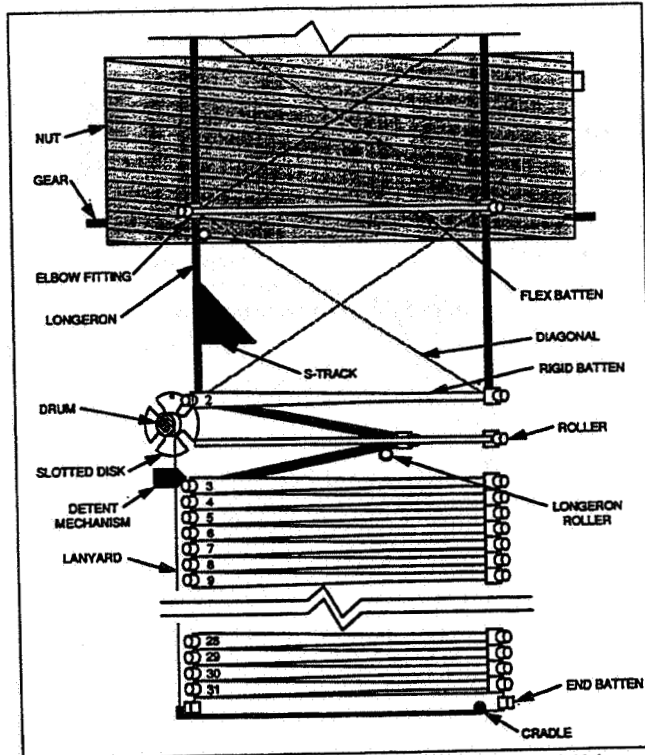
- The second rigid batten actuates the stack advance mechanism (i.e., rotates it 90 degrees and lifts the stowed stack.
- Steps Two, Three and Four repeat until all bays are erect.

Figure 13. Step Four: Next Bay - Deploying
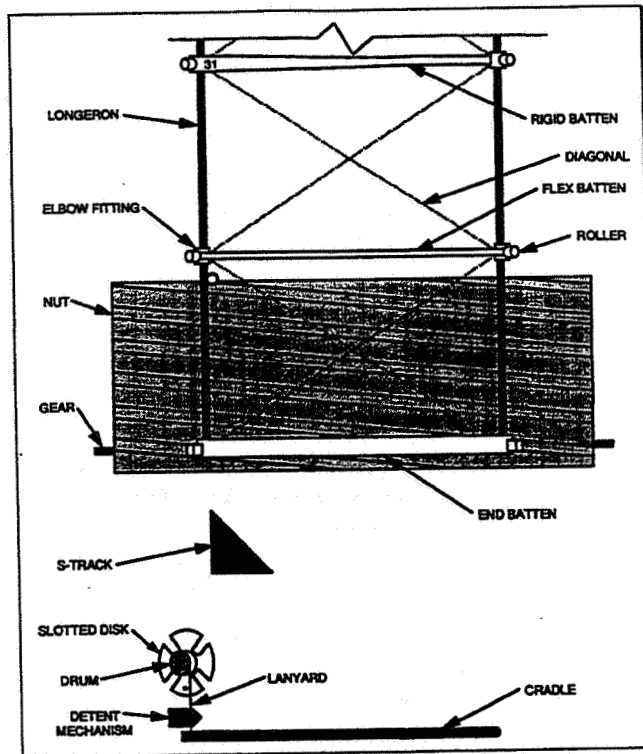
- The end batten separates from the cradle and enters the deployment nut.
- The retraction sequence is the reverse of the sequence shown.

Figure 14. Step Five: Mast - Fully Deployed

10

Load Path Description

The FASTMast is designed to have two nominal and theoretically independent load paths. One load path involves the longerons that transmit axial and bending moment loads. The other load path involves the diagonal cables that transmit transverse and torsion loads. In reality, these load paths are dependent when the bending moment is induced by a large transverse load at the mast tip.

The longerons are loaded in tension or compression when an axial load, a pure bending moment (i.e., a force couple on the mast tip), or a bending moment induced by a transverse load is applied to the mast. Even though the longeron axles, corner fittings, and elbow fittings are all involved in the load path, longeron buckling will limit the ultimate capability of the mast in compression. This failure mode is true only if the elbow fitting is fully stabilized.

The load path for transverse and torsion loads in the mast is much more complicated. The flex-battens are installed in the FASTMast in a post-buckled condition. These battens transmit a force to the rigid battens by evenly preloading the diagonal cables on all faces of the mast. The compressive load on all the rigid battens and flex-battens remains nearly constant and is approximately equal to the flex-batten buckling force, P_{crit}. When a transverse and/or torsion load is applied to the mast, the preload of one diagonal in each face increases and applies a compressive force to the flex-battens. The preload of the other diagonal in the same face decreases.

This transverse/torsion load path continues to work as designed until the unloading diagonal goes slack. At that point, it is conceivable that a compressive load, greater than P_{crit} could be applied to the ends of the flex-battens. The flex-batten has such low stiffness in the post-buckled configuration (~1 lb/in.), it will deflect under even a small increase in the load until an "alternate" load path is activated. It should be emphasized that the "true" batten load remains essentially unchanged from zero applied loads on the mast all the way to the ultimate applied load.

Predicting which path the load will take once the diagonal goes slack is difficult. One possible "alternate" load path forms when transverse load is transferred from one batten frame to the next by bending loads in the longerons. For a given load direction only one of the four elbows is aligned to fold up; two are loaded across the hinge and the fourth rotates backwards until it hits the elbow fitting hard stop. The mast is not designed to accommodate any alternate load paths and will reach ultimate capability fairly soon after it is activated, depending on the applied load combination.

3-BAY FASTMAST TESTS OBJECTIVES AND SCOPE EVOLUTION

In July 1991, Lewis Research Center (LeRC) began an in-house test and analysis program using three (3) bays of the SSF Development Unit #2 (Dev-2) FASTMast Design. The LeRC 3-Bay Test program was initially set up to better understand the strength and possible failure modes of the Solar Array FASTMast. The program evolved to encompass the test and analysis of four principal test series: (1) eccentric axial load, (2) transverse load, (3) combined eccentric axial and torsion loads, and (4) combined transverse and bending loads. Also, the 3-Bay program involved structural analysis at the mast system and component level.

At the beginning of the 3-Bay Test program, the loads specified to the contractor were well within the capability of the mast, as determined by simplified analysis. These hand calculations used empirical data on the local buckling strength of a longeron to determine the bending capability of the FASTMast. The LeRC Structural Analysis Branch had performed independent local buckling analyses using classical and Finite Element (FE) methods and the results were not always consistent with those reported by the contractor. The 3-Bay FASTMast testing was implemented since the SSF program had no planned activity to verify the ultimate strength and failure modes of the FASTMast. Furthermore, as RCS Jet Plume impingement loads continued to increase, the full capability of the mast became more important to determine accurately.

The mast contractor provided a limit load bending strength capability for the FASTMast design. They translated this capability from the ultimate axial compressive load sustained by a longeron. The initial 3-Bay FASTMast longeron test load level was to fall between the advertised ultimate bending moment capability and 90 percent of the theoretical ultimate axial compressive load (i.e., Euler buckling load) of a longeron. The best result hoped for was that no failure would occur up to this maximum test load. Had a failure occurred at or before reaching the maximum test load, it would have been necessary to review the nature of the failure mode and possibly revise the method of calculating ultimate bending capability of the FASTMast. Reference 2 outlined the results of this test. In summary, this test gave good confidence that the 3-Bay FASTMast met advertised strength values based on Euler buckling of a single longeron.

A year after the 3-Bay test program had begun, the experimental determination of the FASTMast capability to resist a transverse applied load became critical in July 1992. This issue came to light when the Level II SSF Control Board approved the latest On-Orbit Loads Data Book (SSP-30800). It was apparent the FASTMast design, developed prior to the release of this document, had near zero margins of safety against shear/torsion internal loads associated with the latest SSF "design to" configuration (i.e., SC-17). The FASTMast resists applied torsion and transverse loads primarily due to the action of the flexible battens. Since the 3-Bay FASTMast Test Program had not planned to exercise this load path, it was deemed prudent to add transverse load testing to the test matrix. The results of these tests are found in reference 3. The test article sustained 120 lb of applied transverse load without an obvious failure, although, an inflection point in the force versus tip deflection curve was observed. At the time, it was unclear what effect the bilinear nature of the system response had on the mast capability.

Another concern of the WP-04 engineers was the unknown effect on the FASTMast capability when bending and transverse/torsion loads occurred simultaneously on the mast. The mast contractors reported that for linear responses of the FASTMast, no load coupling existed between bending and transverse/torsion applied loads due to independent load paths in the design. However, once the mast entered a nonlinear response state, there was no guarantee against failure. The concern was that applied load coupling would alter the anticipated longeron Euler buckling failure mode to a general instability mode involving the entire mast system. Thus, it became incumbent upon the 3-Bay test program to consider more realistic combined loading conditions. The goal of initial combined loads testing was to learn if applied load combinations had an effect on strength capability or failure mode type. The results of the first series of combined loads testing is outlined in reference 4. The test article sustained the combined applied loads of 1600 in-lb torque and the advertised ultimate compressive load in a longeron. No visual indication of system instability was evident during this test.

The next series of tests combined transverse loads with a bending moment until the mast failed, reference 5 describes the results of this test. The test article exhibited no signs of instability when the contractor stated ultimate bending moment was applied in combination with a transverse load in the linear regime (i.e., a transverse load below the inflection point on the force versus tip deflection curve). However, once the FASTMast was subjected to transverse loads associated with a nonlinear response, the application of moment loads did result in a failure mode identified with instability.

Due to the uncertainty of the load levels this structure would encounter in its service life on SSF, it was apparent there was a need to develop the failure envelope for the FASTMast. This could be done by running the appropriate load cases with a correlated FE Model. Reference 6 was the first step in this phase.

The final phase of the LeRC 3-Bay FASTMast test program involved the following activities: (1) identification of failure modes associated with combined load states and (2) the development of an instability load prediction methodology. Nonlinear test and analyses tasks were integrated in an attempt to fully characterize the stability of the structure to a service-like applied load environment. The 3-Bay FASTMast was subjected to a series of individual and combined load types that would invoke responses typical of the on-orbit flight mast. In addition to structural testing, nonlinear FE analyses were performed to support the test activities as well as the development of analytical prediction methodology. A complete description of the final phase of the LeRC 3-Bay FASTMast characterization is presented below.

OVERALL APPROACH TO FASTMAST STABILITY ASSESSMENT

Problem Definition

The 3-Bay FASTMast characterization effort involved integrated test and analysis phases. This resulted in a test verified methodology for identifying failure modes and predicting instability loads. In order to achieve this end, it was very important to design the effort with exercises that would provide insight into the behavior of this fascinating structure. Complex testing and analyses were attempted only after simple response states could be predicted and demonstrated in the lab. Utilizing this approach, a wealth of knowledge pertaining to the FASTMast structure was realized.

The overall objective of the 3-Bay structural characterization effort was to combine test and analysis elements in an attempt to characterize instability failure modes. Furthermore, due to the bilinear nature of the FASTMast structure the 3-Bay effort was further divided into linear and nonlinear assessments. The focus of previous test and analysis efforts was essentially twofold: (1) verification of the contractor specified strength values associated with linear responses, and (2) development of a better understanding of structural behavior. Test and analyses up to

this point in time emphasized simple load states resulting in primarily linear responses. However, as the service load envelope increased so did the likelihood of nonlinear FASTMast operations. The need to better understand FASTMast nonlinear response states required an immediate shift of focus in the 3-Bay structural effort. Therefore, the emphasis during the final phases of 3-Bay testing and analyses would require subjecting the structure to combined load states at levels inducing nonlinear behavior. Also, FE stability assessments would now be required to provide the basis for failure surface development. The need for accurate and reliable FE stability results led naturally to a need for test-verified analytical models. Therefore, the final 3-Bay test and analysis effort would focus on correlation of FE models using results of nonlinear tests that involved the combination of transverse, moment, and torsion loads.

The fundamental redirection of the FASTMast characterization effort given above was motivated by a need to develop stability failure surfaces enveloping FASTMast nonlinear response states. Attempting to test-derive failure surfaces in this case was deemed impractical due to the large amount of required data and the limitations imposed by test hardware availability. Even though the focus of the 3-Bay FASTMast test and analysis task shifted during the final phase, project goals were achieved without expensive modifications to the original plan.

Preliminary Failure Mode Identification

In order to determine the capability of this structure, it was necessary to identify all potential failure modes. The load level at which the structure will fail is a function of its design and the anticipated failure mode. Determination of the maximum allowable loads requires a clear understanding of structural behavior during loading events and identifying the appropriate mode of failure. Once these two goals have been achieved, a valid analytical model can be constructed and the allowable load of the structure can be determined.

From the discussion of the loading environment it is clear that the solar array mast will be subjected to a combined loads state. The moment (M), axial (A), transverse (V), and torsion (T) loads are graphically depicted in figure 15. This figure merely attempts to present a simplified representation of all possible applied loads at a system level. In addition to a material yield, the slender makeup of the mast implies instability is also a possible failure mode. Therefore, load levels associated with stability and yield failure modes were examined in order to identify which is more likely to occur. The results of that investigation clearly identified stability as the most likely failure event for the FASTMast. Once probable failure modes were clearly established, linear and nonlinear failure theories were developed in order to quantify critical load levels.
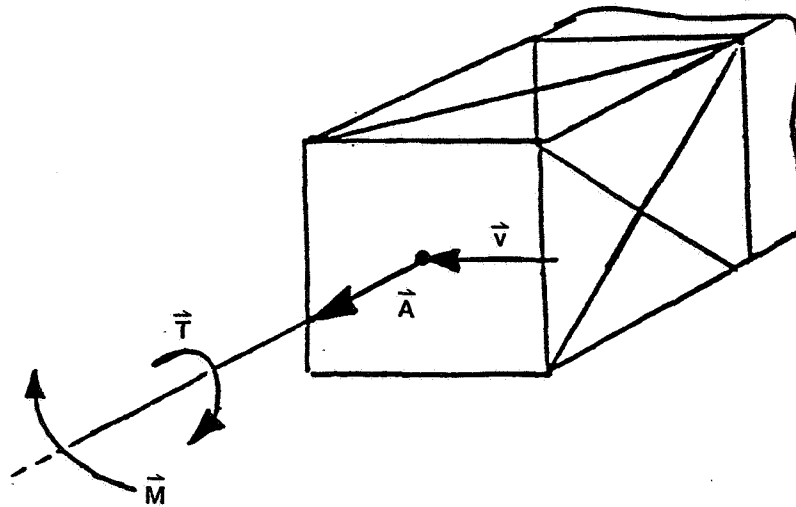
Figure 15. General Schematic of FASTMast Service Loads

13

Unique to this space truss is the fact that as diagonal elements become slack during certain loading events, the stiffness of the FASTMast system is then greatly reduced. The reduction in system stiffness transforms the FASTMast to a nonlinear structure. Kinematic instability involves large displacement of the elbow joints which results in collapse of one or more bays and is associated with a nonlinear system. A second possible failure mode for this structure is Euler buckling of a single longeron which is shown in figure 16. Moreover, as diagonals lose tensile preload the FASTMast system can enter a state of kinematic instability as shown in figure 17. The buckling of a single longeron in this case may also lead to catastrophic collapse of the structure due to a reduction in column compressive strength. The final failure mode of interest for the FASTMast system is that of general instability which involves the solution of the eigenvalue problem for the entire system. Note that Euler buckling of a single longeron and the case of general instability are linear stability problems. Therefore, it was concluded that a complete stability assessment should include linear and nonlinear stability evaluations. The segregation of FASTMast stability assessments into linear and nonlinear components was first presented in reference 7.
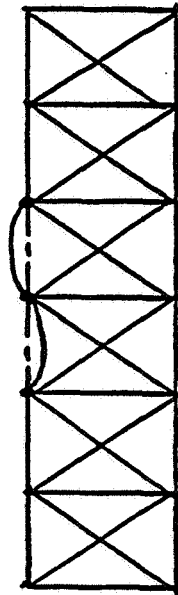
Figure 16. FASTMast Longeron Euler Buckling Failure Mode
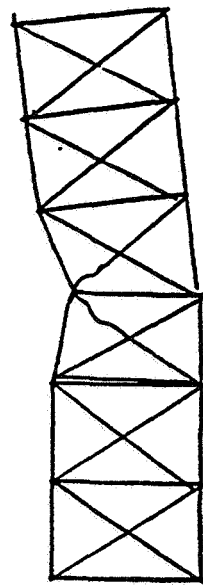
Figure 17. FASTMast Kinematic Instability Failure Mode

14

Linear and Nonlinear Stability Analysis

FASTMast stability assessments have to date included linear and nonlinear stability analyses. Linear stability analysis of the 3-Bay FASTMast has been performed using a variety of failure models. A complete description of the FASTMast linear stability problem and solution is given in reference 8. The FASTMast structure is said to be in a linear state when all of the diagonals are in a state of tension. Initial linear analyses included one-dimensional eigensystems that explored the possibility of longeron and truss panel failure modes. From the knowledge gained during preliminary studies, a three-dimensional FE model was created and general instability was examined utilizing MSC/NASTRAN. Critical buckling loads were generated for a series of FASTMast failure modes and service loads.

Nonlinear behavior of the FASTMast involves system state changes as the structure undergoes large changes in geometry. This phenomenon can be described by demonstrating the reaction of a preloaded mast face to a transverse load. Initially the truss, see figure 18, is preloaded by a force P exerted by the flex-batten. The load P in this case is the critical buckling load of the fiberglass flex-batten. Figure 19 shows the reaction of one face of FASTMast to a transverse load V. Note that for this discussion it is assumed that the transverse load is reacted equally by the diagonals. While the diagonal element is taught, it can react compressive loads by "shedding" tensile preload. As V reaches a value equal to, or greater than initial preload level P, the diagonal becomes slack and the system stiffness of the FASTMast is reduced dramatically. The change in stiffness associated with diagonal slackening is an indication the FASTMast structure has become nonlinear. A nonlinear response of this type can be caused by either a transverse or torsion load state applied to the mast. The development of nonlinear FE models required for stability assessments was the primary focus of the final phase of the LeRC FASTMast effort.

MAST TOP
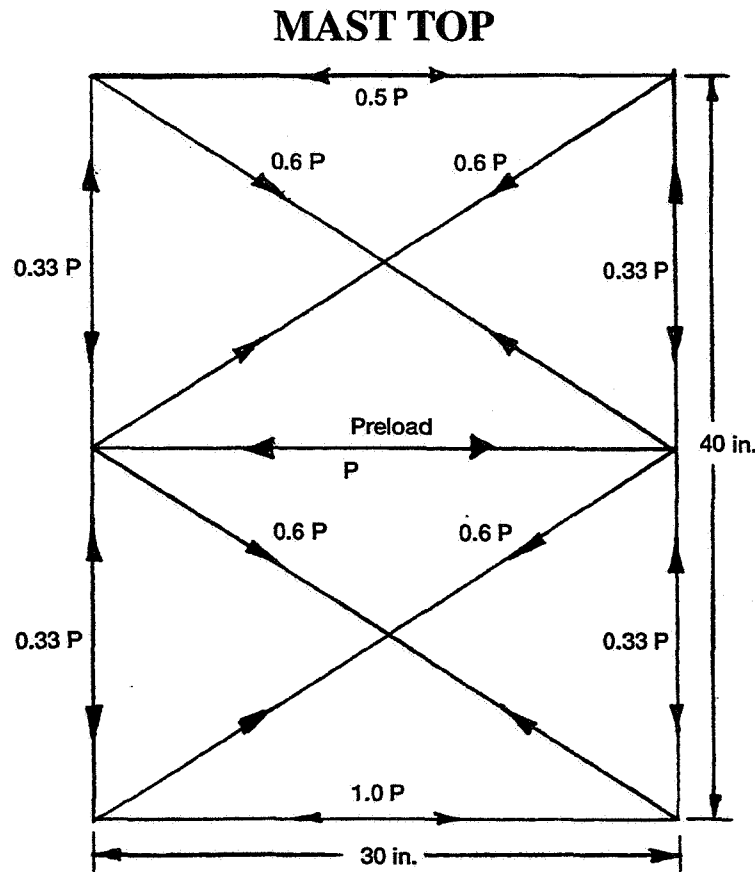
Figure 18. FASTMast Reaction of Flex-Batten Preload (P) in linear state.

MAST TOP
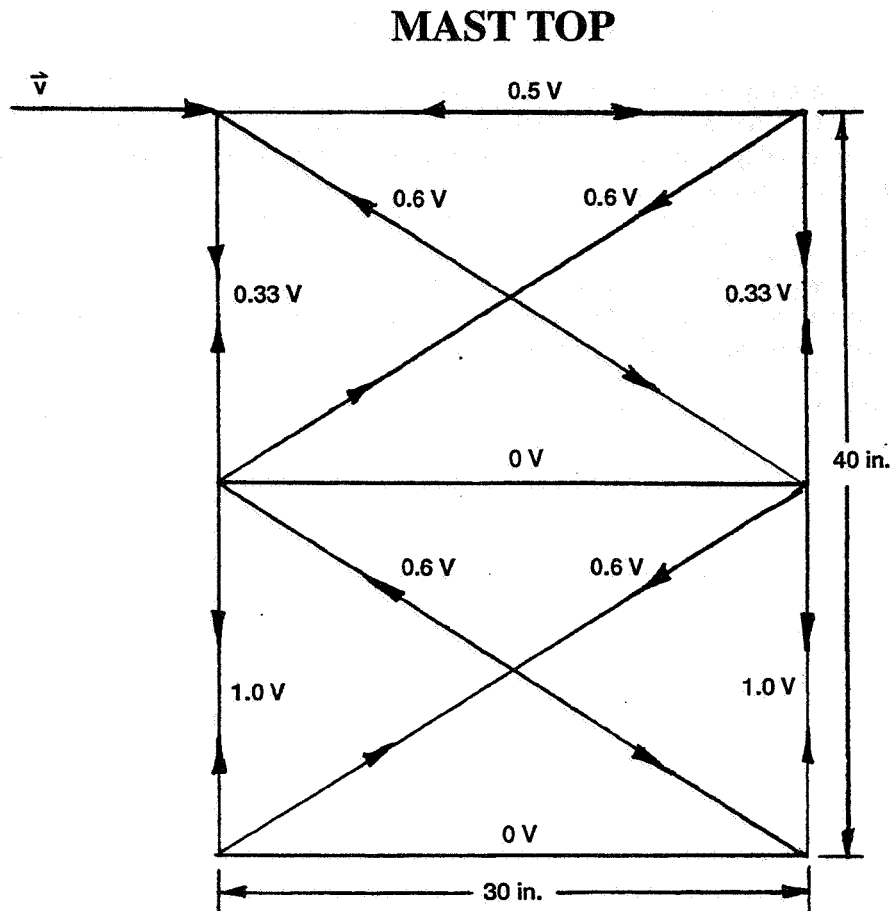
Figure 19. FASTMast Reaction of Transverse Load (V) in linear state.

Combined Load Testing

The general approach for 3-Bay FASTMast testing involved a gradual progression to the loading environment expected during service. Initial testing involved singularly applied loads that would provide insight to structural behavior required for more complicated loading sequences to follow. The need to generate a large sample of failure load data and the lack of test units, dictated a necessity to develop accurate FE models and minimize test article damage. The 3-Bay FASTMast combined loads test and analysis effort was intended to include a combination of mast loading most likely induced by the thruster plume and docking/berthing events. It is clear, from these excitation sources, the mast structure will be subjected to a combination of transverse, torsion, and moment loading. Therefore, the principal objective of this test effort was to generate a test database that could be used to increase the accuracy of FE model stability predictions. Through the process of FE model updating, stability prediction uncertainties are eliminated by judicious use of test data required to improve model performance. Model correlation was deemed absolutely necessary if FE techniques were to yield valid instability load levels. However, the applicability of extending the 3-Bay FE model to represent the flight unit would depend on several factors. The most important concern relative to model extension was thought to be the effect large geometry changes would have on internal load paths. A more thorough discussion involving the relevance of FE model extension is presented later in this report.

In addition to the primary goal of FE model correlation, the combined testing effort was used to focus on other important phenomena. Of considerable interest was the nature of the failure mode itself. Would the mast fail due to general instability of the system or would a local instability such as Euler buckling of a longeron lead to collapse? Another area of concern, which developed early in the test effort, was a lack of understanding of the test boundaries and how they could affect test results. During earlier 3-Bay tests there was some concern that the top plate could be imparting an undesirable load into the top bay. In order to produce structural responses required for successful model correlation the effects of the test boundary must be clearly understood. Therefore, several test sequences were designed to

16

reveal undesirable boundary interactions between the test article and support structure. Other structural performance data to be extracted from this test, included the ultimate axial load capability of a longeron system and a demonstration of failure modes under combined load states. In order to develop and present a clear understanding of mast behavior, it was a belief of the test team that all objectives must be met to a reasonable level of engineering accuracy.

DESCRIPTION OF TEST CONFIGURATION AND PROCEDURES

Test Article

The 3-Bay test article consisted of Dev-2 fidelity hardware. Principal features of this level of hardware maturity include tapered longerons, tapered rigid batten corner fittings, and nonlinear diagonal elements as described earlier. Figure 20 shows Thomas H. Acquaviva standing next to the 3-Bay FASTMast structure that supported combined loads testing. Figure 21 displays a schematic of the critical elements of the test support structure. The interfaces to the test support structure at the top and bottom of the 3-Bay mast reflects flight boundary conditions by using simulated longeron end fittings. Longeron ends at the top and bottom plates had rotational capability about centerline axes that are illustrated in figure 22. The top plate, shown in figure 23, was designed to be much stiffer than the FASTMast thereby minimizing boundary effects and maximizing load transfer into the structure.
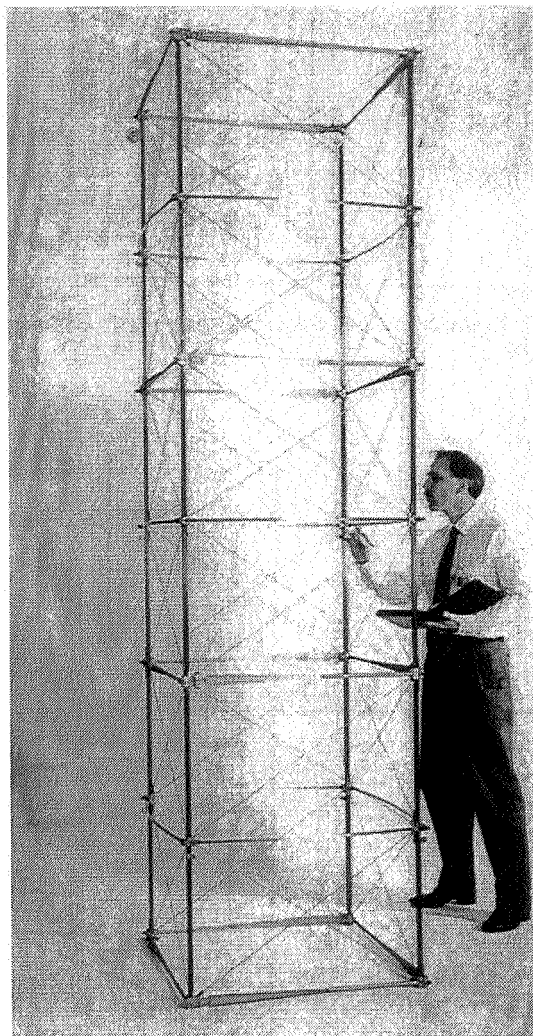
Figure 20. 3-Bay FASTMast Test Article

17
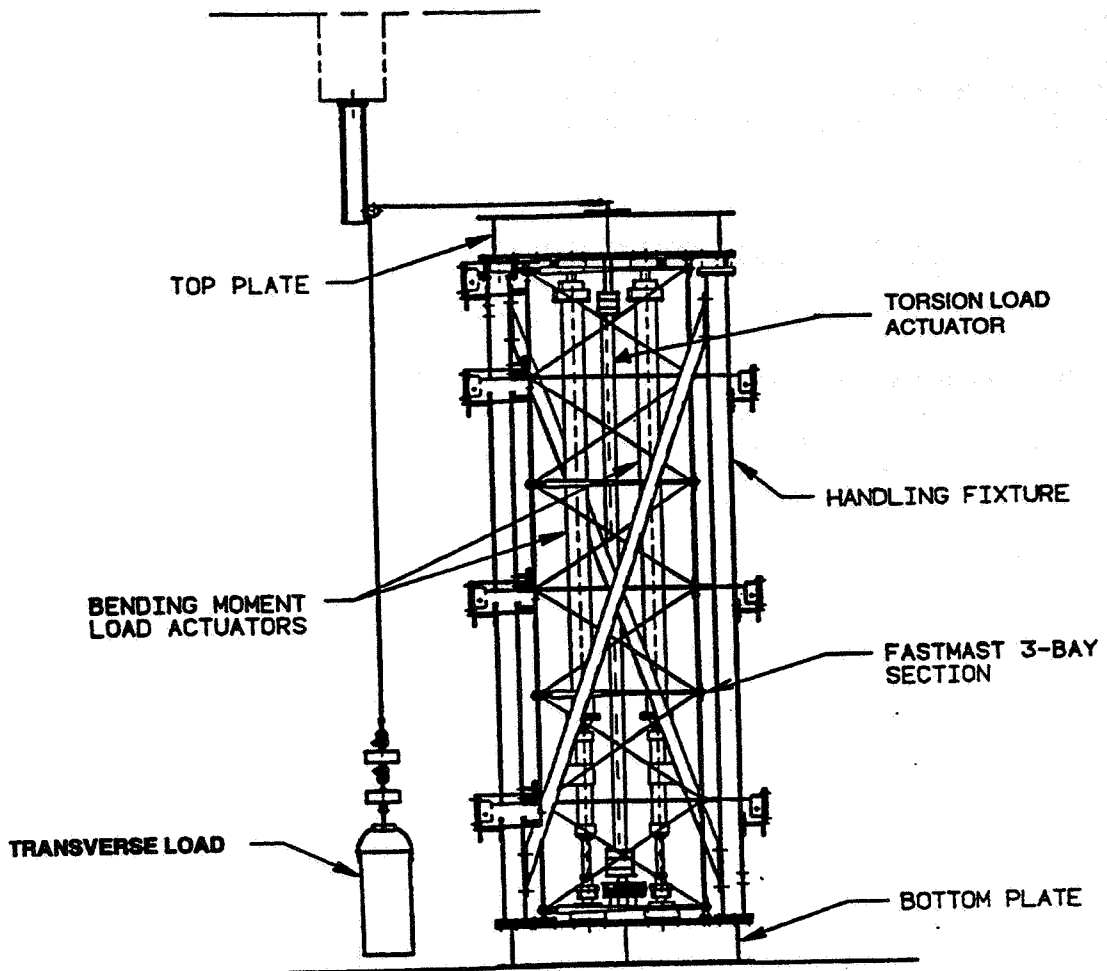
Figure 21. 3-Bay FASTMast Combined Loads Test Setup
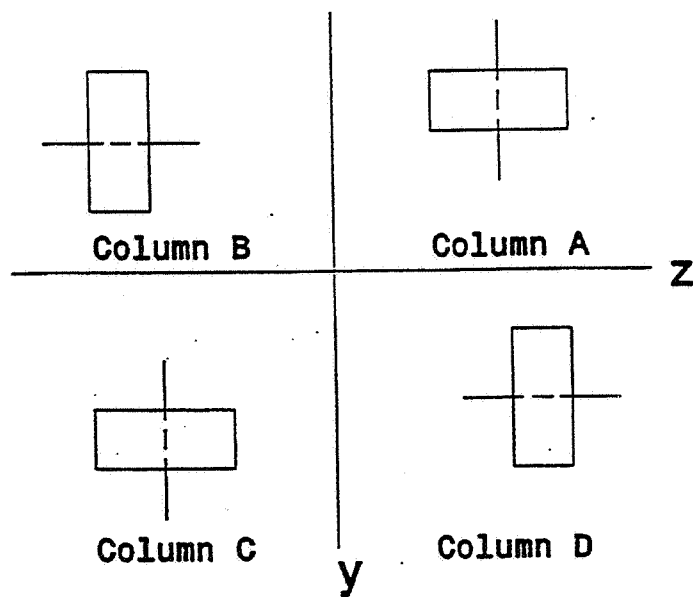
Figure 22. Orientation of FASTMast Elbow Joint Rotation Axes.

18
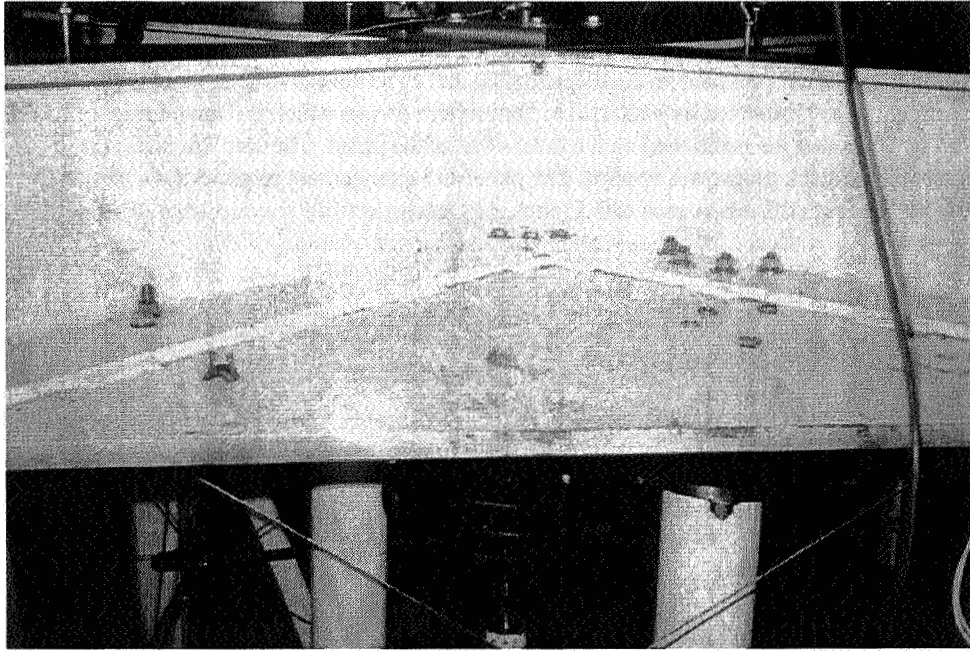
Figure 23. 3-Bay FASTMast Top Loading Fixture Assembly.

Description of Applied Loads and Application Sequencing

Applied loading was achieved through the use of dead-weight and hydraulic systems. The hydraulically driven moment and torsion loading rams are located inside the support frame. Moment loads were generated using hand pumps which energized the tension and compression loading cylinders with application points shown in figure 24. The manner in which moment load was applied to the structure resulted in a ramp profile. Each moment loading cylinder was attached to the base of the support structure using spherical ball joints which decoupled the ram stiffness from the test article during lateral excursions. The manner in which transverse loading is achieved is also shown in figure 24. The load is applied by a cable/weight tray system in a direction 45 degrees from the applied moment load. Desired load levels were achieved by using individual weights ranging from 2 to 20 lb in a combination that provided a "smooth" load profile.
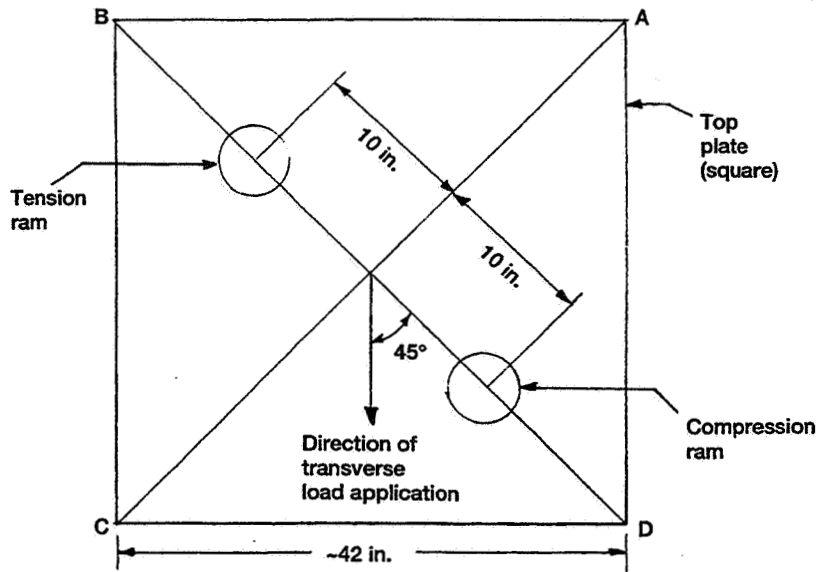
Figure 24. 3-Bay FASTMast Moment Ram Orientation (Top View).

Torsion loading was induced by an electro-hydraulic actuator which drove a load ram positioned at the mast center. A ramp load profile of 10 in-lb per second was developed and controlled by an electronic servo controller. Applying the torsion load in this manner provided an even application and close control of load magnitudes. Undesirable torsion ram stiffness effects were eliminated by a top and bottom fixture design which is shown in figure 25. The steel plates are separated by studs that are positioned on the outer edge of the plates. The stud orientation on a given plate varies by 180 degrees as the stack progresses upward. The plate/stud arrangement provides for a torsionally stiff interface in addition to low bending stiffness at each end. Preliminary testing verified the adequacy of the torque fixture design in terms of its ability to induce torsion loads and avoid undesirable coupling with the test article.
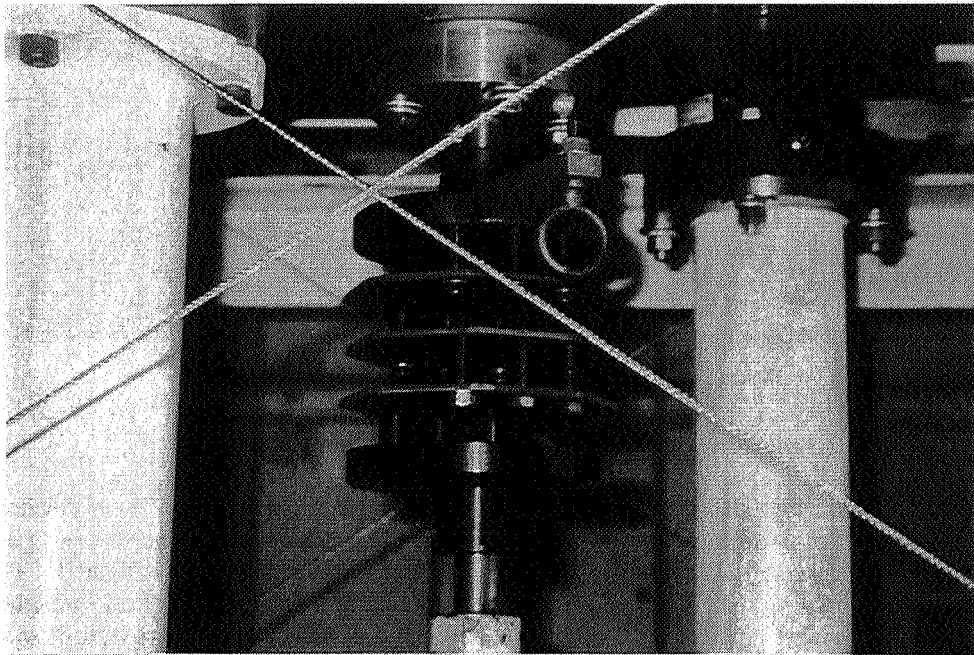
Figure 25. 3-Bay FASTMast Torsion Load Fixture.

The applied load history for this test program reflects the fact that the top priority was acquisition of model correlation data. Only after generation of FE model test verification data was the FASTMast subjected to potentially damaging loads. For cases of combined loading states, individual load types were applied in totality before the structure was subjected to an additional load type. For example, in the case of a combined transverse and torsion load the entire transverse load was applied to the structure prior to the introduction of a torsion load. The sequence of load application is indicated in table 2 by the order of load designation (left-to-right) in the test number.

The first test series involved torsion only loading in order to assess the performance of both the structure and the loading fixture. The manner in which the torsion loads were applied in addition to the large magnitudes, represented new activities relative to 3-Bay FASTMast testing. The torsion load was applied in both directions in order to assess if responses were direction dependent. The data produced during torsion direction studies, in addition to previous test results, revealed little difference in counter clockwise (CCW) and clockwise (CW) torsional stiffness. Therefore, torsion loads were applied to the mast in (CCW) direction for reasons of convenience. Once confidence in the ability to accurately apply torsion loads was established, combined torsion and transverse loads were introduced into the test sequence. In general, tests involving large ratios of torsion to transverse loads were performed later in the sequence due to potential for test article damage.

The next test performed involved a pure transverse load of 120 lbs which provided data to compare to previous test results at similar load levels. Following the completion of the transverse load test, the torsion-only testing levels known to induce nonlinear behavior resumed. The fourth load combination making up this test series involved combined transverse and moment loads. The combination of transverse and moment loads produced test results that could be compared to earlier tests in addition to providing a known failure producing load combination.

Once reasonable confidence was established working with single and multiple applied load states, the 3-Bay unit was subjected to combinations of transverse, moment, and torsion loads. With the completion of the

20

combined transverse/moment/torsion load sequences enough data had been obtained for purposes of model correlation. With all required model correlation data developed, the final test series involving determination of moment-only load capability was carried out. In order to obtain repeatability both columns (D) and (B), see figure 27. Each column was subjected to a moment-only load which caused mast instabilities. The completion of ultimate moment-only testing marked the end of the test program.

Instrumentation

In order to measure the response of the structure, a series of force and deflection measurement devices were installed into the test article system. Instrumentation was placed on parts of the structure critical to stability response measurements. Response parameters of interest included structural deflections, global stiffness, internal and applied load distributions. Deflection data were recorded using string potentiometers. Strain gages were placed on structural elements in order to gain insight into internal load levels and distributions. Load cells for moment, torsion, and transverse loads were used to measure excitation input to the structure. With a good understanding of load application, displacement response, and distribution of internal structural loads, good model correlation was deemed an attainable goal.

Instrumentation used to gather the required test data included the following:

1. 24 string potentiometers for displacement measurement.
2. 44 strain gages monitoring 26 structural elements.
   a. 350 Ohm bridge resistance and 1000 micro-Ohm/volt sensitivity.
3. 30 strain gage conditioners for amplification and bridge completion.
4. Total of 58 data channels.

There was a total of five load cells available to measure the applied moment, torsion, and transverse loads. Instrumentation locations are given in figures (26), (27), and (28). The data acquisition system included analog transducers with a Kiethley A/D converter system. Data reduction software included Labtech Notebook and Microsoft Excel. Reference 9 describes the test setup as well as the instrumentation layout and calibration.
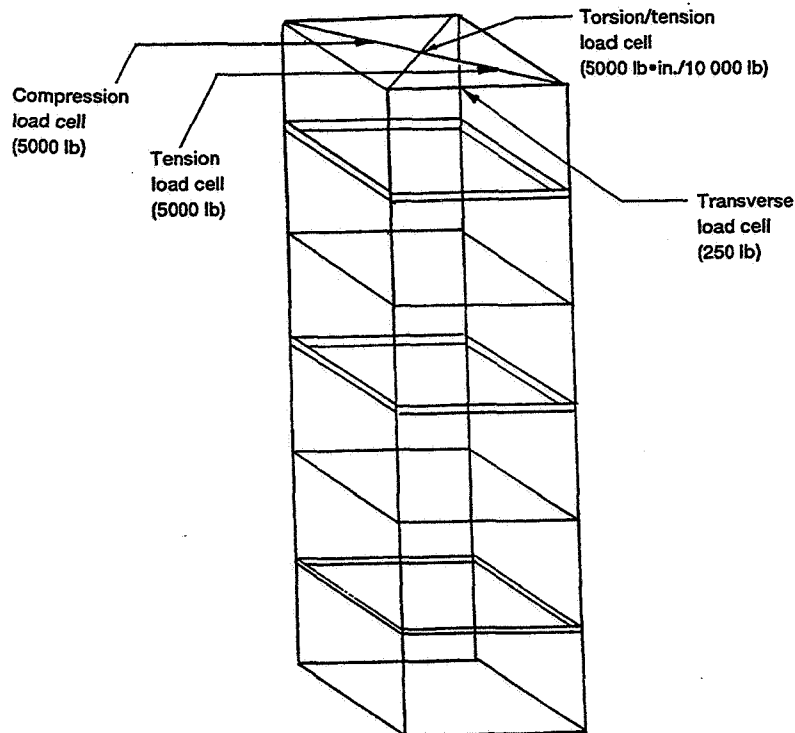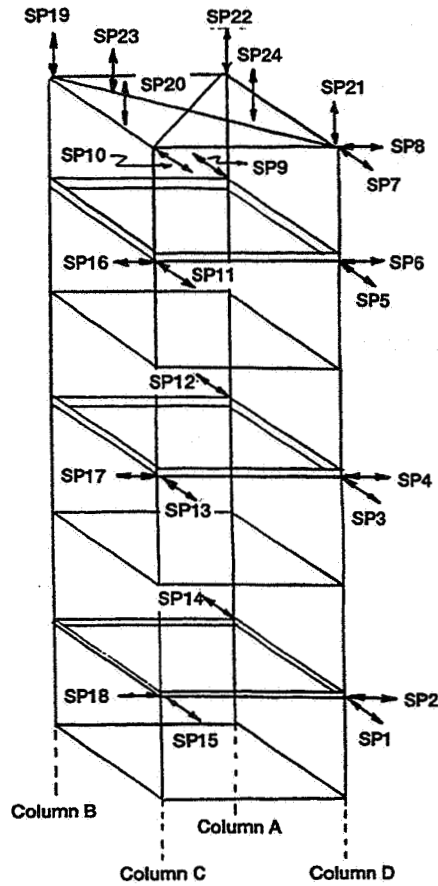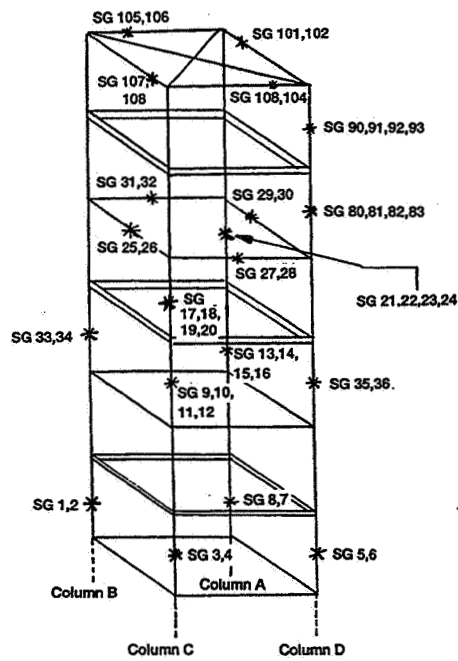

Figure 26. 3-Bay FASTMast Load Cell Locations.

21

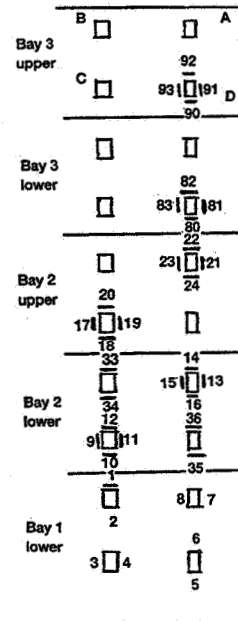**Figure 27.** 3-Bay FASTMast String Potentiometer Locations.

Figure 28. 3-Bay FASTMast Strain Gage Locations.

22

Procedures

The general test procedure included the following elements:

1. Calibrations of the string potentiometers.
2. Calibrations of the strain gages.
3. With the FASTMast unbolted and unloaded, strain gage bridges were balanced.
4. The data acquisition boards were balanced to a zero reading.
5. With the FASTMast bolted down, a visual inspection was made for equilibrium state.
6. The data acquisition system was initiated and "zero" state established.
7. The video camera was positioned and pointed at the expected failure region.
8. Test loads applied to structure.
9. Monitor critical real time load input and response data.
10. Visually monitor test article during load application.
11. If a failure occurred 35mm photos were taken of the failed section.
12. Loads were removed in reverse order of application.
13. Data files were closed and the results processed.
14. Mast was shaken in order to achieve longeron realignment.
15. Initiate a new test if necessary.

After each test was completed, the mast was inspected for structural degradation that could compromise future test data. The mast was examined visually for structural yielding. Diagonal tensions were examined qualitatively by plucking and determining if the pitch was uniform throughout bays. The unloaded state was also examined in order to determine if it had returned to its original shape. Finally, all engineering notes gathered during the test were assembled, discussed and documented for future reference. A complete description of the test configuration, loads, instrumentation, and procedures can be found in reference 9.

PRE-TEST NONLINEAR ANALYSES

Analysis Approach

The development of valid analytical models required to support the 3-Bay FASTMast effort was considered paramount to the overall success of the program. Although there was limited use of two-dimensional models for theory support, three-dimensional nonlinear FE models served as the activity foundation. Using available test and design data, a preliminary model was developed utilizing the commercial code ANSYS. The ANSYS nonlinear FE model was used to generate all pre-test predictions of the mast response under the expected loading conditions. The ultimate goal of model development was to capture the nonlinear nature of the structure while minimizing computational requirements.

Analytical characterization of mast stability for nonlinear events is much more complicated than that required for linear mast states. Nonlinear stability assessments involved performing large displacement analyses which accounted for nonlinear geometry effects. Pre-test nonlinear analyses were performed using a three-dimensional ANSYS FE model of the 3-Bay structure. Due to the hybrid nature of the FASTMast structure it presents an immediate modeling challenge. Of particular concern was obtaining an accurate representation of diagonal and jointed elements of the structure. Phenomena such as joint friction and wire rope nonlinearities presented obvious shortcomings during the initial nonlinear FE modeling efforts. The availability of test data provided an opportunity to update areas of the nonlinear model that possessed modeling uncertainties. The ANSYS FE model was correlated to test data in order to produce 3-Bay test-verified stability predictions. Furthermore, it was felt that after a successful correlation effort the 3-Bay FE model could be extended to 32-bays if internal load symmetry could be shown to exist. Upon successful completion of model expansion, stability results for the FASTMast flight unit could then be generated.

Nonlinear Model and Analysis Description

Both the pre-test and final ANSYS models represent the Dev-2 FASTMast hardware design. Hardware design properties were derived from engineering drawings or information provided at the numerous design and

status reviews held during FASTMast development. There are several differences between the Dev-2 and flight hardware and they are discussed later in this report. The initial ANSYS model contained 292 nodes, 300 elements, and an estimated 1332 active degrees of freedom (DOF's).

The longerons were modeled as straight members with a 0.59 by 0.59 in. square cross-section. Although the longeron possesses a taper, its effect on kinematic motion of the elbow joint, and therefore nonlinear behavior of the mast, was deemed minimal. Furthermore, including the taper at this point would have increased the model size, thereby placing undesirable restrictions on required pre-test analyses. It should be noted that the cross-section given above represents the largest of the Dev-2 longeron. Each longeron was modeled using one three-dimensional beam element. The rigid batten frame was modeled using a three-dimensional tapered beam element for the corner fitting and a three-dimensional truss element representing the batten tube. All diagonal elements were modeled using a linear two-dimensional tension only spar, this aspect of the model represents the second simplification. The Dev-2 diagonal stiffness is nonlinear as shown in figure 29. The linear stiffness used for preliminary modeling was that of an equivalent constant section cable reported by ABLE Engineering early in the design effort. Each fiberglass flex-batten was modeled using ten three-dimensional beam elements. In order to represent the flexibilities at the elbow and corner fittings nonlinear hinge elements were introduced to these parts of the structure. At each elbow joint there are four hinge elements (one at each longeron and flex-batten end) and at each corner fitting there are two hinge elements (one at each longeron end). At each longeron end there is a hinge that allows for ninety-degree rotation plus a 0.6 degree over-rotation required to model stopping action of the deploying mast. As the elbow joint achieves the 0.6 degree over-rotation, the joint is no longer free to rotate and behaves as a torsional spring with a very high torsional stiffness. Also included in the hinge element is a test-derived translational stiffness of 4.3×10^5 lb/in. in the direction along the length of the longeron. The hinges on the flex-batten ends do not have rotational limits and possess a very high translational stiffness.
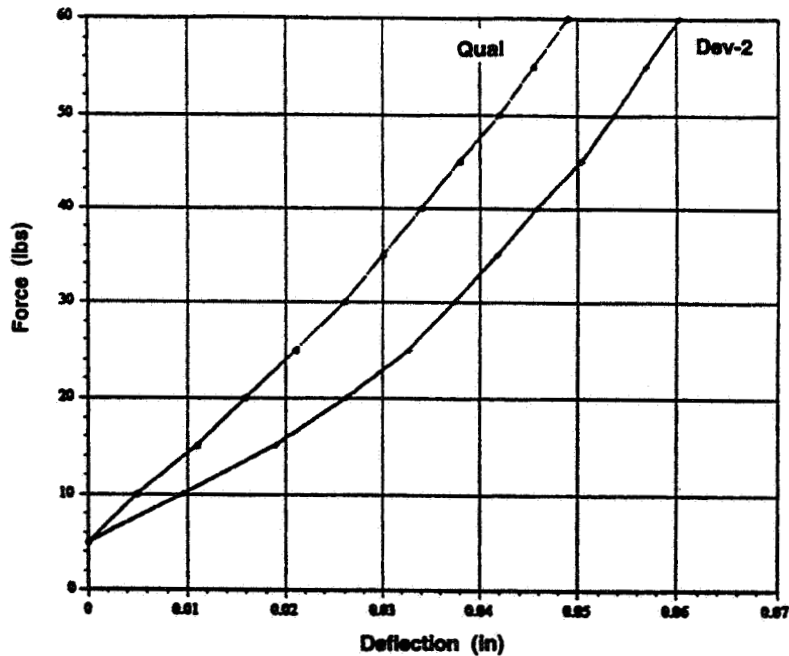
Figure 29. FASTMast Diagonal Stiffness Curves (Dev-2 and Qualification Hardware).

Pre-test analysis data was used to guide the test procedures and prevent undesirable structural damage. Since this test series was to involve nonlinear structural behavior, pre-test analysis consisted of a regiment of large displacement analyses. A summary of the loading histories for pre-test analyses can be found in table 1. The magnitude of each applied load corresponded to a planned test applied load level. Some deviations from initial planned test levels did occur principally due to unforeseen and potentially damaging structural behavior.

24

TABLE 1.—3-BAY FASTMast PRE-TEST ANALYSIS SUMMARY

TRANSVERSE LOAD (V) (LBS)	MOMENT LOAD (M) (IN-LB)	TORSION LOAD (T) (IN-LB)	KNEE VALUE
120	0	0	V=100 LB
0	180000	0	NONE
0	0	3800	NONE
140	0	600	V=90 LB, T=600 IN-LB
140	0	1200	V=75 LB, T=1200 IN-LB
40	0	2700	V=40 LB, T=2200 IN-LB
60	0	2100	V=60 LB, T=1590 IN-LB
80	0	1600	V=80 LB, T=970 IN-LB
0	40000	2000	NONE
0	80000	1400	NONE
40	80000	1000	NONE
60	50000	2500	V=60 LB, M=50000 & T=1600 IN-LB
70	40000	2000	V=70 LB, M=40000 & T=1300 IN-LB
80	50000	400	NONE
70	60000	2500	V=70 LB, M=60000 & T=600 IN-LB

The nonlinear large displacement static analyses were performed using ANSYS 5.0. The data recovery items for pre-test analyses included member forces, displacements, and strains at or near instrumentation locations on the test structure. Instability was not developed analytically, even though the mast did transition into the nonlinear phase for several pre-test load states. During the analysis, the inability to converge from one phase of static equilibrium to another would indicate unstable behavior of the structure. In addition to the convergence criteria, valid instability states were also required to involve acceptable model behavior. During these analyses, proper model behavior was evidenced by development of kinematically admissible displacement states prior to the lack of convergence. Although nine out of fifteen pre-test analyses runs involved excursions into the nonlinear regime, there were no cases of instability. This was consistent with the overall test approach which involved the acquisition of data required for model correlation and not test derivation of a failure surface. Typical displacement curves that were used to assess structural behavior are shown in figures 30 to 32. When possible, the pre-test data was compared with earlier 3-Bay FASTMast test results. The overall assessment of pre-test results, including comparisons against existing test data, revealed the model behaved well despite being overly stiff.
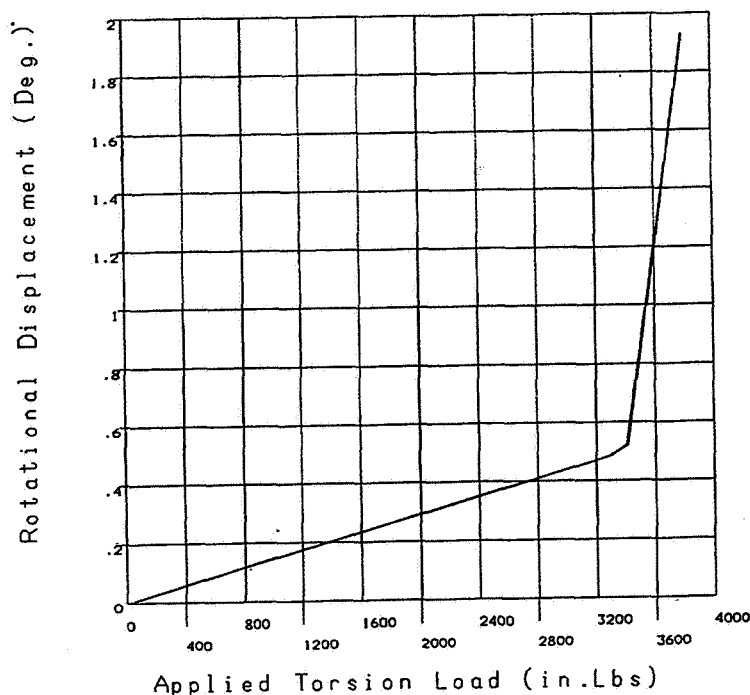
FAST-MAST, PURE TORSION

Figure 30. Pre-test Prediction for 3-Bay FASTMast Top Plate Rotation Due to Pure Torsion Load.

SP10

SP7

FAST-MAST. COMBINED SHEAR & TORSION. Constant Torsion load = 1200 in.Lbs

FAST-MAST. COMBINED SHEAR & TORSION. Constant Torsion load = 1200 in.Lbs
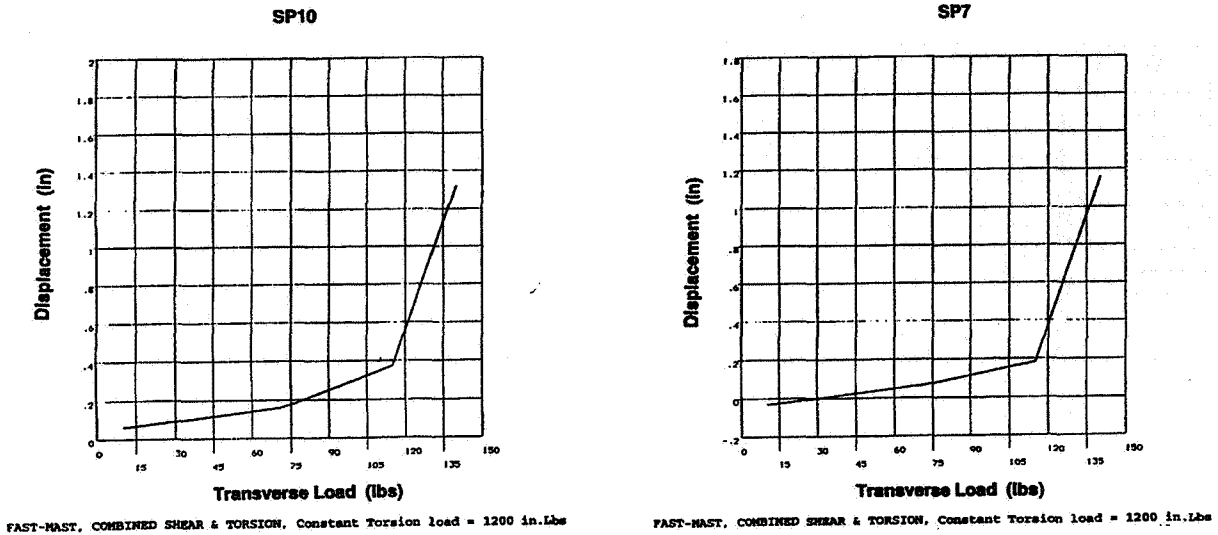
Figure 31. Pre-test Prediction for 3-Bay FASTMast Top Lateral Displacement Due to Transverse Load.

SP7

SP10

FAST-MAST. COMBINED SHEAR. MOMENT & TORSION. S=60 Lbs. M=50000 in.Lbs

FAST-MAST. COMBINED SHEAR. MOMENT & TORSION. S=60 Lbs. M=50000 in.Lbs
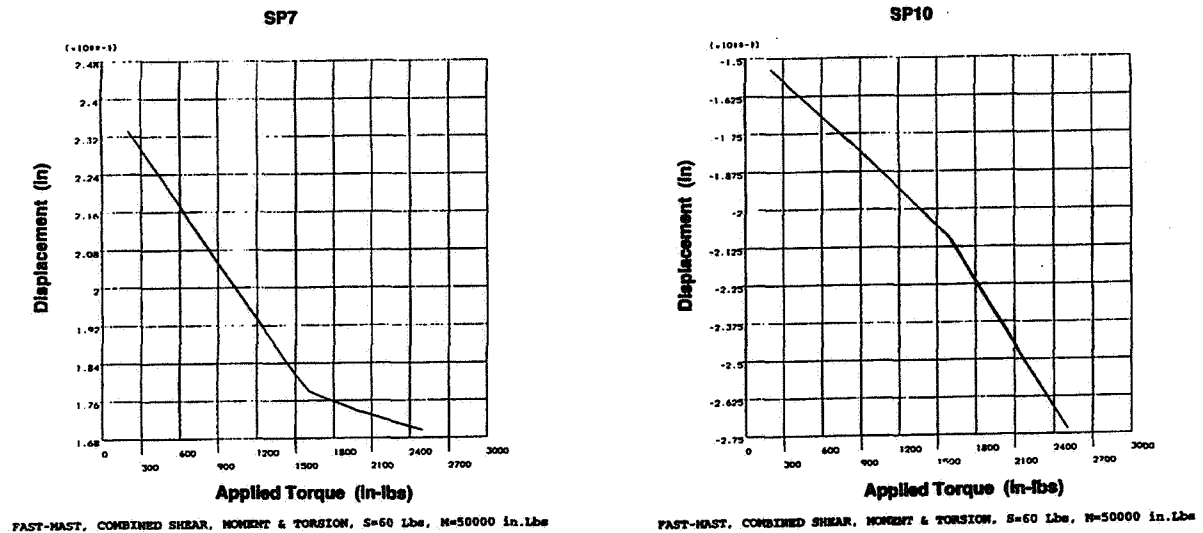
Figure 32. Pre-test Prediction for 3-Bay FASTMast Top Displacements Due to Combined Transverse/Moment/Torsion Load.

DISCUSSION OF TEST RESULTS

Pre-Test Evaluation of Test Article Damage

In order to assess the structural fitness of the 3-Bay test article, several pre and post-test integrity measurements were incorporated into the test process. Pre-test examination of the structure included visual inspections and elbow joint stiffness testing. Post-test mast health was assessed by performing flex-batten stiffness testing, comparing test results to earlier test data, and determining final longeron straightness tolerances. The goal of this segment of the test effort was to identify and eliminate the possibility of mast damage that could cause spurious test results.

The visual inspection being the easiest to implement was the first inspection performed on the mast. Of particular concern were regions that had been exposed to the effects of rapid mast folding failures during the combined transverse/moment load testing performed in 1993. Due to the fact that the failures occurred in the top bay, these members were inspected first. Visual inspection of this area revealed no startling evidence of damage. However, diagonals anchored at elbow joints with a folding direction in the plane of the diagonal, appeared to possess a larger tensile preload. The opposite diagonal in the same face tended to be less taut and the subsequent

26

variation of diagonal preloads existed throughout the mast. A qualitative assessment of this variation was made by plucking each and listening for pitch variations. Longeron straightness was also visually examined by sighting down a column from a vantage point near the top of the mast. Column misalignment did not appear to be detrimental.

The next area of consideration included the stiffness characterization of the elbow joint region. Understanding deficiencies in this region is essential since transverse and torsion load resistance is heavily influenced by this part of the structure. The elbow joint stiffness test was performed with the device shown in figure 33. Relative deflection between the two end points of the test device are recorded in addition to the load required to affect that translation. This test, shown in figure 34, was performed on elbow joints installed in the mast. Test results obtained for three mast locations were compiled and compared to an identical test performed in July of 1992 and documented in reference 9. Note that 1992 stiffness testing was performed on a 3-Bay unit which had not been loaded to a point of instability. The force-displacement curves from the 1992 and 1994 stiffness tests are given in figures 35 to 37.
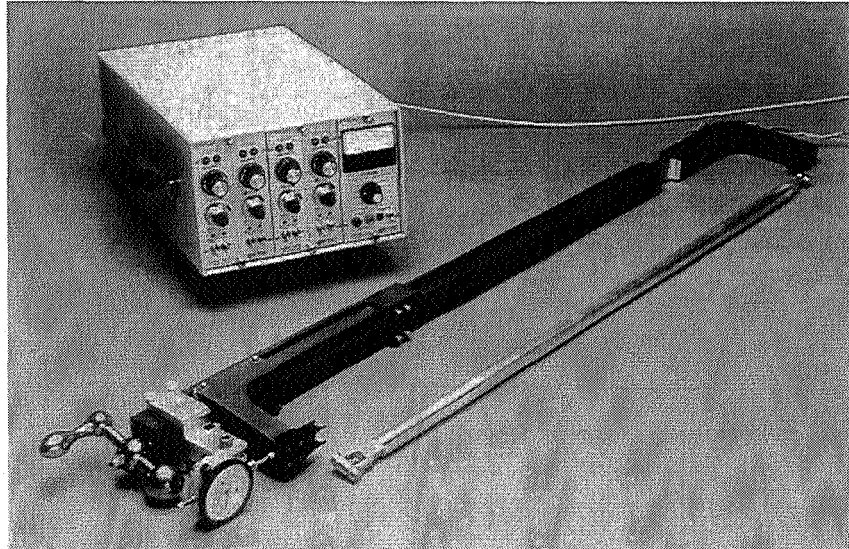
Figure 33. Elbow Joint Stiffness Testing Device.
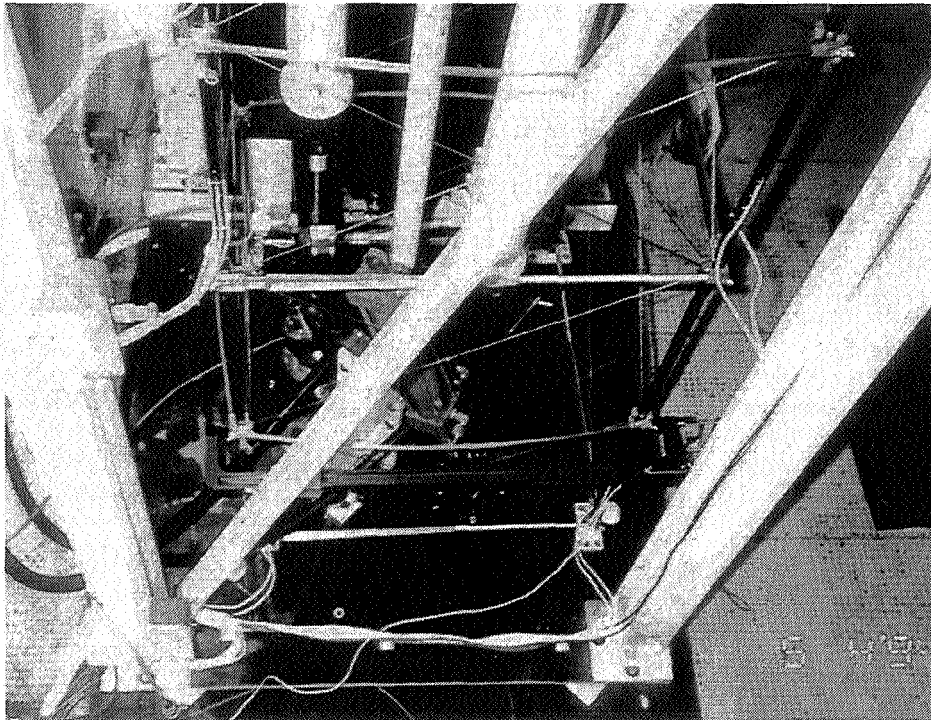
Figure 34. Elbow Joint Stiffness Device Test Installation (Typical).

27

BATTEN A-D BAY 1 RUN 1; 7/21/92
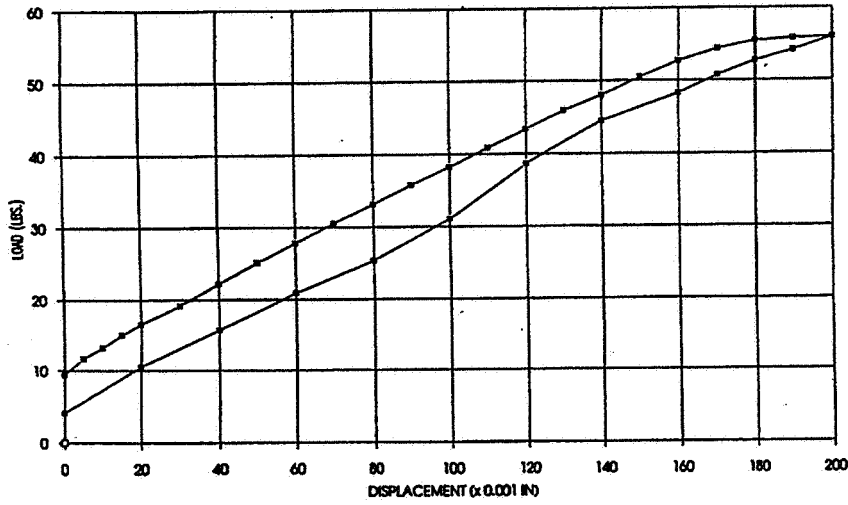
**JULY 1992 ELBOW JOINT
STIFFNESS TEST**

FLEX BATTEN - BAY #1 - D to A
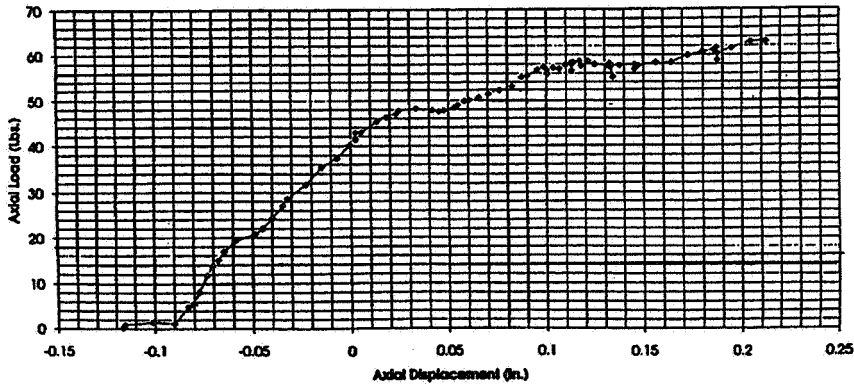
**AUGUST 1994 ELBOW JOINT
STIFFNESS TEST**

Figure 35. Comparison of Elbow Joint Stiffness for 3-Bay FASTMast Damage Assessment (Bay 1/Face AD)

28

BATTEN A-D BAY 2 RUN 2; 7/21/92
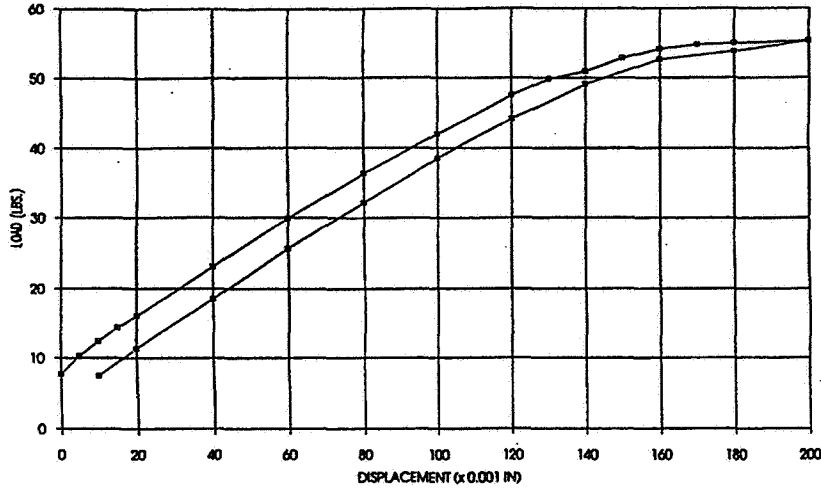
JULY 1992 ELBOW JOINT
STIFFNESS TEST

FLEX BATTEN - BAY #2 - D to A
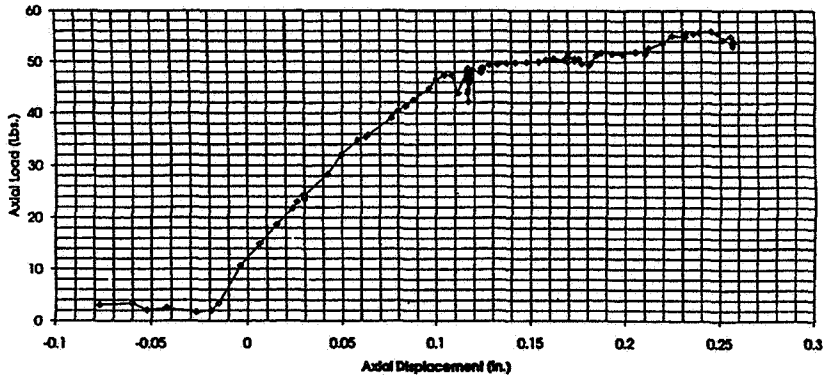
AUGUST 1994 ELBOW JOINT
STIFFNESS TEST

Figure 36. Comparison of Elbow Joint Stiffness for 3-Bay FASTMast Damage Assessment (Bay 2/Face AD).

BATTEN B-C BAY 2 RUN 1; 7/21/92

JULY 1992 ELBOW JOINT STIFFNESS TEST

FLEX BATTEN - BAY #2 - B to C
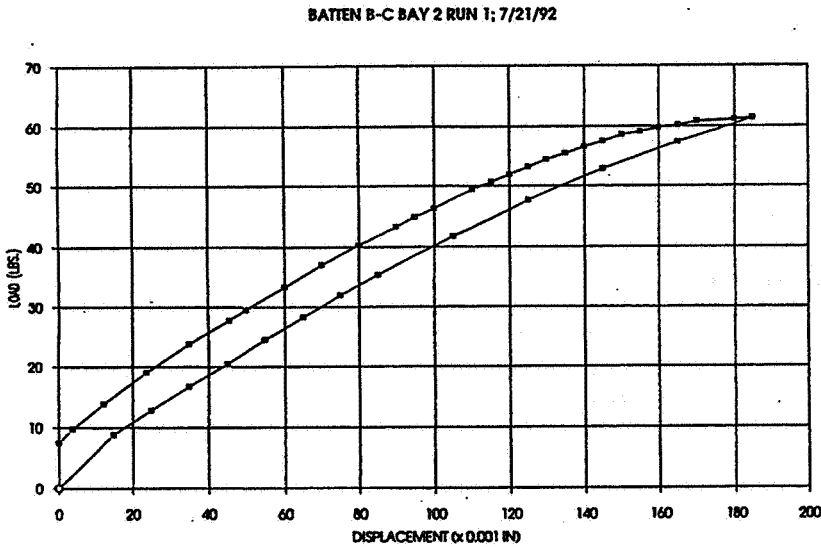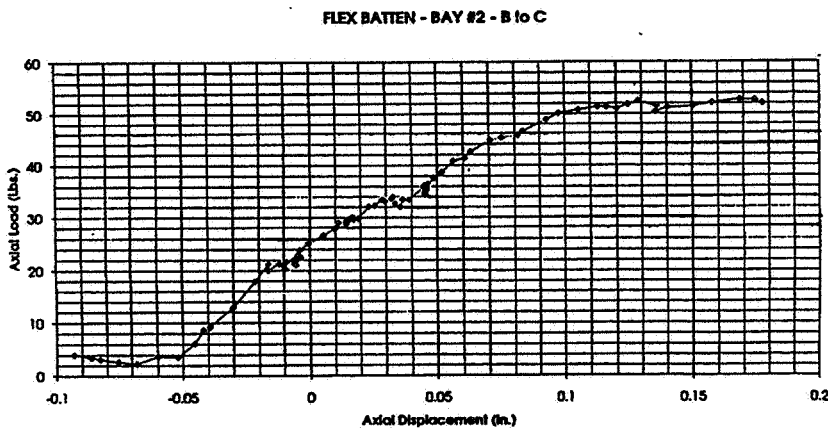
AUGUST 1994 ELBOW JOINT STIFFNESS TEST

Figure 37. Comparison of Elbow Joint Stiffness for 3-Bay FASTMast Damage Assessment (Bay 2/Face BC).

The first interesting result that is extracted from these curves is the nonlinear nature of the elbow joint stiffness. This is consistent with the fact that the stiffer load path offered by the prestrained cables is a nonlinear wire cable. A measure of the relative stiffness between the two structures can be defined by the maximum load each mast reached prior to large decreases in the stiffness curve slope. In general, when decreasing slope occurs at a larger axial load, this indicates larger elbow joint stiffness. Although the response curves for both tests compare well, the test article of 1992 possessed an elbow joint that offered greater stiffness. Bay 1 is the only exception to this trend, see figure 35. It appears the current test article elbow joint stiffness eclipsed that of the previous test by 3 lb/in. However, the irregular nature of the 1994 stiffness curve for bay 1 cast some doubt on the validity of the data. Positioning the tension test device for the 1994 test was difficult due to the support structure and may have compromised the test results. Providing comparisons to other mast faces was desirable but the 1992 test data was limited to the three positions, reflected by figures 35, 36, and 37.

In general the mast testing was divided into three fundamental phases: (1) pre-test assessment of test article viability, (2) development of linear and nonlinear response data required for model correlation, and (3) structural tests at failure load levels for failure mode investigations. Each of these test phases was deemed critical to the success of FASTMast structural characterization effort and is discussed below. A complete summary of the test results can be found in reference 9.

30

Post-Test Evaluation of Test Article Damage

To thoroughly investigate the possibility of existing test article damage combined loads test data was used to identifying structural anomalies. Of particular interest was the validation of assumed applied loads and load paths. Verifying the pre-test assumptions was accomplished by evaluating test data.

The first step in the assessment of structural performance was to determine if the applied loads were imparted to the structure as required by test design. Figure 38 illustrates a typical moment load history for the tension and compression rams. Although hand pumps were used to develop the necessary hydraulic pressure, the load curve is smooth and even over the entire range of applied loads. Mast top deflections under a moment-only load given in figure 39 indicate a smooth and even displacement profile. The distribution of a moment load into the structure can be examined by evaluating the axial load response in the longeron. Shown in figure 40 are strain gage readings from the tensile and compressive longerons for a moment-only load. This data shows favorable tensile load distribution with some bending occurring at the base of the mast on the compressive leg. The longeron load curves in figure 41 have been normalized to represent the axial load as if the longeron assemblies in columns (D) and (B) were located at the position of the hydraulic rams. The actual axial load in the longerons is much lower as revealed in figure 40. The data presented in figure 41 confirms an uneven distribution of the internal axial load at the base of column (D). This may have been the result of test article damage.

Evaluation of the torsion load input was made by examining the compressive loads in the rigid battens shown in figure 42. The curves show an evenly applied torsion load until the load magnitude increases to a point near the mast nonlinear response state. The erratic rigid batten frame behavior during nonlinear response state is associated with "bowing" outward of the batten tube.
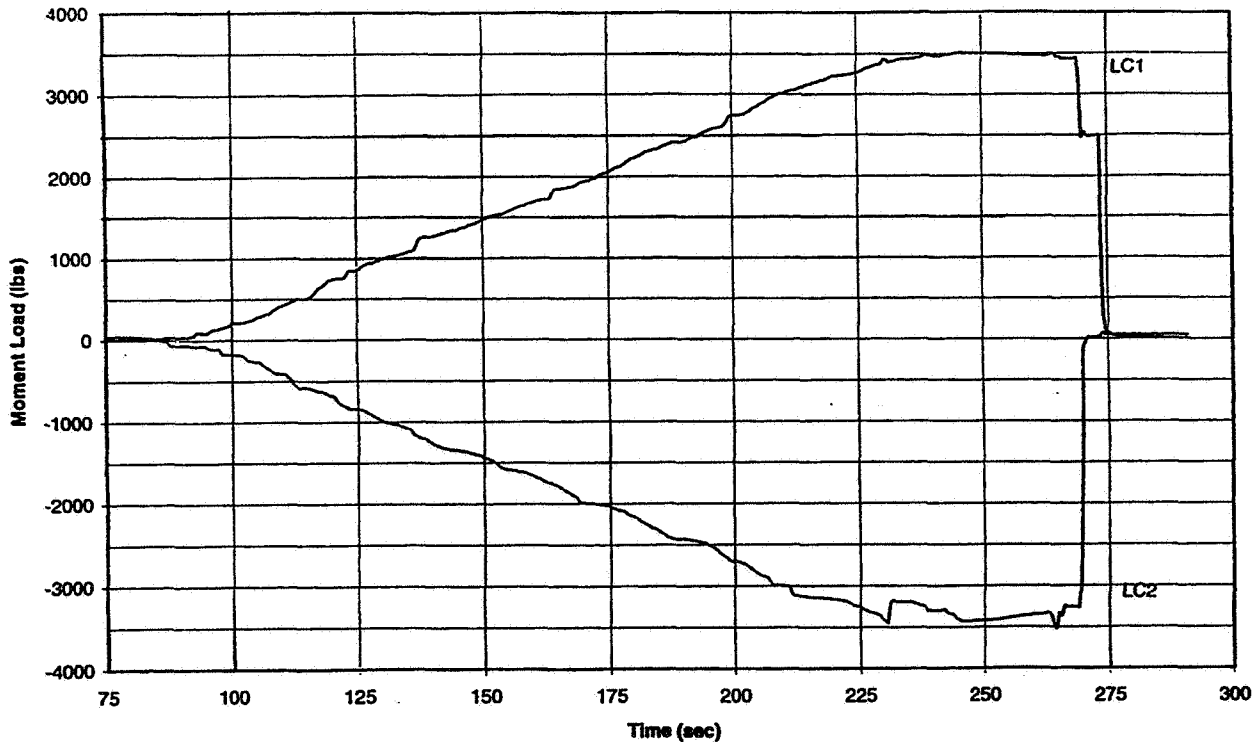

Figure 38. Moment Load Cell Recording During Pre-test Check.
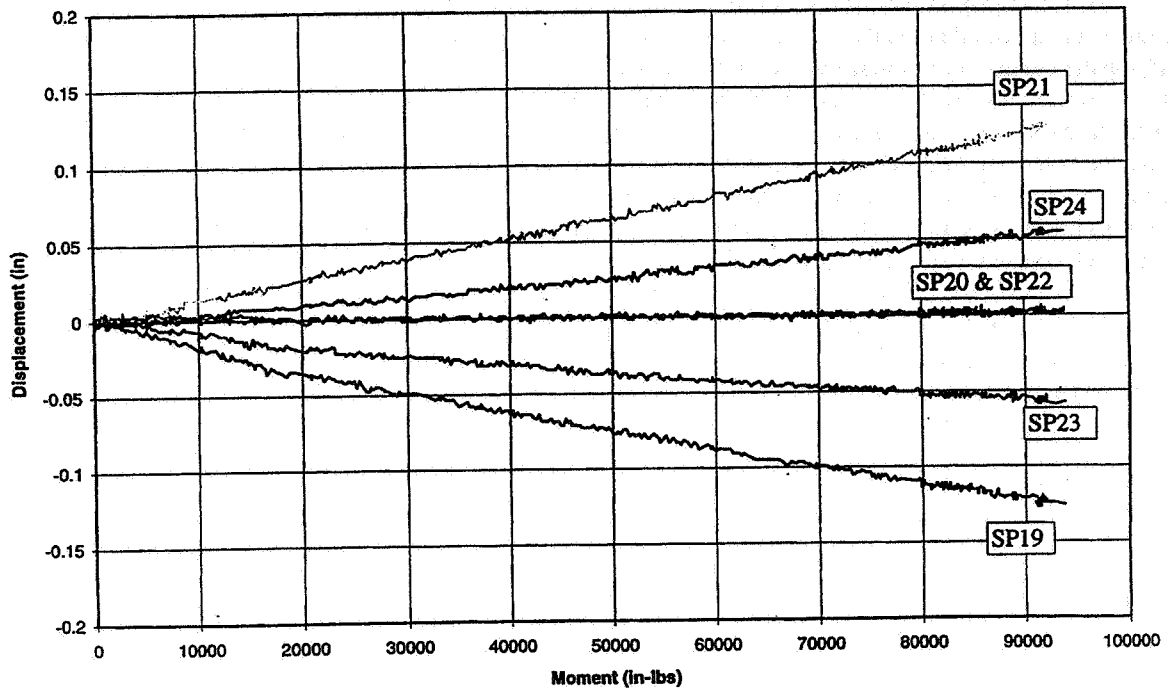
Figure 39. Vertical Displacements at 3-Bay FASTMast Top for Test (M1).
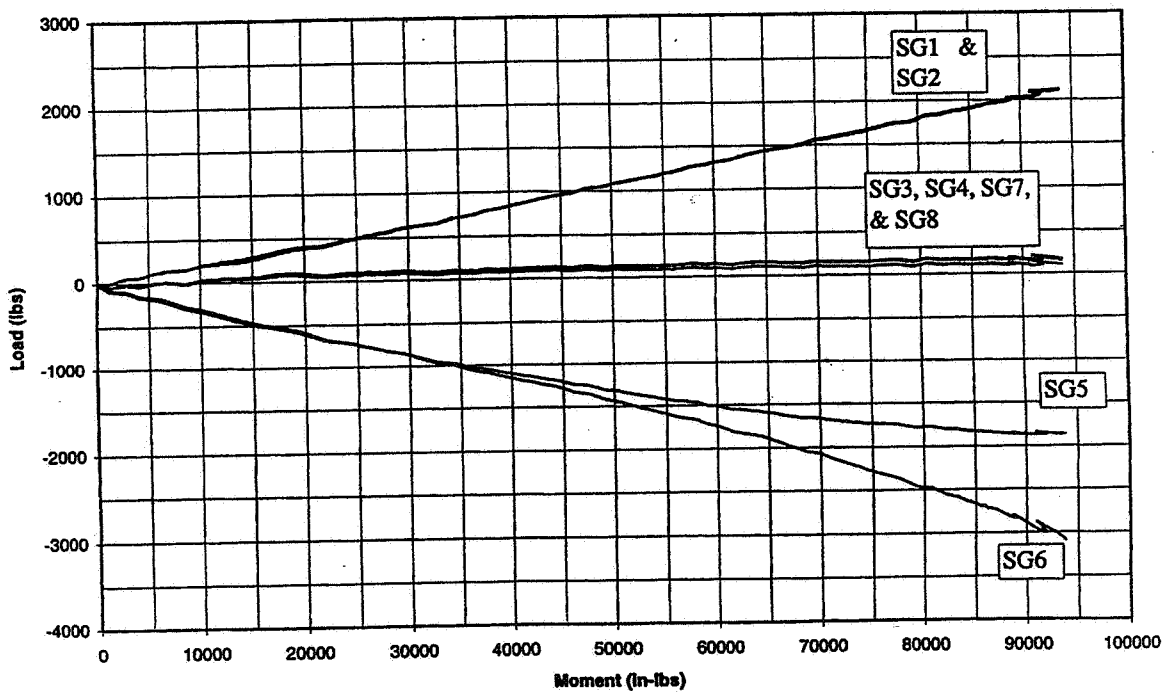

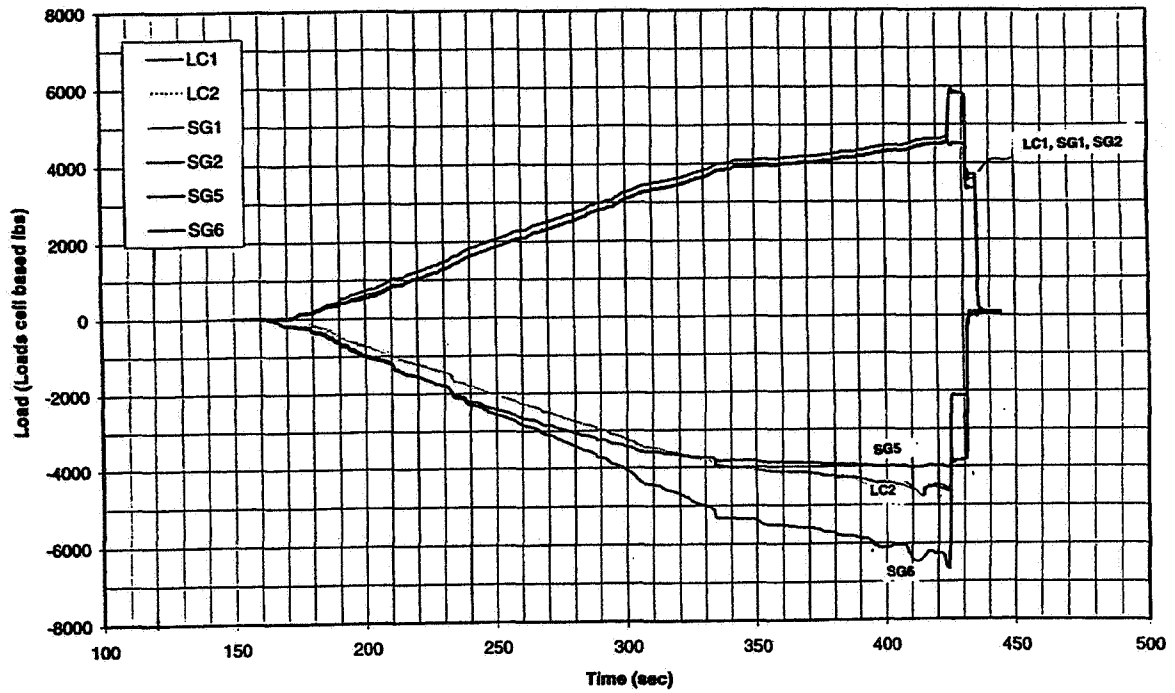
Figure 40. 3-Bay FASTMast Longeron Loads for Test (M1).

32

Figure 41. 3-Bay FASTMast Longeron Loads for Test (M1) in Terms of Load Output.
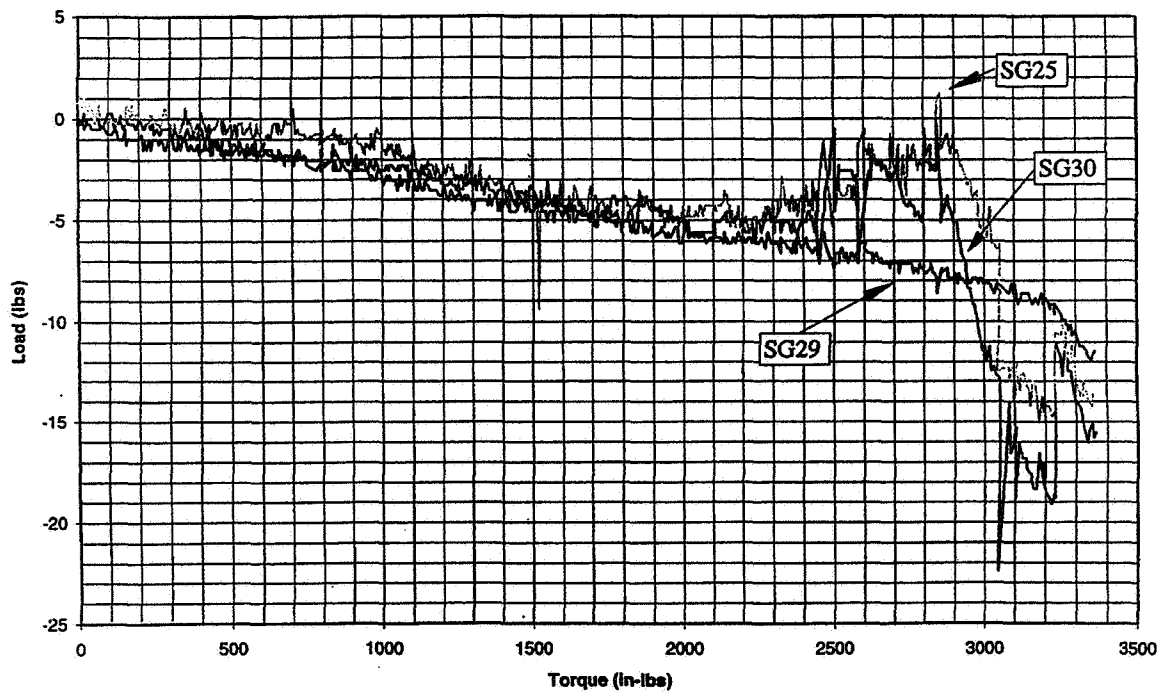
Figure 42. Rigid Batten Tube Load for Torsion Test (T4).

33

The final load application to consider is the mast transverse loading. Since a transverse load is controlled solely by properly positioning the required dead weight into the weight tray, little ambiguity exists for this load state. There are small parasitic losses due to pulley friction which can be overcome by increasing the amount of dead-weight. Figure 43 reveals that the mast top lateral motion under the transverse load was smooth and even.
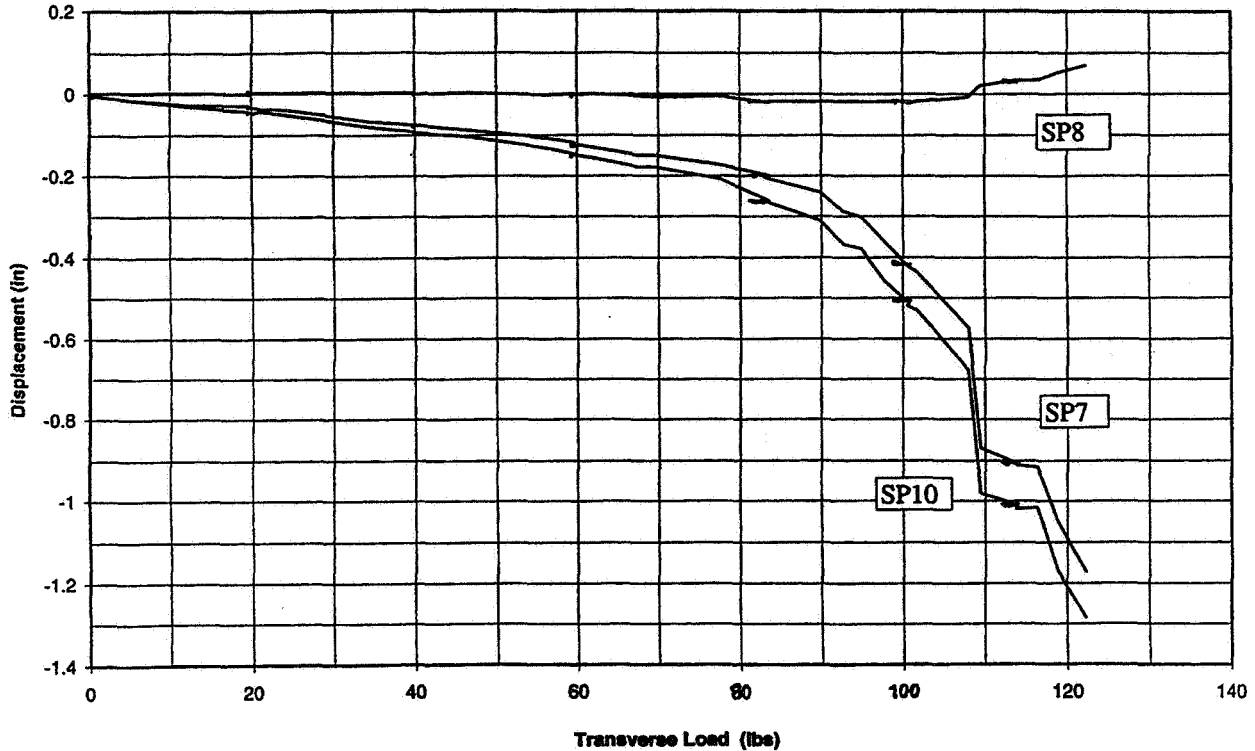
Figure 43. 3-Bay FASTMast Top Displacements for Test (S1).

In addition to validation of applied load histories, an assessment of anticipated load path activation was examined in an attempt to identify structural damage. The logical first step was to compare the latest test results to earlier tests. The focus during this phase of the test effort involved individually applied loads since combined loads data was not available from the earlier tests.

The first comparison is between moment-only test results given in figures 44 to 46. For mast corner displacements, shown in figure 44, the responses for the most recent test match closely to earlier results over the entire range of applied loads. Figures 40 and 45 reveal the data from both tests compare well when the response of column (D) is taken from strain gage SG6. However, longeron axial load path performance displayed in these figures shows unanticipated irregularities for both tests under examination. The observed irregularity is a disparity between the absolute value of tensile and compressive longeron axial loads. For the ideal case, axial loads in column (B) and (D) should be equal in magnitude but opposite in sign. However, the absolute value of the compressive load is nearly 43 percent higher at 35000 in-lb of applied load. As the applied moment load increases beyond 35000 in-lb, not only does the disparity between the column axial loads continue, but column (D) exhibits some form of misalignment behavior. This fact is indicated by the decrease in compressive strain recorded at SG5 relative to SG6. The longeron compressive loads should be equal over the length of the column but a closer look at the internal loads of column (D), displayed in figure 46, shows the column axial loads do not compare well even during low-level loading. The readings from SG5, SG6, and SG80 through SG83 should be equal throughout the loading cycle. The data shown in this case indicates that the longerons in bay 3 and 1 are translating in both the (YZ) and (XZ) planes as shown in figure 47. In other words, there is a two-plane misalignment in column (D) which is altering the load path in the compressive leg of the mast. The effect of the load path alteration is the disparity, stated above, between the absolute values of internal axial loads in columns (B) and (D).

34
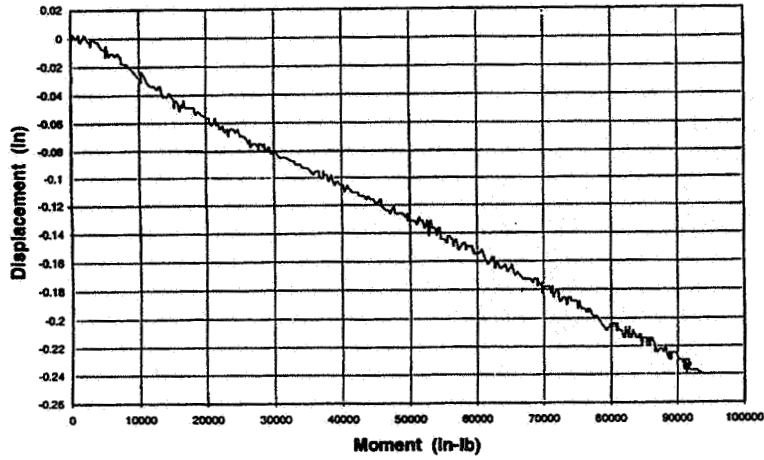
AUGUST 1994 MOMENT
LOAD TEST
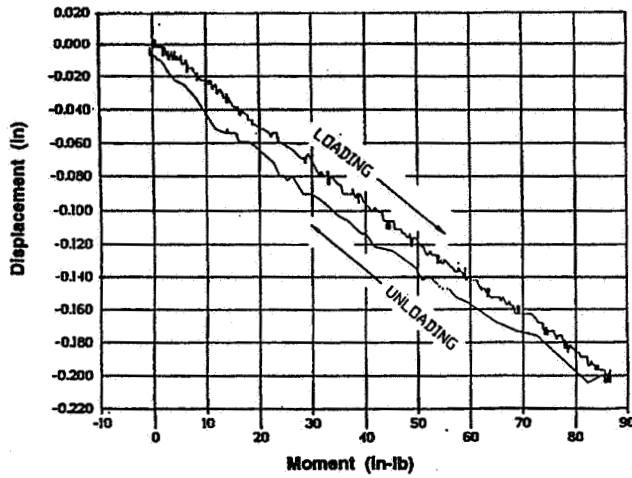
FALL 1993 MOMENT
LOAD TEST

Figure 44. Comparison of Moment-only Test Results for 3-Bay FASTMast Damage Assessment.
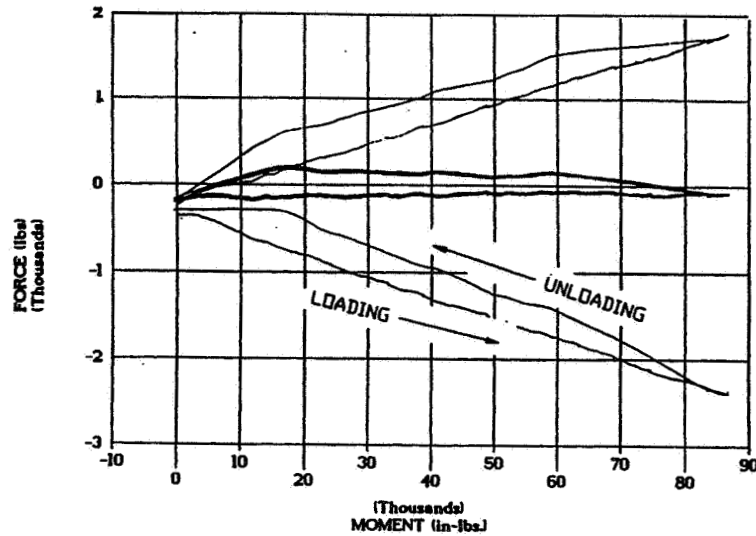
Figure 45. 3-Bay FASTMast Longeron Loads for 1993 Moment-only Test (M1).

35
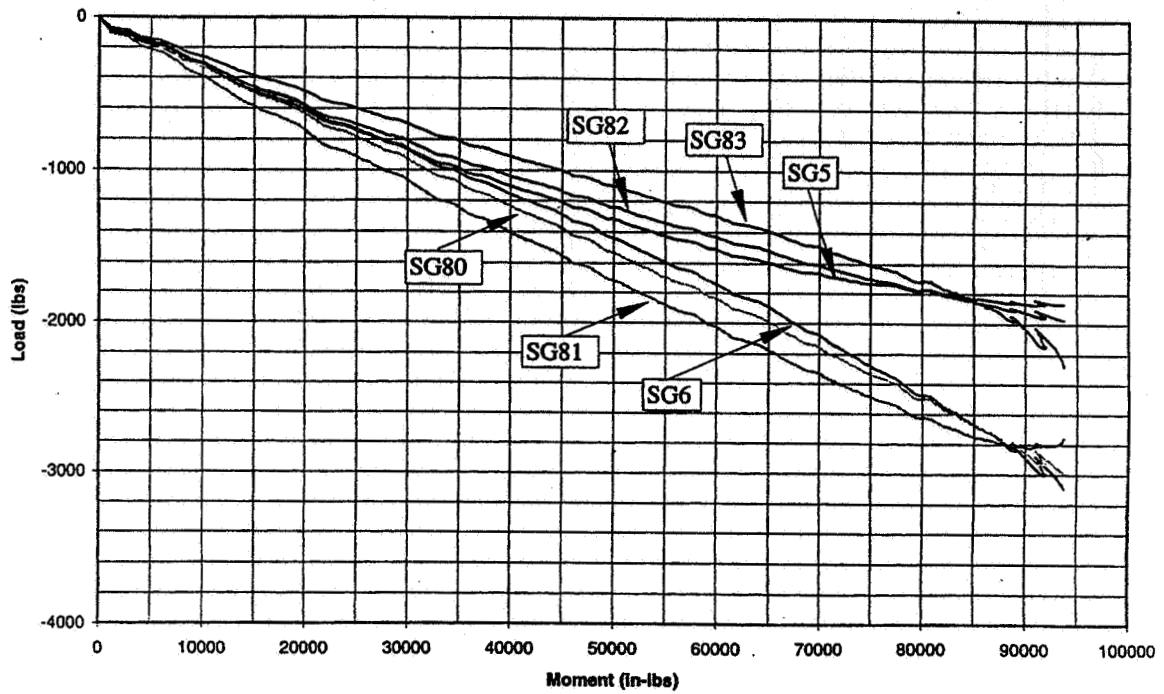
Figure 46. 3-Bay FASTMast Longeron Loads for 1994 Moment-only Test (M1).
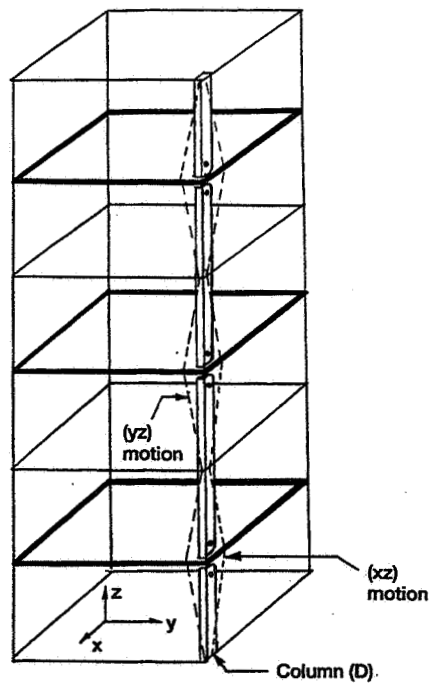
Figure 47. Schematic of 3-Bay FASTMast Failure Shapes.

Comparisons of the transverse load test results offer additional insights to the structural performance of the mast and confirms the interpretations of mast behavior during moment-only loading. Comparing the tests of an applied transverse load, figure 48 shows good agreement for mast top displacements in the linear regime and only small deviations in the nonlinear regime. The nonlinear nature of the FASTMast response is vividly evident from this figure. A gradual transition to the nonlinear behavior begins, in both cases, at an applied transverse load of 80 lbs. As the transverse load increases to 85 lbs, the diagonals will transition to a totally slack state and mast stiffness is rapidly reduced to 10 percent of its original level.
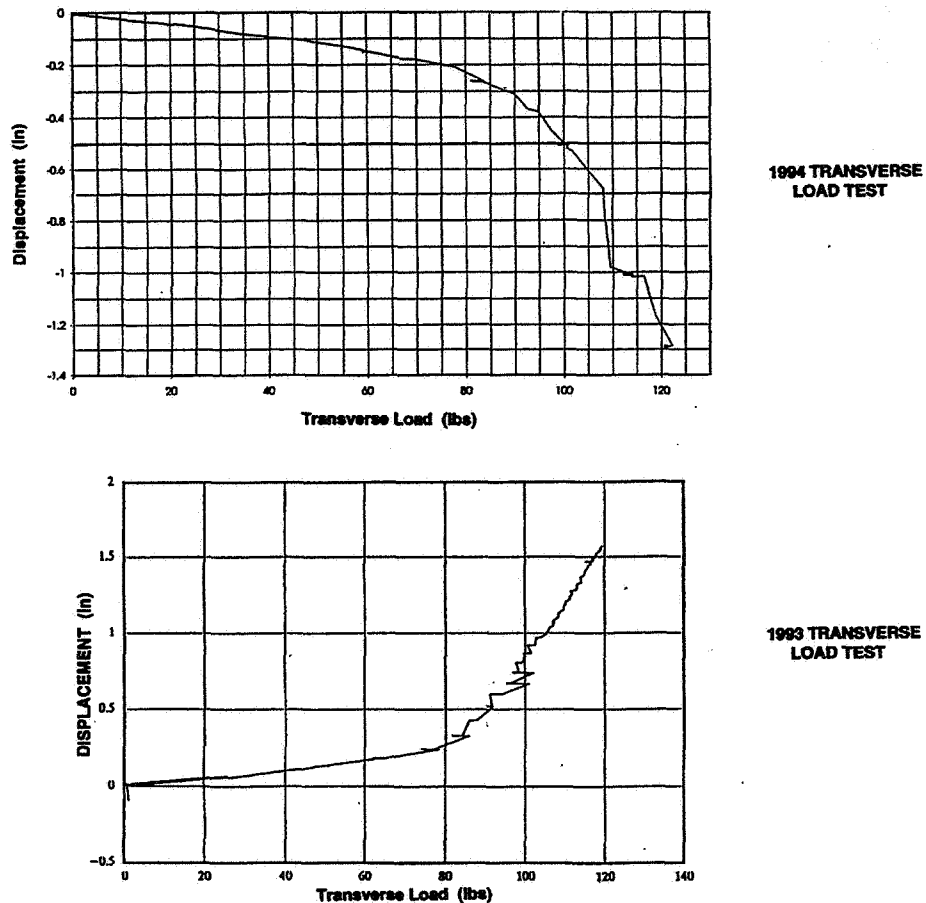
Figure 48. Comparison of Transverse Load Test Results for 3-Bay FASTMast Damage Assessments.

Two points of comparison, illustrated in figure 49, include the tensile and compressive reactions in the front and back columns, as well as the axial loads in the compressive columns. Examination of data obtained during these two tests indicates three trends: (1) the absolute value of compressive and tensile internal axial loads agree well in each test, up to moderate levels of applied load, (2) tensile and compressive internal loads are smaller in the latest test for the same applied transverse load, and (3) compressive load distribution between columns (C) and (D) exhibits an unanticipated disparity at moderate to high levels of applied load. The fact that the most recent results show lower internal loads over the entire applied load regime indicates load paths have changed relative to the earlier test. Figure 49 displays the distribution of internal compressive loads in columns (C) and (D) and it is clear the symmetry of these internal loads is decreasing as the applied load increases. As in the case for moment-only loading, high levels of transverse load causes misalignment effects at the base of columns (C) and (D). Misalignment effects in this case are more pronounced in column (D), this is evidenced by larger deviations between SG5 and SG6 than the deviations between SG3 and SG4. Furthermore, it appears that as the transverse load increases, the misalignment effects on column (D) are aggravated, causing additional disparity between the internal loads of columns (C) and (D). The final comparison of interest pertains to the results of 3-Bay FASTMast torsion testing. Figure 50 exhibits the response curves of two torsion tests performed on the 3-Bay test article. In both cases the torque was applied in a (CCW) direction. The earlier test involved only a linear mast response. The maximum applied torque was

37
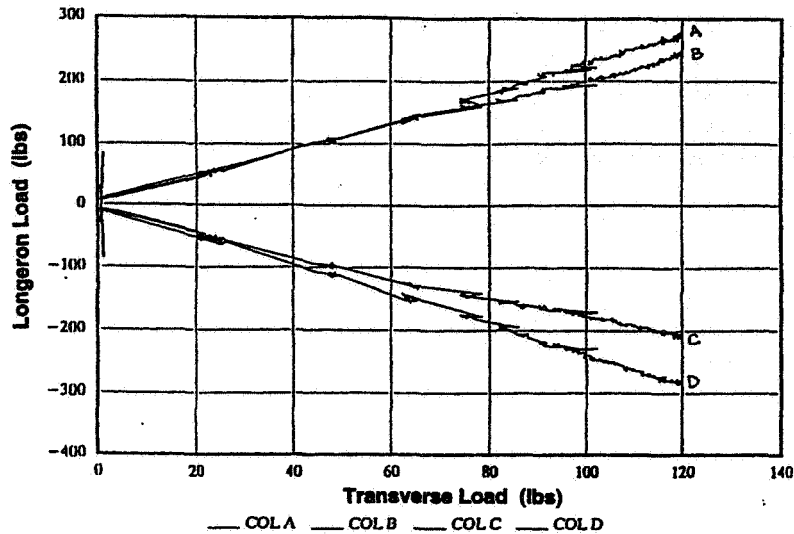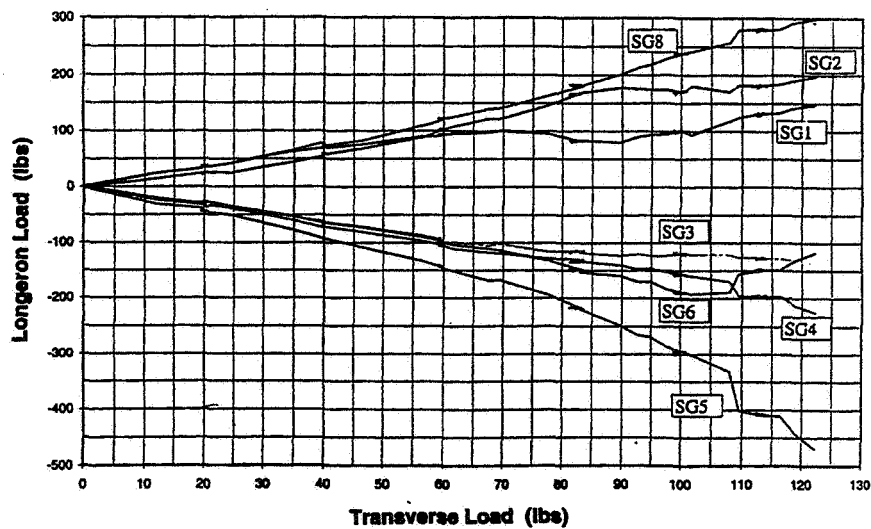
Figure 49. Comparison of Longeron Load Results for 3-Bay FASTMast Damage Assessment.

1600 in-lbs. The rotation response of the mast top, based on SP7 and SP10 displacements, agrees very well within the linear response regime. For example, at a load of 1500 in-lbs the most recent test invoked a response of 0.420 degrees and the earlier test yielded a rotation of 0.400 degrees. Note that the zero point for the 1994 torsion test was inadvertently shifted to the right. The larger rotation occurring during the more recent test represents a 5 percent decrease in torsional stiffness of the 3-Bay mast. An interesting phenomenon revealed in the nonlinear data of figure 51 is the trilinear nature of the response curve. The data given in this figure is the translation of the mast top at column (C). Note that there are inflection points located at approximately 1800 and 2700 in-lbs. The trilinear response is due to the fact that mast "twist", resulting in slack diagonals, begins at the mast top and proceeds downward. The rate of the downward "twist" dictates the position of the inflection points on the response curve. This type of nonlinear behavior was the first indications that load paths accommodating torsional loading would present a formidable challenge during model correlation. Finally, from figure 52 it is clear that the mast top remains parallel to the floor throughout the linear torsion loading.

38
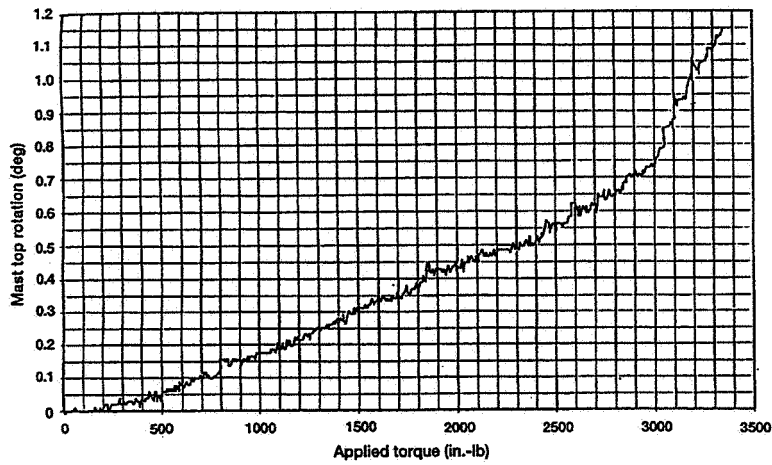
AUGUST 1994 TORSION TEST
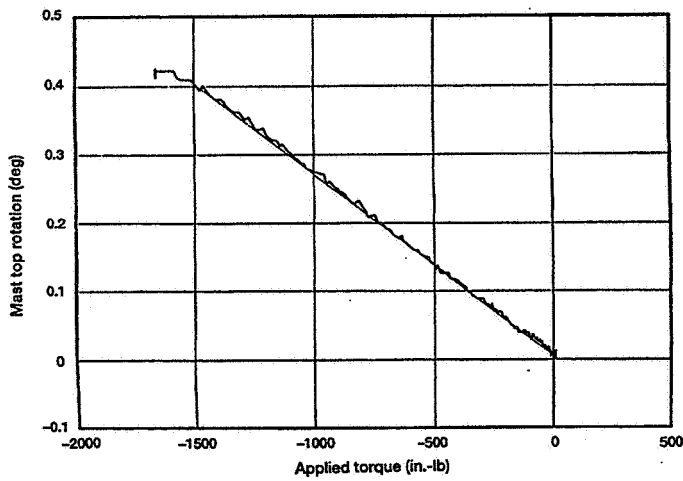
FALL 1992 TORSION TEST

Figure 50. Comparison of Torsion Load Test Results for 3-Bay FASTMast Damage Assessment.
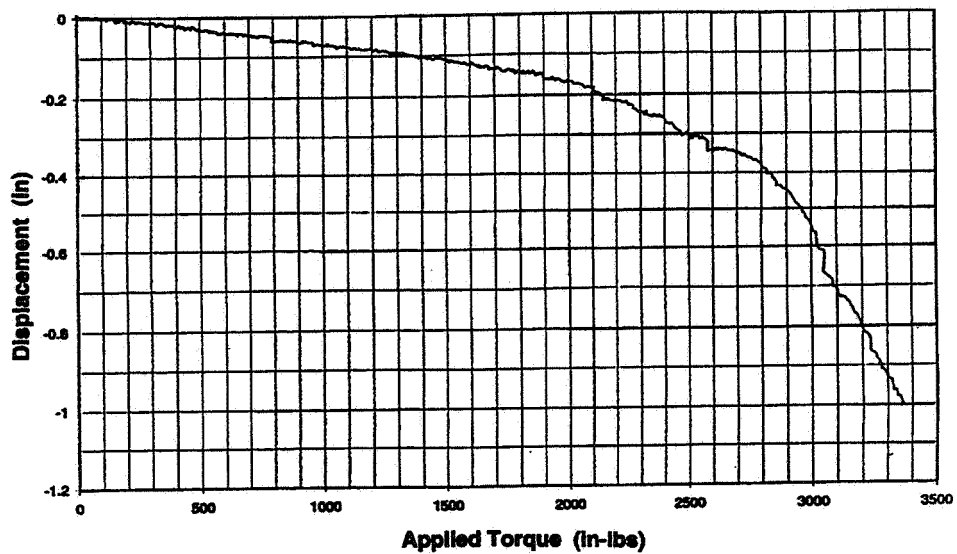
Figure 51. 3-Bay FASTMast Top Displacement at SP10 for Test (T4).
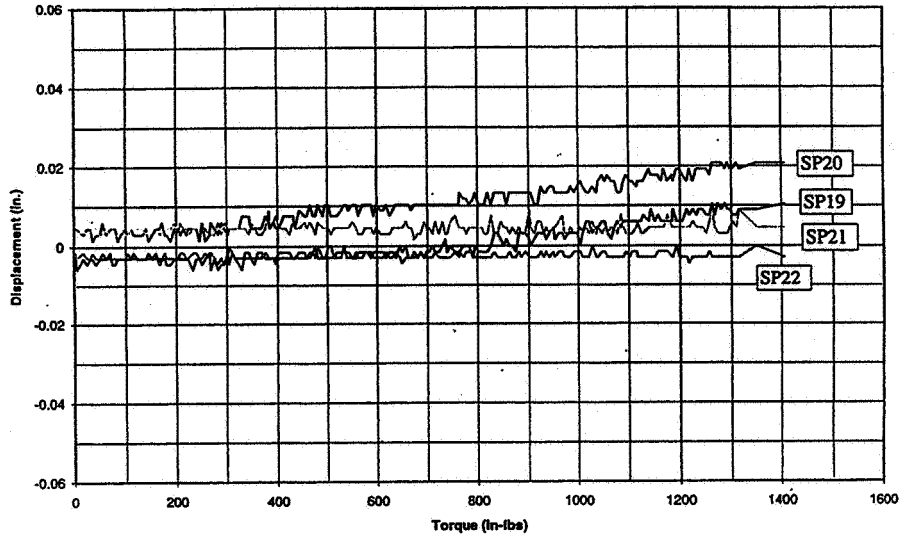
Figure 52. 3-Bay FASTMast Top Vertical Displacements for Test (T4).

Load Path Anomalies Due to Column Misalignment

For the most part, the 3-Bay FASTMast response curves developed during the initial phases of the combined transverse/moment/torsion testing matched the results of earlier tests on an undamaged test article. However, there was data collected during this test sequence that would seem to suggest that load paths were altered from those expected from design intention. In theory, a transverse load applied at the top center of the structure should be reacted equally by affected shear faces and longerons. However, it is clear from the test data that columns (C) and (D), and faces (AD) and (BC), do not react applied loads in a manner consistent with symmetry of the structure and applied load. The fundamental reason for this deviation from expected behavior is believed to be a nonuniform rate of longeron misalignment throughout the structure especially as the response becomes nonlinear. Note that this discussion involves the mast during a loaded condition and does not apply to an unloaded situation. It is the belief of the authors that the ultimate consequence of nonuniform misalignments at the four mast columns manifest itself into an overload situation most pronounced at column (D). The causes and consequences of nonuniformity of column misalignment are presented in the following discussion.

The first source of nonuniform misalignment was assumed to be the result of nonuniform diagonal preloads caused by flex-battens possessing different stiffness properties. In order to identify flex-batten stiffness variations throughout the mast, one batten from each bay was stiffness tested prior to combined loads tests. The results of initial flex-batten stiffness testing are given in figure 53. The data presented here clearly shows the existence of a flex-batten preload variation that ranged from 46 to 48 lbs. At the conclusion of combined loads testing, each flex-batten was stiffness tested and the results support the trend presented in figure 53. Shown in figure 54 is the stiffness curve of a virgin flex-batten delivered to LeRC in 1992. The flex-batten stiffness testing performed in 1992 is documented in reference 10. Upon comparing the curves of figures 53 and 54 there appears to be an overall degradation in flex-batten stiffness which contributed further to the variation of diagonal preload throughout the mast.

A second source of diagonal preload variation identified and analytically predicted during this phase of the effort involves diagonal fixity at the elbow joint. As was stated earlier, pre-test inspection of the mast revealed diagonal preload variations witnessed primarily by the different vibrational tones emitted when a diagonal was "plucked". This result was due to the fact that at one end of the flex-batten there is a pinned boundary condition and at the other end there is a fixed constraint. Manual inspections of diagonal preloads were performed throughout the test program and in all cases indicated variation throughout the mast.

The reduction in flex-batten stiffness and the resulting nonuniform distribution of diagonal preload was a likely cause of longeron misalignment. Misalignments of this type could precipitate undesirable elbow joint translations under loading conditions of interest. Furthermore, elbow joint translations could be in a direction parallel or perpendicular to the axis of joint rotation. Joint translation in either direction is consistent with the column (D)

40
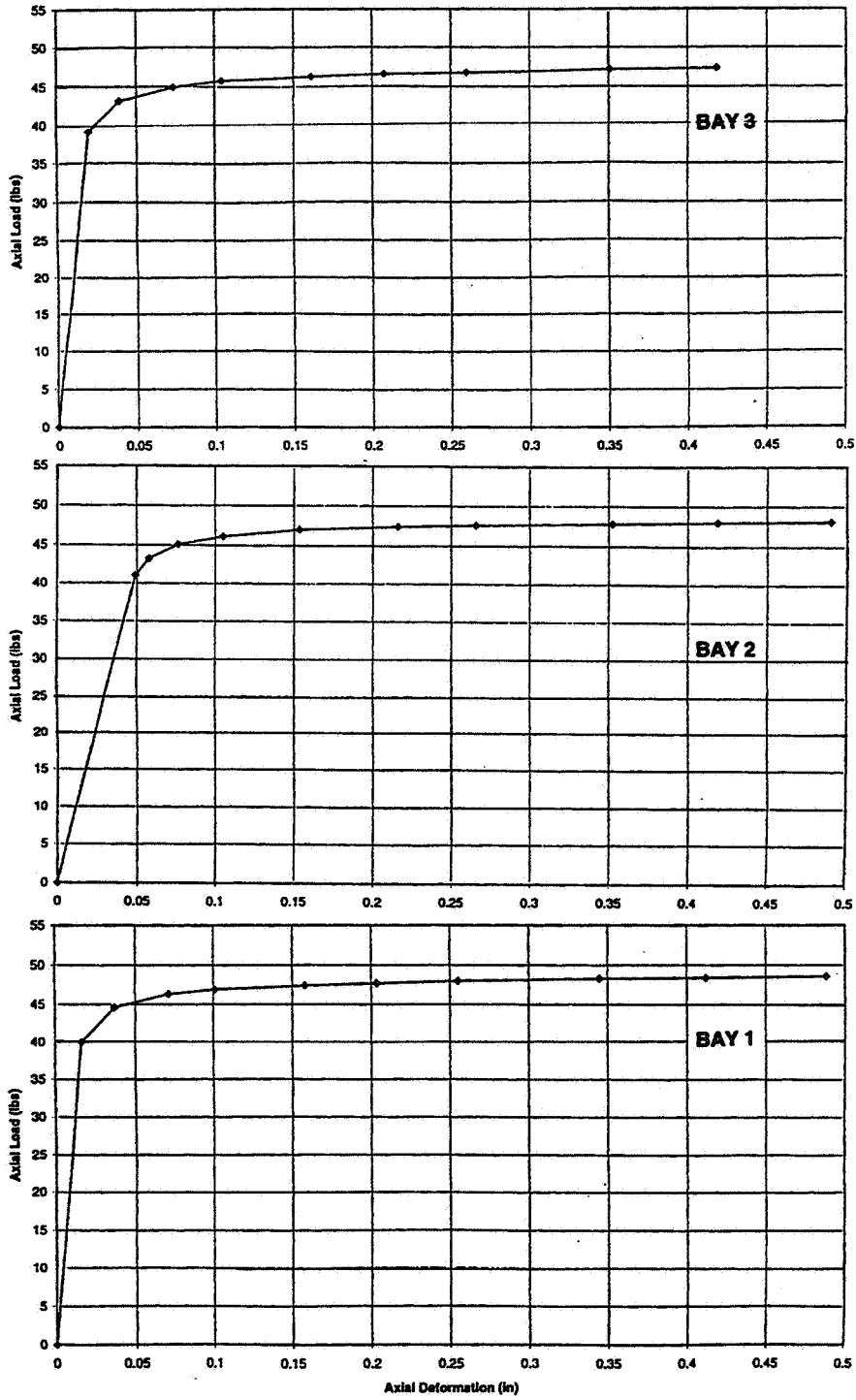
AUGUST 1994 FLEX BATTEN STIFFNESS TESTING

Figure 53. 1994 3-Bay FASTMast Flex-batten Stiffness Test Results.

41
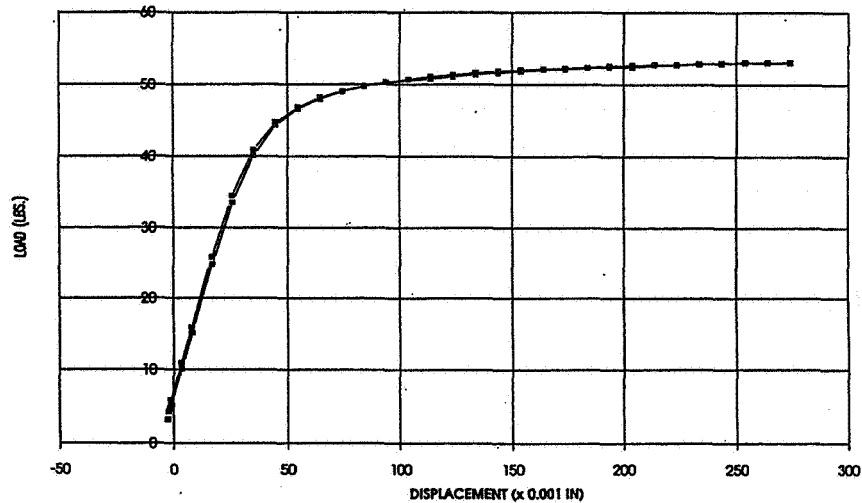
Figure 54. 1992 3-Bay FASTMast Flex-batten Stiffness Test Results.
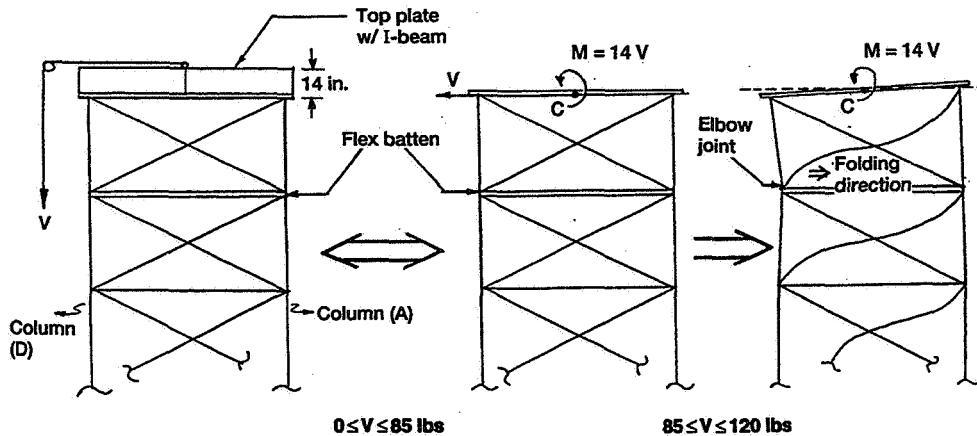
Figure 55. 3-Bay FASTMast Top Plate Assembly Motion for Transverse-only Loads.

misalignment mode described earlier during moment-only applied loads. Misalignment effects in the direction per-
pendicular to the axis of elbow joint rotation may also be amplified due to the taper of the longeron itself.

Another source of nonuniform longeron misalignment observed during testing involved only transverse
loading of the mast structure. In this case load path corruption appeared to result from an undesirable interaction
between bay 3 and the top plate structure. Given in figure 55 is a two-dimensional representation of events leading
to inadvertent misalignment of the top longeron in column (D). The fourteen inch offset of the applied transverse
load V is equivalent to a force-couple system represented by V and M acting at the plate level. The transverse force
V tends to displace the mast in a horizontal direction while the couple, left unresisted, will cause the plate to rotate
in a counterclockwise fashion. In this case plate rotation occurs because the motion restraint provided by longeron
columns is reduced as the mast top displaces. There is also a compressive dead-load of 200 lbs acting on each col-
umn from the weight of the plate-beam assembly. When the diagonals are taught, load V is reacted by the diagonals
and rigid battens as design would dictate. However, as load V increases to a level larger than the preload induced by
the flex-batten, the diagonals become slack. The elbow joint of column (D) located in bay 3 is now free to translate
in the folding direction and a small misalignment develops between the upper and lower longerons. With the align-
ment of column (D) now compromised in bay 3, the resistance to the rotation induced by the couple and plate dead-
load decreases and the elbow joint is forced further inward. As the elbow joint moves inward, the top of column (D)
begins to move downward and an interaction at the boundary of the top plate and the mast exists. Due to this interac-
tion, the rate of misalignment in column (D) will accelerate.

42
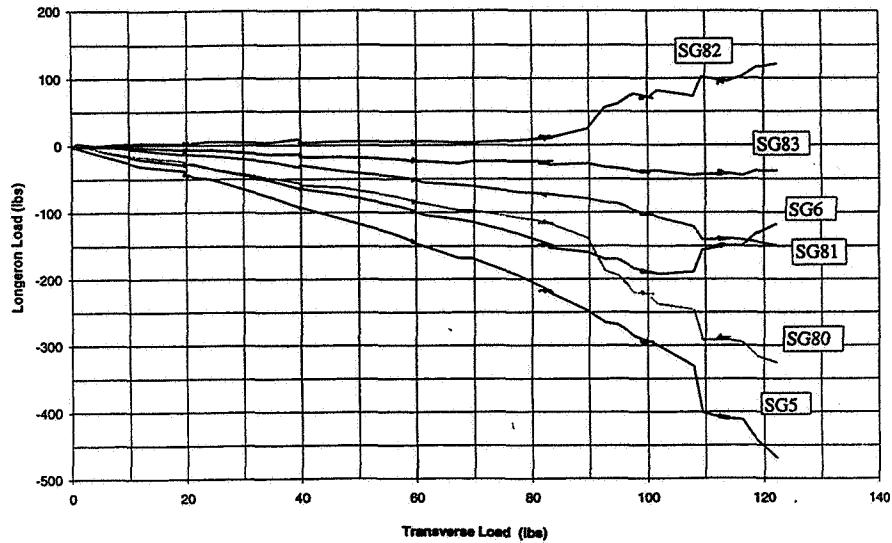
Figure 56. 3-Bay FASTMast Column (D) Loads for Test (S1).
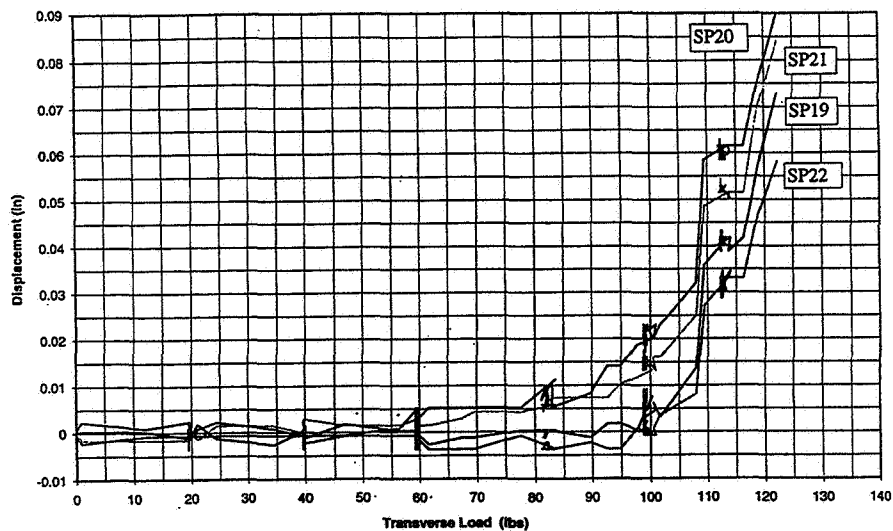
Figure 57. 3-Bay FASTMast Top Plate Vertical Displacements for Test (S1).

To verify this theory, a transverse load test was performed to a level of 120 lbs. The strain data obtained during this test is given in figure 56. The data is very similar to the moment-only test results presented earlier for column (D) base reactions. In order to accommodate the misalignment of column (D), the load paths within the top-bay longeron assembly are altered. Indication of load path alterations is provided by the divergent nature of strain records for SG80 and SG82. Furthermore, figure 57 shows that as the magnitude of the transverse load reached 90 lbs the plate corner at column (D) moved rapidly downward as theorized. The existence of plate-mast interaction was first made evident by mast tip deflection data generated during transverse load tests. From figure 48, the onset of nonlinear behavior occurs at a transverse load of approximately 85 lbs. However, if the theoretical flex-batten preload is 50 lbs and it is assumed that the structure is reacting the load as intended, the structure would become nonlinear at an applied transverse load of 100 lbs. This was verified by performing a nonlinear FE analysis of the FASTMast subjected to a transverse load. The analysis was performed using an ideal FASTMast structure which precluded a state of diagonal preload variation. The results of this analysis are given in figure 58 and as expected the structure becomes nonlinear at an applied load of 100 lbs. However, early FE analyses did not include the plate assembly and therefore boundary effects, unfortunately, went undetected. Upon closer examination of the transverse load test strain data, it was observed that column (C) reacted 40 percent of the compressive load and column (D)

43
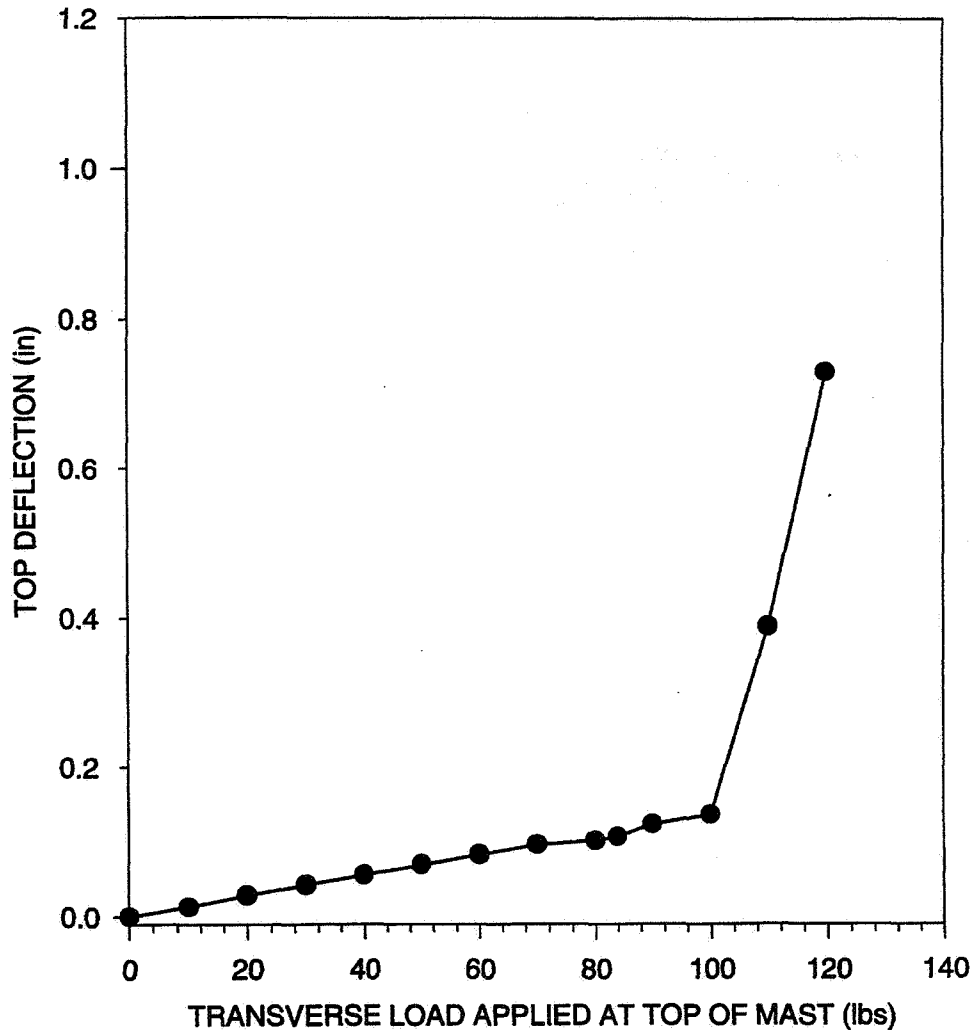
Figure 58. 3-Bay FASTMast Top/Center Lateral Deflection from ANSYS Nonlinear Large Displacement Analysis.

reacted the remaining 60 percent. In order to determine if the model was performing properly, and to assess the reality of the interaction problem, the FE model without the top plate was subjected to an applied transverse load in the ratios given above. In other words, columns (C) and (B) were subjected to 40 percent of the transverse load, and columns (A) and (D) received the remaining 60 percent. The results of that analysis are given in figure 59. The data confirms that a redistribution of the longeron load in columns (C) and (D) could cause the mast to be nonlinear at a lower applied load. The final verification of this effect was established by performing a nonlinear analysis of the mast with the complete test support structure.

From the above discussion it is clear that nonuniform longeron misalignments did occur during combined loads testing. Furthermore, behavior of this type did alter load paths and structural responses from those expected from theory. The source of nonuniform longeron misalignments was due to test article interaction with support structure and degradation in flex-batten stiffness. It was the opinion of the test team that the two parameters with the largest potential for negative impact on achieving model correlation were diagonal preload variations and plate/mast interactions. Although the likelihood of yielding a joint, longeron, or rigid batten was considered remote, it was not possible to perform detailed inspections required to discount the existence of this type of damage. The effects of test article damage on the model correlation effort and failure mode assessments are presented in the discussion to follow. Using accepted FE modeling techniques, every attempt was made to isolate problem areas from the load path and also account for irregularities due to the mast design and/or effects of the boundary conditions between the mast and the support structure.

44
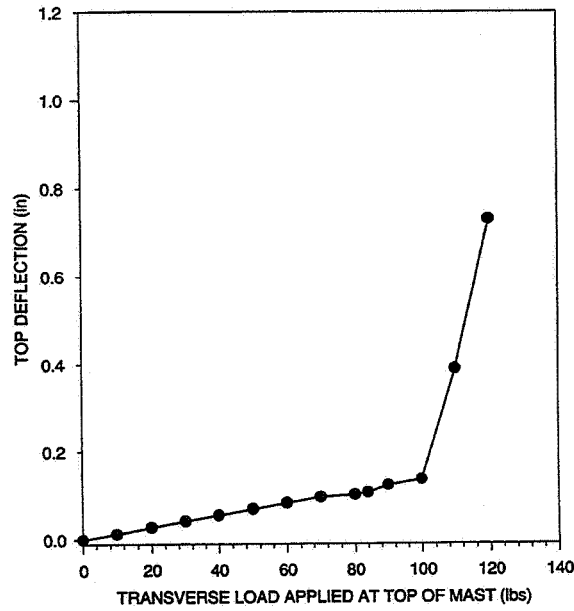
Figure 59. 3-Bay FASTMast Lateral Deflection Comparison of Plate Interaction Study.

Assessment of Combined Loading Test Data

Presented in table 2 is a summary of all structural tests performed during the 3-Bay FASTMast combined loads test program. The first item of interest is the type of load used for various tests. In addition to the combined loads which are of fundamental interest, the structure was subjected to individually applied transverse, moment, and torsion loads. Although the service environment of the FASTMast structure will, for the most part, include a combination of applied loads, test results involving individual applied loads can be used for model correlation purposes and interpretations of mast behavior.

TABLE 2.—3-BAY FASTMast COMBINED LOADS TEST RESULT SUMMARY

TEST NUMBER[1,2]	TRANSVERSE (LB)	MOMENT (IN-LB)	TORSION (IN-LB)	RATIO (T/S)	FAILURE LOCATION	ELBOW FOLDED	ELBOW BUCKLED	COMMENTS
T1	0	0	1000	n/a	NONE			TORSION CHECK
T2	0	0	1000	n/a	NONE			REPEATABILITY CHECK
ST1	60	0	1000	16.67	NONE			LINEAR MAST
ST2	60	0	1000	16.67	NONE			REPEATABILITY
TS1	120	0	600	9.76	NONE			NONLINEAR MAST
TS2	100	0	900	9.00	NONE			NONLINEAR MAST
TS3	100	0	1200	12.00	NONE			NONLINEAR MAST
ST3	80	0	1400	17.50	NONE			LINEAR MAST
S1	120	0	0	n/a	NONE			NONLINEAR MAST
T3	0	0	2500	n/a	NONE			NONLINEAR MAST
T4	0	0	3300	n/a	COLUMN C	√		ONSET OF FAILURE
SM1	100	37000	0	n/a	BAY 3 (AD)	√		COLUMN (D) FAILURE
SMT1	75	38860	2000	26.67	NONE			LINEAR MAST
SMT2	70	39540	2280	31.43	NONE			NONLINEAR MAST
SMT3	70	48980	2400	34.29	NONE			NONLINEAR MAST
SMT4	70	49920	2500	35.71	NONE			SHARP KNEE
SMT5	90	40300	1900	21.11	NONE			NONLINEAR MAST
SMT6	70	58540	2500	35.71	NONE			POWER FAILURE
SM2	90	54000	0	n/a	NONE			COLUMN (D) FAILURE
SMT7	90	50180	1000	11.11	BAY 3 (CD)	√		COLUMN (D) FAILURE
M1	0	94000	0	n/a	BAY 1 (AD)	√		COLUMN (D) FAILURE
M2	0	68000	0	n/a	BAY 1 (AD)	√		COLUMN (D) FAILURE
M3	0	68000	0	n/a	BAY 1 (AD)	√		COLUMN (D) FAILURE
M4	0	66000	0	n/a	BAY 1 (CD)		√	VERY NONLINEAR MAST
ST4	120	0	2500	20.83	BAY 1 (CD)	√	√	CORRELATION DATA
TR	0	0	2000	n/a	NONE			ABORT TEST
MR1	0	0	0	n/a	NONE			COLUMN (B) FAILURE
MR2	0	100000	0	n/a	BAY 3 (AB)		√	COLUMN (B) FAILURE
MR3	0	66000	0	n/a	BAY 3 (AB)		√	

[1] T - TORQUE(CCW) ONLY, TS - TORQUE(CCW)+TRANSVERSE, ST - TRANSVERSE+TORQUE(CCW), SMT - TRANSVERSE+MOMENT+TORQUE(CCW), M - MOMENT ONLY, S - TRANSVERSE ONLY, TR - TORSION REVERSE (CW)
[2] TESTS LISTED IN ORDER THEY WERE PERFORMED

45

The first two tests involved performance checks of the torque load application device in addition to generation of test article integrity assessment data. Following the torque load checkout, the ST1, ST2, ST3, TS1, TS2, and TS3 tests were performed in order to assess response traits involving combinations of low-level transverse and torsion loads. The data obtained included both linear and nonlinear responses required for model correlation. Early transverse/torsion load data provided required insight to the behavior of a very complicated load path. Much of the test data confirmed what had been predicted during pre-test analyses involving application of combined transverse and torsion loads to the FASTMast structure. One consequence of various levels of torsion and transverse load, is the different rate of cable slackening on the mast faces that are reacting the pure transverse load. Recall that a torsion load can be treated as a transverse load reacted equally on all four faces. The disparity in cable slackness is due to the torsion load increasing the transverse load effects on one shear face and reducing the effects on the other. The FASTMast system remained essentially linear until both faces reacting the direct transverse load achieved cable slackening. Also, as the ratio of a torsion load to a transverse load increased, there was a decrease in the rate of transition to a nonlinear state. This effect can be observed by comparing the curves shown in figure 60.
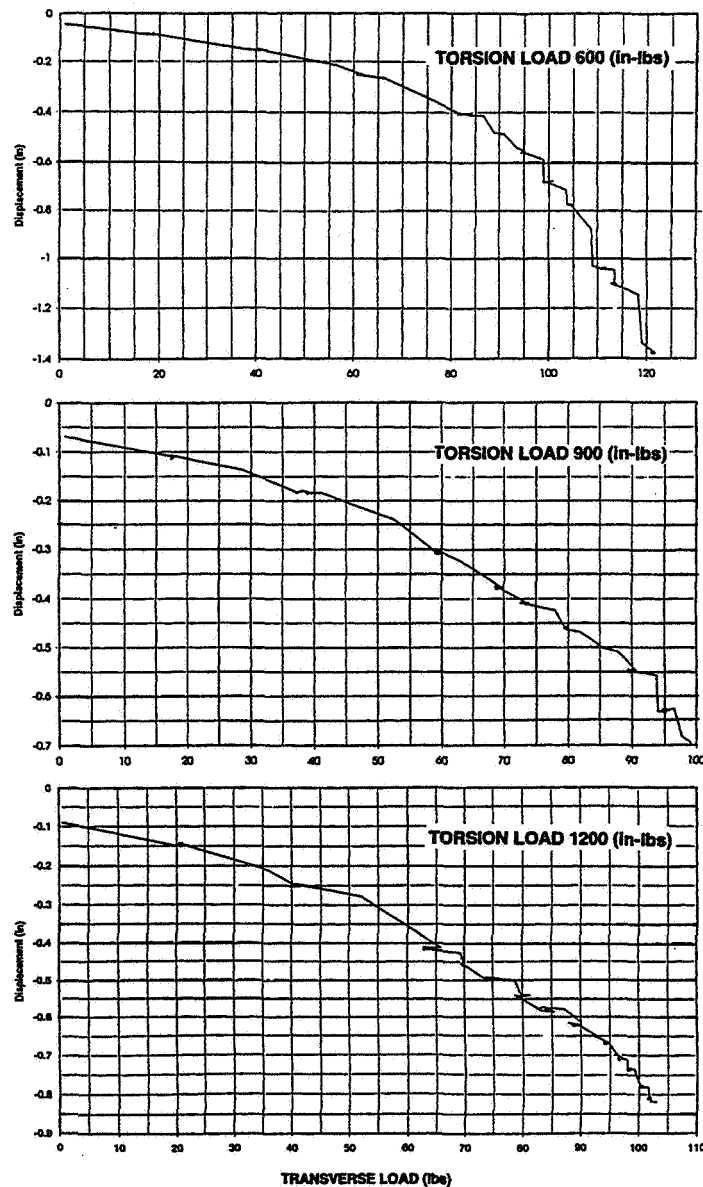
MAST TOP DISPLACEMENT VERSUS TRANSVERSE LOAD

Figure 60. 3-Bay FASTMast Top Displacement Due to Combine Transverse and Torsion Load Tests (TS1), (TS2), (TS3).

46

Test ST3 involved reversing the sequence of torsion and transverse loading to determine if the order of application affected mast response. The results obtained during ST3 indicated that the order of load application does not alter mast response. A comparison of mast top displacements for both sequences of transverse and torsion load applications is given in table 3. This data indicates that mast displacement response is independent of load application order for low and moderate levels of transverse and torsion loads. However, due to a lack of understanding of high-level torsion load effects on joint stiffness, a decision was made to apply the transverse load before the torque load in order to avoid joint binding.

TABLE 3.—DISPLACEMENT RESPONSE FOR CONSTANT TRANSVERSE LOAD OF 80 lbs

TEST NUMBER	TORSION LOAD	DISPLACMENT	
	(IN-LB)	(IN)	
		SP7	SP10
TS1	600	-0.180	-0.400
TS2	900	-0.150	-0.450
TS3	1200	-0.140	-0.550
ST3	600	-0.180	-0.380
	900	-0.165	-0.420
	1200	-0.150	-0.500

Following the first series of combined transverse/torsion load tests, the mast was subjected to a single transverse load of 120 lbs. The data obtained during this transverse load test was used for mast health assessments and plate/mast interaction studies, both of which were described earlier.

The next item of investigation involved the effects of high-level torsion loads on the mast. Test T3 and T4 involved the application of 2500 and 3300 in-lb (CCW) torque levels respectively. Mast top deflection curves for test T4 are given in figure 61. From the deflections at SP8 and SP10, nonlinear behavior is initiated by a load of 2000 in-lbs or an equivalent transverse load per mast face of 34 lbs. However, significant nonlinear behavior starts when the flex-battens begin to take on load at 2700 in-lbs or an equivalent transverse load of 45 lbs. The action of the mast is consistent with the assumption that nonlinear behavior will result when flex-batten preload is overcome by transverse loads. Note from figure 53 that the installed flex-batten preload in bay three is approximately 46 lbs. The data given here supports the claim that the nonlinear behavior which occurred during S1 was premature and caused by an outside influence. The failure mode which occurred at 3300 in-lbs involved moderate elbow joint displacement in the folding direction of the bay 3, column (C) longeron assembly.

The next series of tests included a repeat of an earlier transverse/moment load test and several cases of combined transverse/torsion/moment loads. Tests SM1 and SM2 were performed to provide additional data necessary to close out the issue of test article damage. A similar test was performed at LeRC in the fall of 1993 and the data was available for comparison purposes. The mast was subjected, first, to a 100 lb transverse load followed by moment load to failure. The mast failure mode in this case was a large displacement of the elbow joint of bay 3, column (D), in the longeron folding direction. The moment load at failure for SM1 was 37000 in-lbs, 8 percent higher than the value reported in the decreasing shear load test case in reference 5 (fig. 5). Test SM2 also demonstrated a greater capacity to resist instability. The moment load was 13 percent higher than what was reported in reference 5 for the 90 lb transverse load case. The reason for the apparent increase in strength is not totally understood. However, it is speculated that additive longeron misalignment inherent to the manner in which earlier tests were conducted probably reduced the level of moment load causing failure.

SMT1 through SMT7 combined loads tests involved transverse, moment, and torsion loads applied to the structure. The load combinations in these tests produced both linear and nonlinear mast responses with no occurrences of instability. The most important revelation from this set of tests, as well as test ST4, was the apparent interaction between the transverse and torsion loads that was briefly discussed earlier. As the ratio (T/S) of torsion (T) to transverse (S) load increased, the transition rate to a nonlinear state was greatly decreased. The indication of this type of behavior was presented in displacement data which was bilinear for small values of (T/S) and trilinear for large values of (T/S). The implications of this behavior are discussed later in this report.

The final sequence of testing, with the exception of test TR, was performed in order to develop 3-Bay mast failure modes. Test TR was a torque case applied (CW) for the purpose of developing correlation data and final verification of torsional stiffness differentials in the (CW) and (CCW) directions. No significant findings can be reported based on the data of test TR. Tests M1 through M4 were performed to assess the ultimate axial load capability of column (D). From the data in table 2 two points are very clear: (1) the maximum moment capability was

SP10 vs. Torque

SP8 vs. Torque
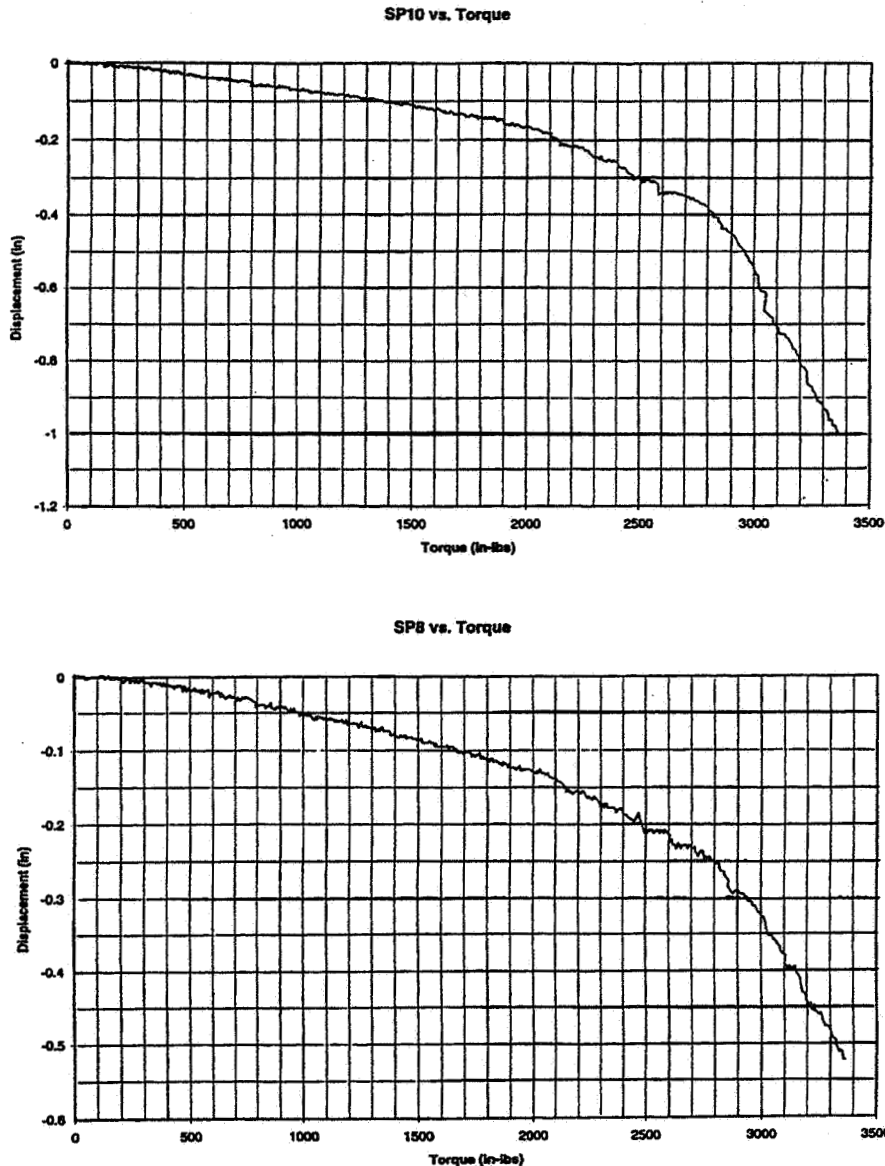
Figure 61. 3-Bay FASTMast Top Displacements for Torsion-only Test (T4).

94000 in-lbs, and (2) once a column has failed, the strength is permanently reduced by a minimum of 30 percent. The failure mode in all four cases involved a large displacement of the elbow joint in a direction either consistent with the longerons folding (elbow fold) or perpendicular to the folding action (elbow buckling). An equivalent longeron load associated with a mast failure load of 94000 in-lbs, would be approximately 2186 lbs, assuming the column is straight at collapse. Note that this value is lower than the Euler buckling load of a single longeron (approximately 2450 lbs) reported in reference 8. However, the actual value of allowable axial load would be somewhat less if the misalignment known to exist at high moment loads was taken into account.

Tests MR1 through MR3 were the final tests of this effort and were performed to demonstrate repeatability of the ultimate longeron compressive load values. The tests involved reversing the moment load and therefore compressing column (B) until failure. The ultimate bending moment was 100000 in-lbs (2325 lb equivalent longeron axial load) and the mast experienced a bay 3, column (B), elbow joint kinematic stability failure. Results from MR3 indicate a strength reduction of 33 percent once the column has failed from an ultimate axial load. The fact that column (B) failed at a higher load is consistent with the fact that it was the least loaded column in compression throughout the three-year service life of the 3-Bay unit.

Failure Mode Discussion

With the test data serving as a basis, a discussion concerning failure modes can now be undertaken. From the observed failure modes several principal points involving mast instability can be stated:

1. FASTMast instability is accompanied by large lateral displacements of the elbow joint(s).
2. Large transverse displacements of an elbow joint, in the direction of folding or perpendicular to the fold direction, are associated with a misalignment between upper and lower longerons in a given bay. Furthermore, the amount of longeron misalignment increases dramatically during nonlinear response states.
3. The likelihood of elbow joint lateral motion is greatly increased when the mast is required to react high transverse loads combined with bending and axial loads. The two things that primarily affect elbow joint motion when the mast transverse load capability is exceeded are (see fig. 62):
    a. The increased diagonal tension load pulls the elbow joint laterally (after one diagonal goes slack).
    b. The horizontal component of the column axial load, P_H, pushes the elbow joint laterally. For a large P the horizontal component can quickly reach the buckling level of a flex-batten. For example, if $\Delta=0.40$ in, and $P=2500$ lbs, then $P_H=51$ lbs.

Note that in figure 62 the vector diagram involving the decomposition of load P is not drawn to scale. From the points (1), (2), and (3), above, it is clear that the FASTMast exhibits a primary failure mode that involves general instability of the system. Furthermore, the instability is precipitated by the kinematic action of the elbow joint responding to a series of externally applied loads. The specific load state that can be associated with instability will vary due to load path alterations brought on by changes in mast geometry.
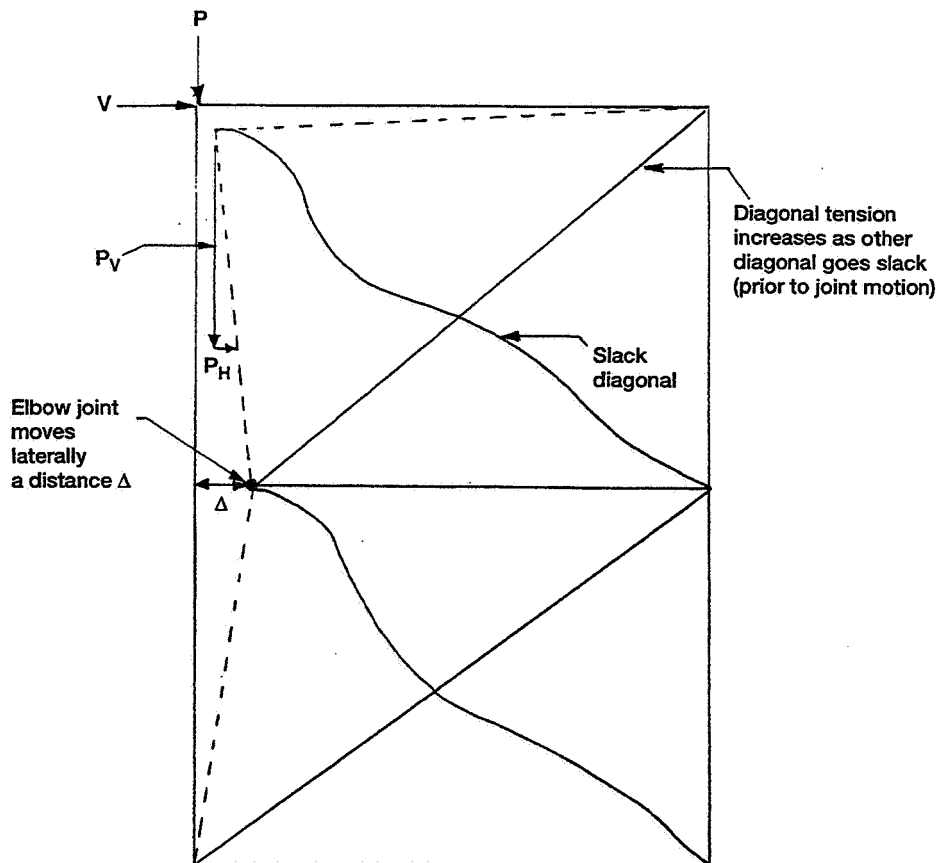

Figure 62. Influence of Column Axial Load on 3-Bay FASTMast Failure Modes.

49

Now that the nature of the stability failure mode has been identified, it is necessary to understand the parameters which most influence the tendency toward an unstable state. The most important state change leading to instability appears to be longeron misalignment. Once an initial imperfection is introduced, relative to longeron assembly straightness, the ability of the mast to resist axial and bending loads decreases dramatically. This fact is consistent with most systems that are susceptible to stability failure modes. Since longeron assembly straightness is a function of elbow joint lateral displacements, the FASTMast stability can be directly related to internal shear load resistance. This is due to the fact that significant elbow joint displacements occur when the mast shear resistance has been reduced to zero and the flex-batten is loaded beyond its buckling limit. Therefore, the most critical parameters relative to mast stability are those related to internal shear creation and resistance. A third important parameter that relates directly to those just mentioned is the altered stiffness state brought about by changing mast geometry. Determination of the effects of geometry state changes on mast stability is the essence of the nonlinear large displacement problem. The problem of FASTMast instability, in its most succinct form, involves a nonlinear mast with longeron assemblies possessing a critical level of misalignment.

In order to better understand mast instability it proves beneficial to examine in detail the three critical factors identified in the preceding paragraph. In general, mast capability can be maximized by: (1) limiting adverse applied loads, (2) increasing strength of structural members, or (3) a combination of the two. It was shown earlier that the onset of nonlinear mast response, which clearly precedes instability, is a function of mast column shear load. The creation of internal shear load is a result of applied transverse and torsion loads. In general the mast axial and bending load capability decreases as the internal shear loads increase. The first obvious solution to mitigate the effects of internal shear load is to reduce the level of applied transverse load. Due to the fact that torsion loads are a result of offset transverse loads, a reduction in transverse load will also decrease torsion load. Torsion loads could also be reduced independently of transverse loads by avoiding array loading that is non-symmetric. An alternate approach to minimizing the effects of applied loads that are associated with mast instability is to increase structural capability. To be able to minimize large elbow joint displacements, it is necessary to increase the transverse load resistance of the mast. The most direct approach when increasing the mast shear strength is to increase the buckling load of the flex-batten. However, any changes in the flex-batten design must be accompanied by analyses which will evaluate the effects on other parts of the mast. For example, an increase in flex-batten stiffness will result in larger column axial loads that may approach the Euler buckling limit for a single longeron. Also, an increase in the flex-batten pre-load will put excessive wear on the mast deployment and retraction mechanisms. Perhaps a combination of applied load mitigation in conjunction with prudent design changes would offer the best solution to increasing current mast stability limits.

In addition to identifying the stability critical parameters, there are those that possess a yet-to-be determined level of significance in terms of mast stability for nonlinear states. The first area of interest is the interaction of transverse and torsion load and its effect on instability loads. From reference 11 it is clear that mast axial/bending capability decreases as the value of (T/S) increases. This, at first glance, appears contradictory to the notion that mast instability is related to the "degree" of mast nonlinearity. The "degree" of nonlinearity in this case can be related to the slope of the force/displacement curve for mast top motion. As the number of slack cables increase, curve slope, or "degree" of mast nonlinearity will also increase. For low values of (T/S) the response curve is trilinear and therefore transition to a final nonlinear state is "slower". However, it was observed from both test and analyses data that for a wide range of (T/S) the final mast stiffness was constant at approximately 30 lbs/in. Therefore, variations in the column shear loads within mast faces appears to have a limiting effect on axial/bending load capability which is independent of the final stiffness state. A second important aspect of the design that must be better understood is the behavior of the elbow joint. The response of this critical element will be influenced by joint stiffness and friction parameters which remain undefined. Other design factors that probably require additional study include (1) effect of longeron taper and hinge-pin offset, (2) variation of diagonal preload due to flex-batten degradation, and (3) effect of nonlinear diagonal stiffness. Once the effects of the elements given above are known, it is possible to develop a complete understanding of FASTMast stability failure modes.

The final point, relative to the failure mode discussion, must address the subject of post-buckling capability of the FASTMast. Post-buckling capability refers in this case to the ability of the mast to resist applied loads after it has reached a nonlinear response state. The significant failure modes, to this point, have been kinematic in nature and leads ultimately to the question of post-buckling strength. There are two very important points that quickly provide focus to this very important question. It is very clear from the ultimate moment tests that once a longeron

column has been involved in an instability event, the axial/bending capability was reduced by 30 percent. The reduction in strength is most likely due to permanent longeron misalignment resulting from local yielding of several mast components. However, the reduction in strength observed from test data is only possible because applied load states are removed during the onset of unstable behavior. It is reasonable to assume that in the actual service environment an applied load causing instability will not be detected and therefore continue unabated. The continuous application of an applied load beyond the critical threshold will obviously result in a catastrophic collapse. Therefore, a conservative engineering conclusion based on available test and analysis data is that the post-buckled strength of the FASTMast is zero.

NONLINEAR FINITE ELEMENT MODEL CORRELATION WITH TEST DATA

Before it is possible to develop analytical failure interaction curves for transverse, moment, and torsion loads it is necessary to verify the FE model represents reality. The model verification approach utilized during the 3-Bay FASTMast effort was to update the nonlinear FE models based on test results. The ANSYS model, used for pre-test analysis, and an MSC/NASTRAN nonlinear FE models were used during the correlation process. The addition of the MSC/NASTRAN model was based on the desire to provide an independent check of the ANSYS model results. The graphical representation of the FE models is presented in figure 63.
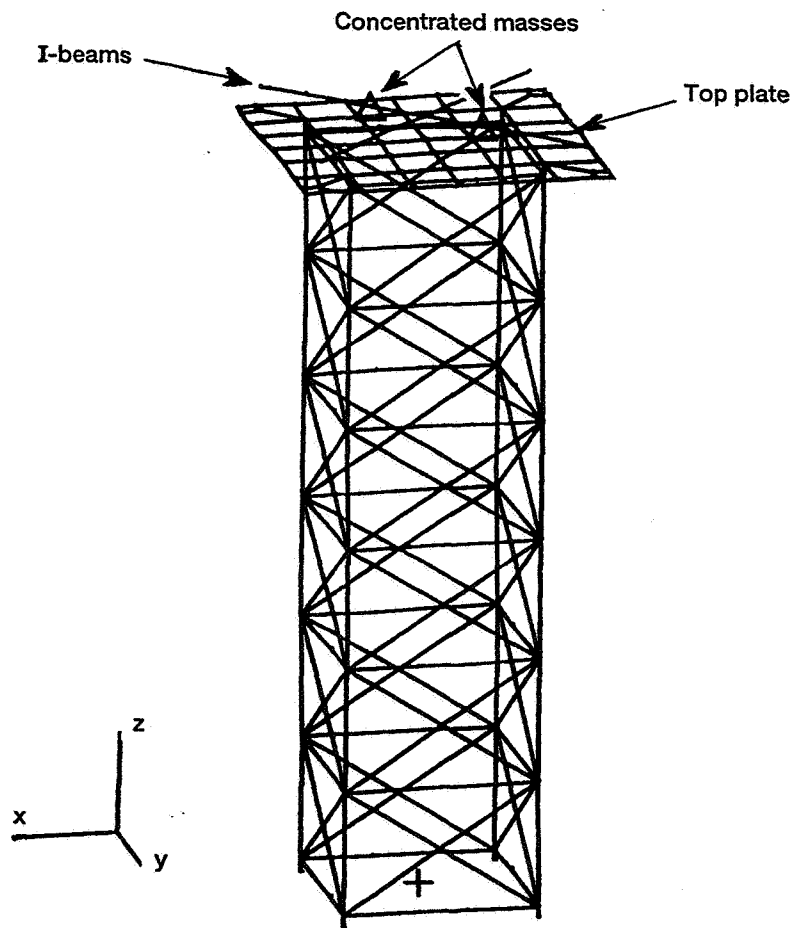

Figure 63. 3-Bay FASTMast Nonlinear Finite Element Model.

51

Finite Element Model Updating and Correlation Approach

Since the ANSYS model was developed prior to combined loads testing, it was updated while the MSC/ NASTRAN model was being created. The principal ANSYS model parameters requiring refinement included the following:

1. Diagonals modified to reflect nonlinear stiffness given in reference 11.
2. Flex-batten stiffness properties were updated based on testing performed at the completion of combined loads testing.
3. Rigid batten and longeron properties were updated to reflect the most recent design data, including all element tapers.
4. Hinge joint separation was included in longeron assembly.
5. Mass and stiffness properties of top plate were updated.

Due to a lack of new joint stiffness data, the ANSYS hinge element stiffnesses were not changed during the updating process. The diagonals were modeled using rod elements with nonlinear material properties required for the proper stiffness characteristics. Diagonal stiffness properties are given in table 4. Listed in table 5 is an ANSYS model element summary. The final model contained 558 elements, 492 nodes, and a total of 2910 degrees of freedom.

TABLE 4.—NONLINEAR PROPERTIES FOR
DEV-2 DIAGONALS

ABLE		ANSYS		
Cable Load, (Lbs.)	Cable Stretch, (in.)	Stress, (Lbs./in.^2)	Strain, (in./in.)	Tangent Modulus
0.0	0.0	0.0	0.0	
		2.00E-09	1.12E-04	56200.00
10.0E+00	1.92E-02	10.0E+00	5.42E-04	18448.00
15.0E+00	2.90E-02	15.0E+00	7.94E-04	19851.51
25.0E+00	4.30E-02	25.0E+00	1.18E-03	26091.27
35.0E+00	5.20E-02	35.0E+00	1.42E-03	40584.42
45.0E+00	6.05E-02	45.0E+00	1.66E-03	42973.79
55.0E+00	6.70E-02	55.0E+00	1.83E-03	56179.78

TABLE 5.—3-BAY FASTMast NONLINEAR ANSYS FINITE ELEMENT
MODEL SUMMARY

Hardware	Item	Number of Items	Number of ANSYS elements					
			LINK10	BEAM4	BEAM44	CONM2	SHELL43	COMBIN7
FAST-MAST	Rigid battens	16	0	0	32	0	0	0
	Flex battens	12	0	120	0	0	0	0
	Longerons (offset)	24	0	0	168	0	0	0
	Diagonals (dev2)	48	48	0	0	0	0	0
	Elbow joint	12	0	0	0	0	0	76
	Joint Link	28	0	0	48	0	0	0
TEST	Clevices	8	0	4	4	0	0	0
	Top plate	1	0	0	0	0	44	0
	I-beams	2	0	0	12	0	0	0
	Shear application fixture	1	0	2	0	0	0	0
	Moment application fixture	2	0	0	0	0	0	0

The MSC/NASTRAN model was developed using the same design criteria as the ANSYS model. The fundamental differences between the two models were the manner in which the joints were represented and the level of fidelity. The MSC/NASTRAN hinges were created using linear stiffness elements and the backstop feature was represented with GAP elements. Element properties, with the exception of those relating to the GAP elements, are given in tables 4 and 6. The MSC/NASTRAN model consists of 327 elements, 243 nodes, and 950 degrees of freedom, this is approximately half the size of the ANSYS model. All aspects of nonlinear FE development in support of the 3-Bay combined loads testing can be found in reference 12.

TABLE 6.—3-BAY FASTMast NONLINEAR NASTRAN FINITE ELEMENT MODEL SUMMARY

Hardware	Item	Number of Items	Number of NASTRAN elements					
			CONROD	BAR	BEAM	CONM2	QUAD	CELAS2
FAST-MAST	Rigid battens	16	0	16	16	0	0	0
	Flex battens	12	12	0	0	0	0	0
	Longerons (straight)	24	0	24	0	0	0	0
	Diagonals (dev2)	48	48	0	0	0	0	0
	Elbow fitting joint stiffness	12	0	0	0	0	0	144
TEST	Clevices	8	0	0	8	0	0	0
	Top plate	1	0	0	0	0	44	0
	I-beams	2	0	0	13	0	0	0
	Moment application fixture	2	0	0	0	2	0	0

The goal of the correlation effort was to develop a test-verified FE model for nonlinear large displacement stability analyses. The principal model attributes required for accurate stability assessments were determined to be system stiffness and representation of mechanistic behavior. The approach was to first make the required updates based on known design parameters. Following preliminary model updating, nonlinear large displacement analyses were performed and displacements of the mast top were compared to those obtained during testing. The applied loads used for both analyses and test data comparisons included individually applied transverse, torsion, and moment loads. It was felt that correlation of the model to individually applied loads over the entire nonlinear response range would result in a test verified system stiffness that could successfully predict responses to combined load states. Any discrepancies between tests and analyses results would be eliminated by updating joint stiffnesses as required. Once model correlation was achieved, the joint stiffnesses were to be evaluated in terms of the design reality.

ANSYS Nonlinear Finite Element Correlation

The ANSYS correlation curves are given in figures 64 to 72. Characteristic displacements were taken at the mast top (SP7 and SP10) and at the bay 3 flex-batten (SP5). For the case of a transverse load, represented by figures 64 to 66, agreement with test results was good in the linear range and effects of plate interaction were captured by the model. FASTMast nonlinear stiffness projected by the ANSYS model was greater than that of the test structure. The majority of this discrepancy is likely due to plate interaction effects combined with the differences between model and test article joint stiffnesses. Correlation results for moment loading are given in figures 67 to 69. Again there is good agreement with test results with a maximum displacement deviation of 0.10 in. at SP7. In general the model was stiffer than the 3-Bay test article. Note that the test record for displacement is mildly nonlinear probably indicating a minor longeron misalignment. Finally, model correlation to torsion loading is given in figures 70 to 72. Of all the applied load conditions, torsion loads represented the biggest challenge relative to model correlation. There is good agreement between tests and analyses results during linear response at all three gage positions. However, once the structure becomes nonlinear, the only reasonable correlation occurred for responses at SP10. The reasons for the large deviations at SP5 and SP7 are not clear but may involve a discrepancy in the hinge rotational stiffness contained in the FE model and/or gravity effects.
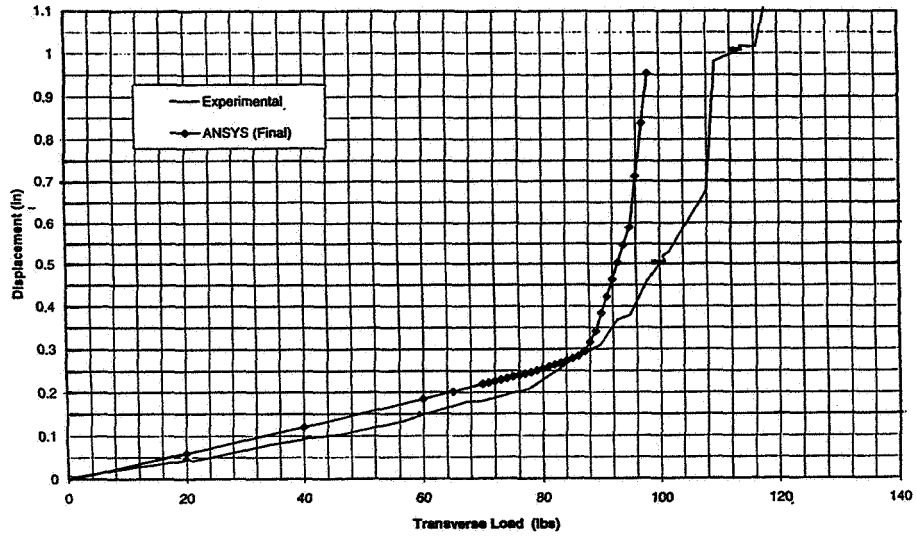
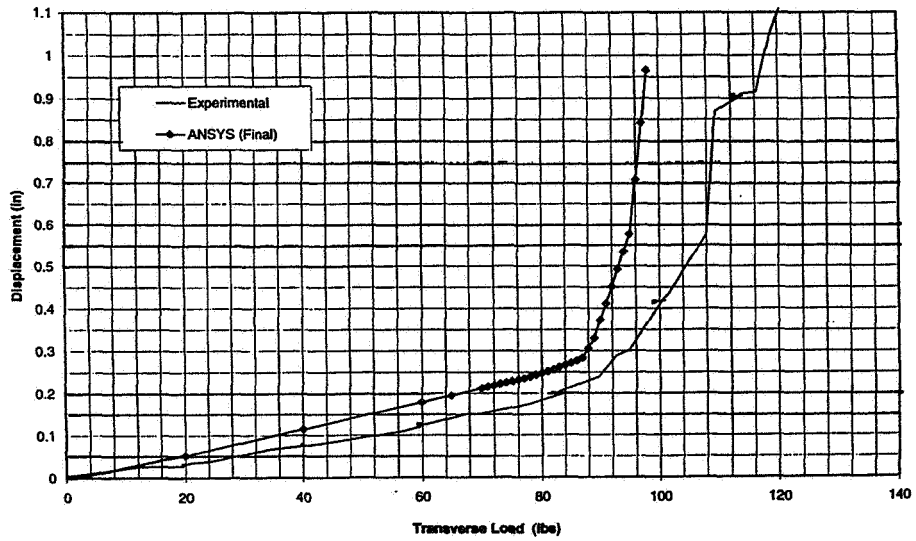**Figure 64.** ANSYS 3-Bay FASTMast Correlation Curve for Transverse Load and SP10 Displacement.

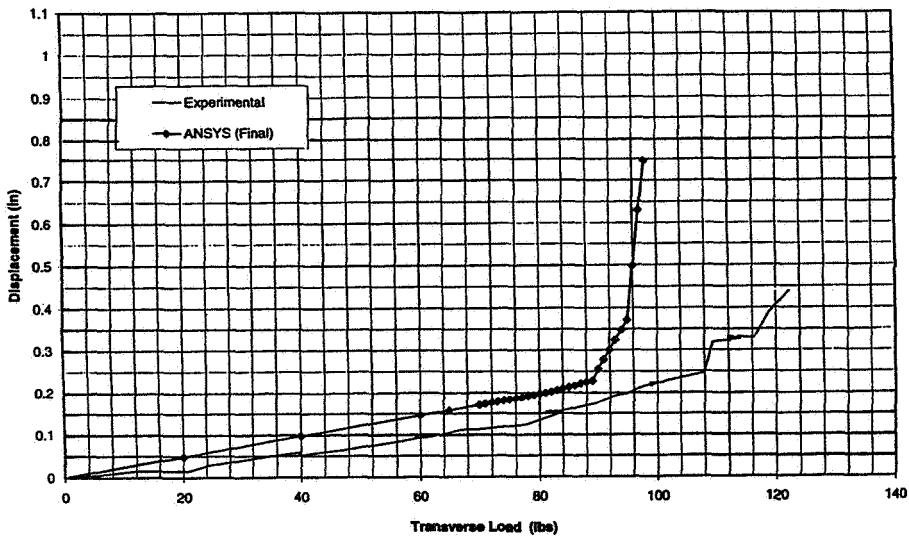**Figure 65.** 3-Bay FASTMast Correlation Curve for Transverse Load and SP7 Displacement.

Figure 66. ANSYS 3-Bay FASTMast Correlation Curve for Transverse Load and SP5 Displacement.
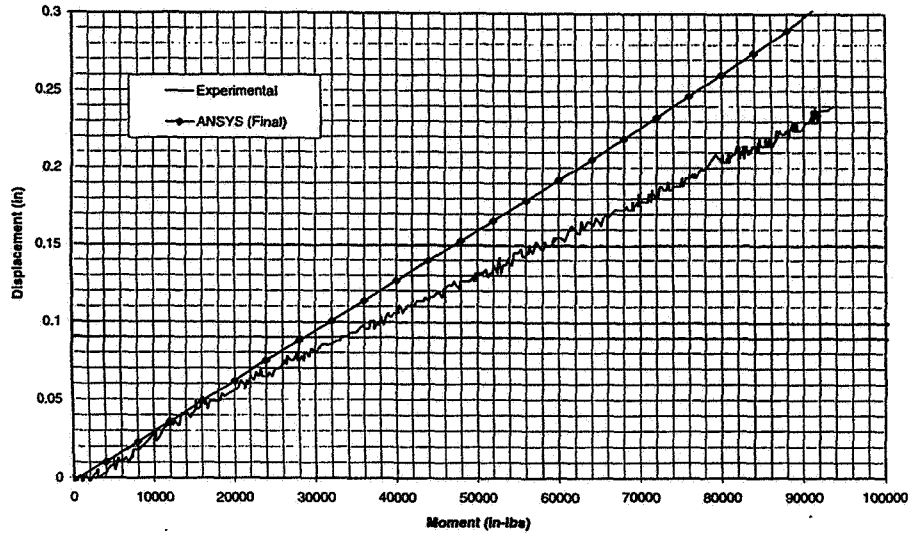
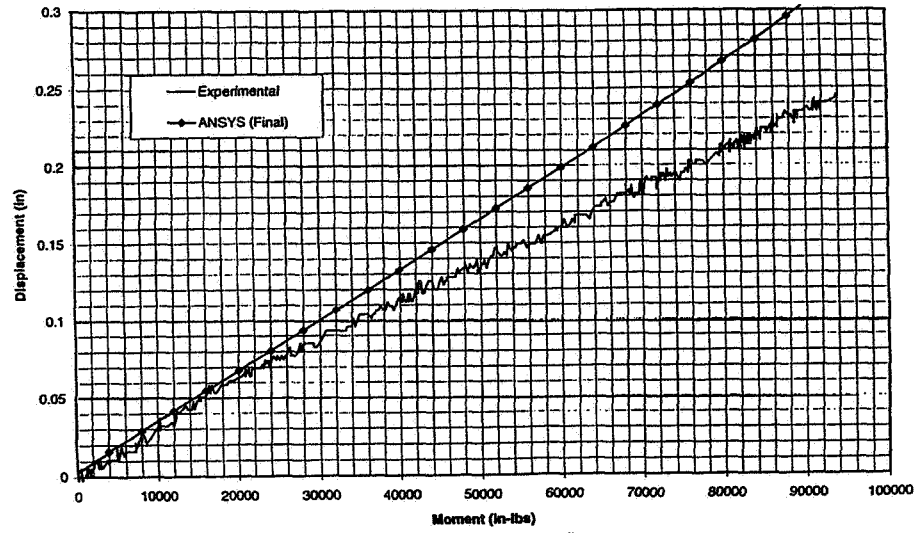**Figure 67.** ANSYS 3-Bay FASTMast Correlation Curve for Moment Load and SP7 Displacement.

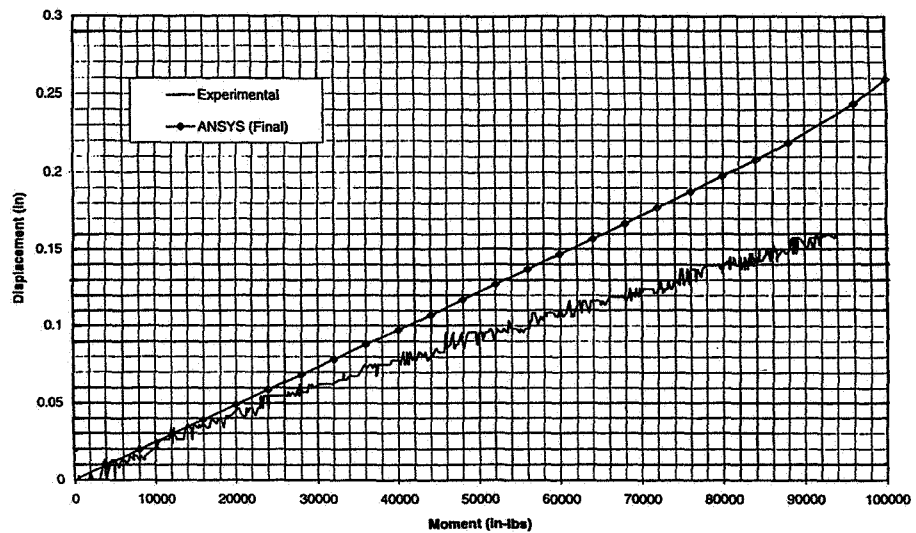**Figure 68.** ANSYS 3-Bay FASTMast Correlation Curve for Moment Load and SP10 Displacement.

Figure 69. ANSYS 3-Bay FASTMast Correlation Curve for Moment Load and SP5 Displacement.
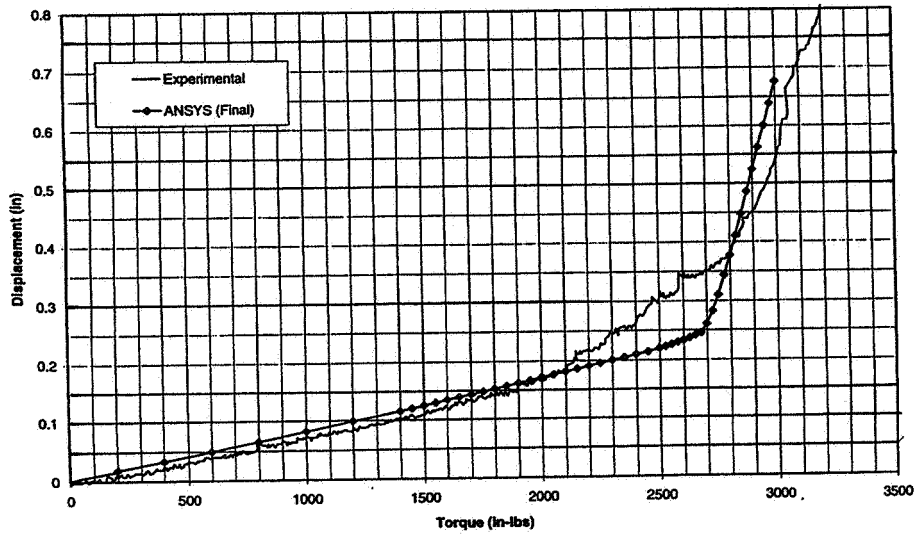
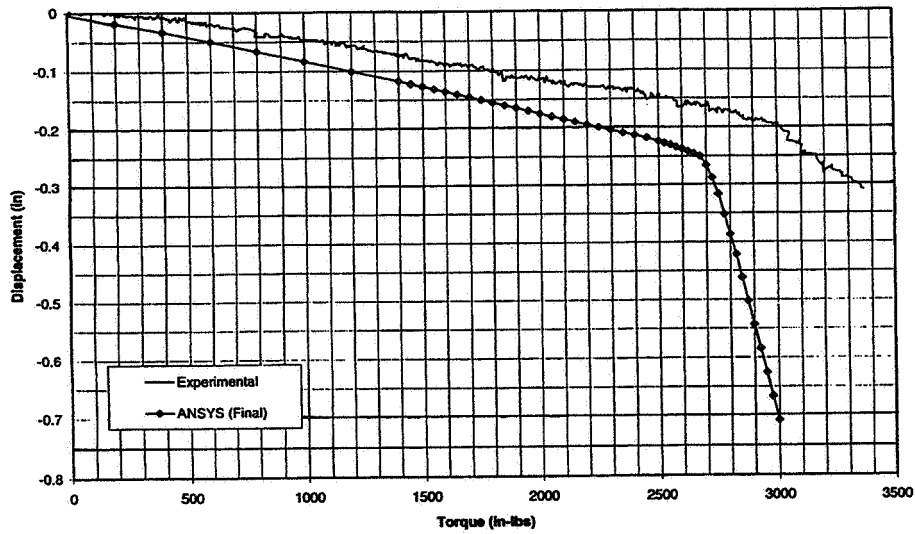**Figure 70.** ANSYS 3-Bay FASTMast Correlation Curve for Torsion Load and SP10 Displacement.

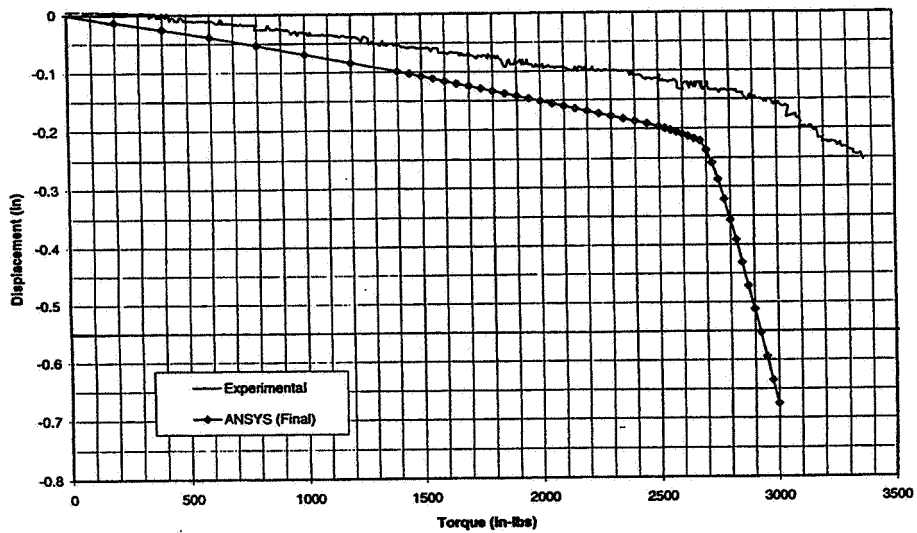**Figure 71.** ANSYS 3-Bay FASTMast Correlation Curve for Torsion Load and SP7 Displacement.

Figure 72. ANSYS 3-Bay FASTMast Correlation Curve for Torsion Load and SP5 Displacement.

56

MSC/NASTRAN Nonlinear Finite Element Model Correlation

The MSC/NASTRAN correlation curves are given in figures 73 to 78. Due to time constraints, correlation to torsion response was not possible. In this case the final MSC/NASTRAN response curve includes an update to elbow joint tensile and compressive stiffnesses. The stiffness updates resulted in values of 83,000 lb/in tension, and 20,000 lb/in. compression. The final joint stiffness values used here were intended to represent a damaged or yielded joint. For the case of transverse loads, model correlation was excellent throughout the linear and nonlinear response regime. Again the effect of plate interaction was captured by the FE model. Deviations for nonlinear response at SP5 were likely due to the inability to anticipate and therefore model load path deviations. Given in figures 76 to 78 are the moment load correlation curves. It is quite clear that reducing joint compression and tension stiffness introduced the required compliance necessary for model correlation. However, the fact that updated joint stiffnesses represents a yield state raises questions regarding model correlation and its effect on subsequent stability analyses for an undamaged flight structure.
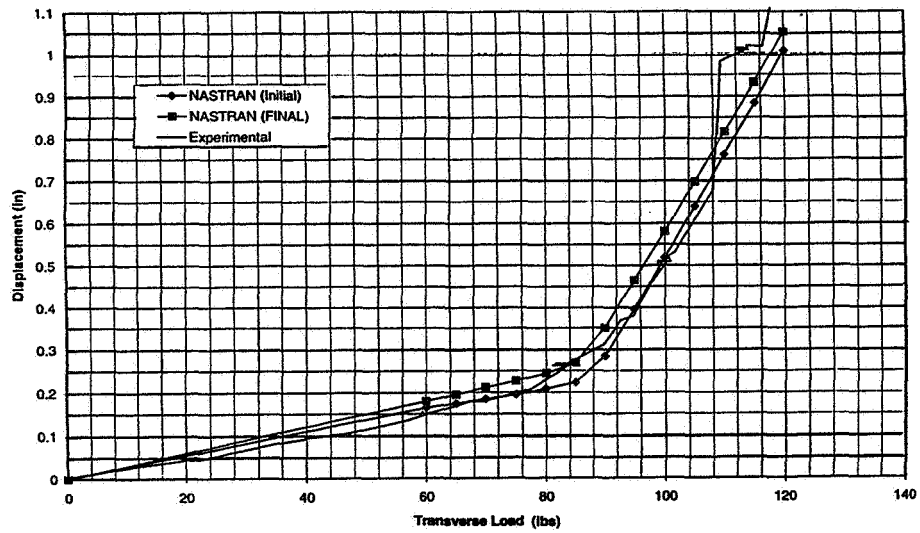

Figure 73. MSC/NASTRAN 3-Bay FASTMast Correlation Curve for Transverse Load and SP10 Displacement.

Figure 74. MSC/NASTRAN 3-Bay FASTMast Correlation Curve for Transverse Load and SP7 Displacement.

57

Figure 75. MSC/NASTRAN 3-Bay FASTMast Correlation Curve for Transverse Load and SP5 Displacement.

Figure 76. MSC/NASTRAN 3-Bay FASTMast Correlation Curve for Moment Load and SP10 Displacement.
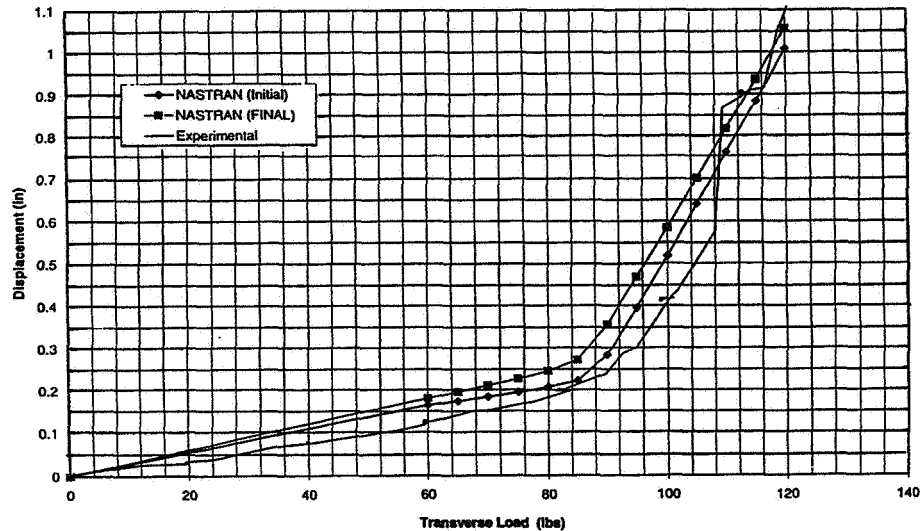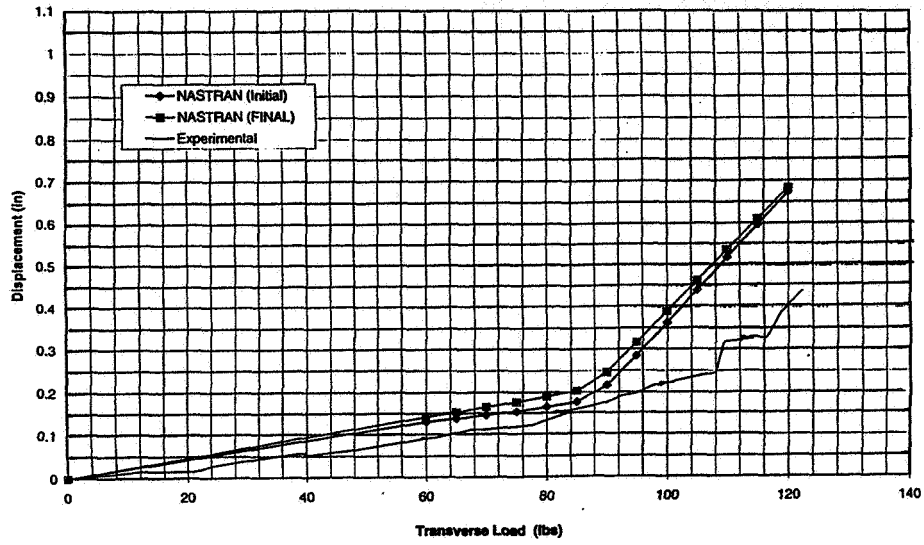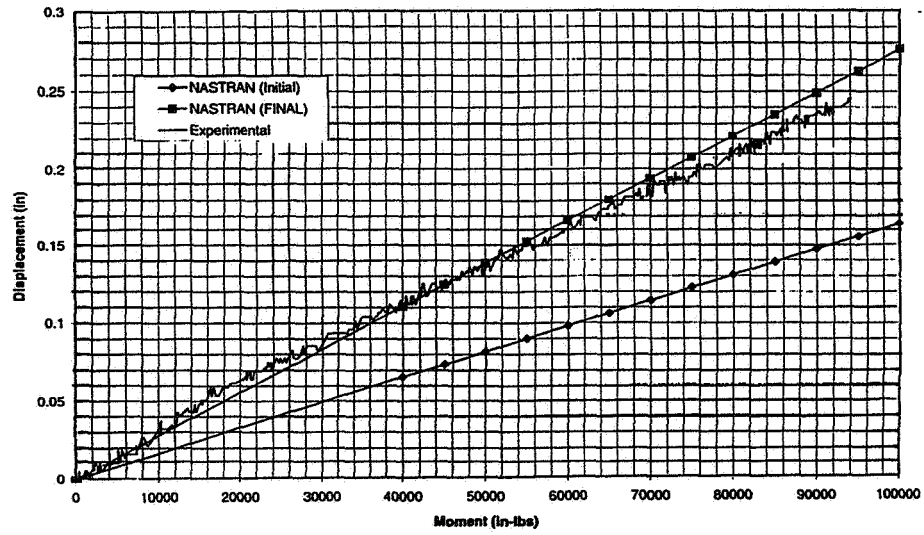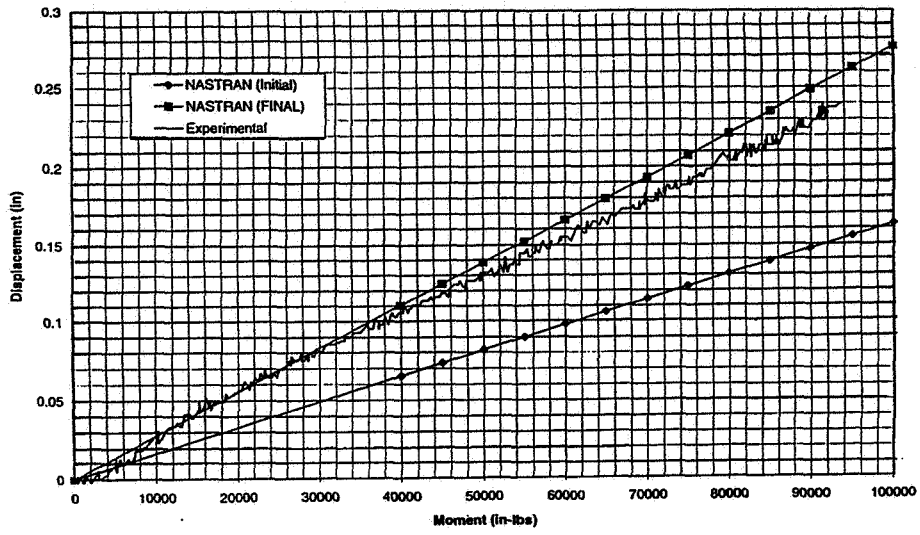
Figure 77. MSC/NASTRAN 3-Bay FASTMast Correlation Curve for Moment Load and SP7 Displacement.
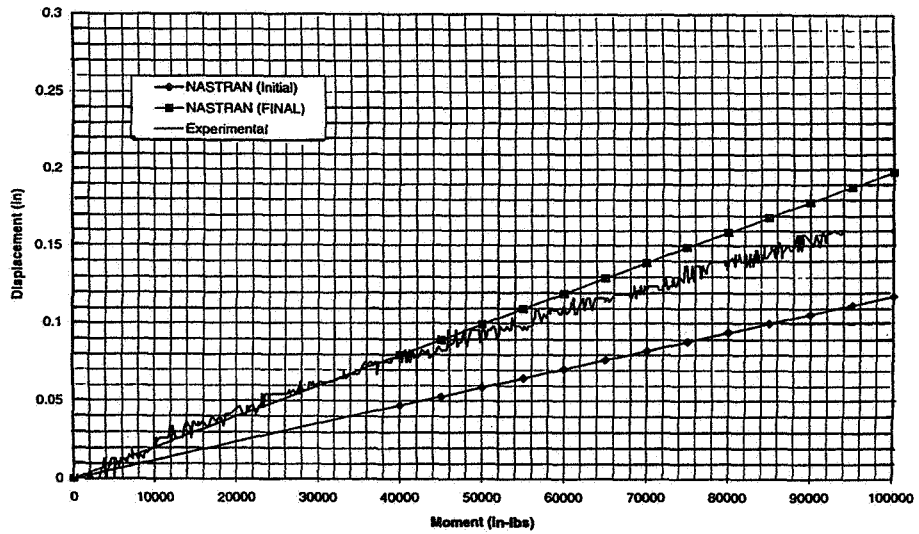

Figure 78. MSC/NASTRAN 3-Bay FASTMast Correlation Curve for Moment Load and SP5 Displacement.

Overall the ability to correlate FE models to individually applied loads proved relatively straightforward. The majority of model updates included design information that was obtained from detailed drawings and component stiffness testing. The only radical change to a FE model involved the joint stiffness changes incorporated in the MSC/NASTRAN model. Once the ANSYS model undergoes joint stiffness updating each model will possess a system stiffness representative of the test article. Although time did not permit correlation checks involving combined load states up to a point of instability, either FE model should provide sound support to nonlinear stability assessments of the 3-Bay Dev-2 FASTMast hardware.

CONCLUSIONS

From the results of the 3-Bay FASTMast effort it appears that within the confines of linear behavior the mast does not present a stability concern. The linear stability failure mode, as reported in reference 8, is Euler buckling of a single longeron for an axial load of approximately 2450 lbs. Before this value of longeron load can be achieved during service, however, diagonals become slack and the problem of linear stability ceases to exist. The problem of FASTMast instability then, in its most succint form, involves a nonlinear mast structure possessing a critical level of longeron misalignment. Once inside the nonlinear response regime, large lateral displacements of the elbow joint(s) result in a state of general instability. As the elbow joint translates, the FASTMast structure transitions from one equilibrium state to another of a different character. The two equilibrium configurations differ greatly and the rate of transition from one to the other varies with the nature of the applied loads. At this point the structure loses its capacity to sustain further applied loads and large deformations render it unsafe for further use.

In order to reliably assess the nonlinear stability limits of the FASTMast structure much work remains. The first problem that must be addressed is the development of a 32-bay FE model of the flight unit. Due to radical changes in load paths associated with nonlinear behavior, extending a correlated 3-Bay FE model to a 32-Bay flight unit is not a viable option. If internal load symmetry had been maintained into the nonlinear state, extending the correlated 3-Bay FE model to 32 bays would have been an acceptable approach to support flight unit analyses. Originally it was assumed by the authors, that nonlinear behavior would not involve radical changes to the mast load paths. However, alternate load paths which develop during nonlinear behavior will surely vary as a function of the mast length and changing geometry.

In addition to load path alterations the fidelity of Dev-2 hardware will also cast doubt upon any effort to extend the 3-Bay model to 32 bays. The fact that flight fidelity diagonals possess nearly linear stiffness may significantly affect the response of FASTMast system. Therefore, the 3-Bay correlation effort supports a class of hardware that no longer represents the flight configuration. However, FE modeling of the structure is straightforward provided the flex-batten, hinged joints, and diagonals are represented properly. The fact that the flight diagonal is linear and flex-batten properties are well-understood, leaves only joint unknowns as the immediate impediment to accurate model development.

A second important consideration before embarking on a nonlinear stability assessment involves the complexity of nonlinear analyses. In general, the time to perform an analysis is a function of model performance and the analysts' ability to predict the failure load. When failure loads are unknown, load increments must be small to avoid stepping" over the failure load. Even when adequate load stepping is achieved, computational difficulties may arise due to model anomalies or instabilities in the equations of motion themselves. Each of the problems given above has the potential capability to increase computational time exponentially. The cost and complexity of a nonlinear assessment would be increased further due to the number of failure load cases required to produce a statistically viable failure surface. The random nature of longeron misalignment, diagonal preload, flex-batten stiffness, and applied loads over the life of the structure should be accounted for within stability analyses. Finally, the determination of margins of safety for nonlinear stability should involve a limit load developed using nonlinear methods.

The FASTMast is a state-of-the-art flight structure designed very carefully by the mast contractor to meet specific service requirements. In order to meet many conflicting demands, the structure has been rendered stability critical. The strength characteristics supporting the original assumption of linear operational behavior are well understood and predictable to a high level of certainty. However, when the FASTMast structure is exercised into a nonlinear response state, the problem of assessing structural stability is complicated at best. A nonlinear structural assessment in this case is not straightforward and would probably involve additional development work for which there is no time. There are perhaps several simple design changes which, when coupled with operational

modifications of the Space Station and Shuttle, may provide additional strength but they must be assessed at the component and system levels. However, until margins of safety are determined with actual flight loads the need for any change is merely speculation.

RECOMMENDATIONS

In order to minimize the likelihood of a stability failure of the FASTMast flight unit the following recommendations are presented for ISS Program consideration:

1. Maintain a linear operational state and retain current limit load reduction factors for flex-batten creep and stability failures. This will require the flight structure to maintain a tensile preload in all diagonals in the service environment.

2. All FE models used for final assessment of flight hardware should be based on released flight drawings.

3. If the mast operation is extended into a state of nonlinearity, develop appropriate nonlinear failure surface(s) necessary to characterize failure loads. Failure surface(s), or failure interaction curves should be defined in terms of FASTMast applied or internal loads required for stability assessments.

4. Develop data that quantifies the effects of elbow joint, diagonal, and flex-batten degradation on component structural performance. Include effects in nonlinear FE models for future structural assessments.

5. Use consistent limit load types for margins of safety determinations involving linear and nonlinear stability strength capability (i.e. nonlinear response analyses should accompany nonlinear capability levels in the equation for margin of safety).

6. Perform a FASTMast structural reliability assessment that will account for the stochastic nature of system strength and applied loads over the operational life of the structure.

REFERENCES

[1] Space Station Program Structural Design Loads Data Book Volume 2: On-orbit Structural Design Loads, SSP-30800 Volume 2, May 1993.

[2] 3-Bay FASTMast Axial Test and Analysis, Lewis Research Center, Engineering Directorate, Structural Systems Division, Structural Analysis Branch, Report No.SAB 93-002, February 1993.

[3] 3-Bay FASTMast Shear Test and Analysis, Lewis Research Center, Engineering Directorate, Structural Systems Division, Structural Analysis Branch, Report No. SAB 93-003, April 1993.

[4] 3-Bay FASTMast Axial/Torsion Test and Analysis, Lewis Research Center, Engineering Directorate, Structural Systems Division, Structural Analysis Branch, Report No. SAB 93-005, May 1993.

[5] Roche, J. M., Combined Shear/Bending Moment Test of the 3-Bay FASTMast, Lewis Research Center, Engineering Directorate, Structural Systems Division, Structural Analysis Branch, Report No. STR No. 93-5, January 1994.

[6] 3-Bay FASTMast Combined Shear/Bending and Analysis, Lewis Research Center, Engineering Directorate, Structural Systems Division, Structural Analysis Branch, Report No. SAB 94-001, April 1994.

[7] Shaker, J. F., Static Stability of Three-Dimensional Space Truss , M.S. Thesis Case Western Reserve University 1994.

[8] Trudell, J. J., <u>3-Bay FASTMast Linear Stability Analysis</u>, Lewis Research Center, Aerospace Technology Directorate, Power Technology Division, Solar Array Branch, Report No. SAB 94-007, November 1994.

[9] <u>Final Test Report 3-Bay FASTMast Combined Loading</u>, Aerospace Design and Fabrication, Inc., Report No. 9404, September 1994.

[10] Smucker, J. E., <u>Flex-batten Spring Rate Test</u>, Lewis Research Center, Space Station Freedom Directorate, Photovoltaic Power Module Division, Solar Array Branch, July 1992.

[11] <u>Mast Canister Failure and Strength Assessment Final Report</u>, AEC-Able Engineering, Corp., Report No. AEC94518R921 Rev. A, May 1994.

[12] <u>Final Finite Element Correlation Report 3-Bay FASTMast Shear, Torque, and Moment Loading Using NASTRAN and ANSYS</u>, Aerospace Design and Fabrication, Inc., Report No. 9405, September 1994.

REPORT DOCUMENTATION PAGE

1. AGENCY USE ONLY (Leave blank)	2. REPORT DATE	3. REPORT TYPE AND DATES COVERED
	August 1995	Technical Memorandum

4. TITLE AND SUBTITLE

Static Stability of the Space Station Solar Array FASTMast Structure

5. FUNDING NUMBERS

WU–478–42–10

6. AUTHOR(S)

John F. Shaker and Thomas H. Acquaviva

7. PERFORMING ORGANIZATION NAME(S) AND ADDRESS(ES)

National Aeronautics and Space Administration
Lewis Research Center
Cleveland, Ohio 44135–3191

8. PERFORMING ORGANIZATION REPORT NUMBER

E–9543

9. SPONSORING/MONITORING AGENCY NAME(S) AND ADDRESS(ES)

National Aeronautics and Space Administration
Washington, D.C. 20546–0001

10. SPONSORING/MONITORING AGENCY REPORT NUMBER

NASA TM–106895

11. SUPPLEMENTARY NOTES

12a. DISTRIBUTION/AVAILABILITY STATEMENT

Unclassified - Unlimited
Subject Categories 37, 39, 15, 18, and 64

This publication is available from the NASA Center for Aerospace Information, (301) 621–0390.

12b. DISTRIBUTION CODE

13. ABSTRACT (Maximum 200 words)

The combined loads test of the 3-Bay FASTMast marks the end of the Lewis Research Center (LeRC) effort to characterize the behavior of the principal Space Station solar array support structure. The primary objective of this test and analysis effort was to develop a method to predict structural stability failure modes under flight-like applied loads. Included at the beginning of this report is a brief historical perspective of the hardware design development and FASTMast structural stability problem evolution. Once an understanding of the solution process has been established, test and analysis details are presented and related to the postulated failure theories. The combined load test series subjected the structure to a combination of transverse, moment, and torsion loads similar to that expected in the service environment. Nonlinear Finite Element (FE) models were developed and large displacement analyses were performed to support the test effort and failure mode predictions. Details of the test configuration as well as test and analysis results are presented. The results were then critiqued to establish valid and successful support of the failure mode assessments. Finally, study conclusions are drawn and recommendations for safe operation of FASTMast structure are presented for consideration.

14. SUBJECT TERMS

Deployable mechanism; Nonlinear; Stability; Large space structure technology; Solar array support structure; Deployable structure

15. NUMBER OF PAGES

74

16. PRICE CODE

A04

17. SECURITY CLASSIFICATION OF REPORT	18. SECURITY CLASSIFICATION OF THIS PAGE	19. SECURITY CLASSIFICATION OF ABSTRACT	20. LIMITATION OF ABSTRACT
Unclassified	Unclassified	Unclassified	